DIPS

AN INTERACTIVE AND GRAPHICAL APPROACH TO THE ANALYSIS OF ORIENTATION BASED DATA

by Mark S. Diederichs
Department of Civil Engineering

ABSTRACT

Many problems in engineering geology are fundamentally problems in three dimensional geometry. Spherical projection is a time tested technique by means of which complex and arbitrary orientation problems can be solved manually with relative ease. In spite of rapid developments in computing hardware, no analytical software has been created which seems capable of adequately replacing spherical projection techniques. Therefore, many attempts have been made to computerize this method. The majority of these attempts have resulted in programs which are static and inflexible in nature. DIPS, a program which was developed as the main component of this work, duplicates, on the computer, the flexibility, graphical visualization potential and interactive nature of the original spherical projection techniques.

ACKNOWLEDGEMENTS

When the opportunity arose to study and research with Dr. Evert Hoek, it certainly appeared to be a golden opportunity to learn from the experience, knowledge and superb teaching style which he would bring to the group. These expectations were indeed fulfilled. What I had not anticipated was the loyal and mutually respectful friendship that has evolved. As a supervisor and as a friend, he has been of seemingly inexhaustible source of patience, support and inspiration.

The Rock Engineering Group at the University of Toronto has provided a stimulating environment for learning. More importantly, it has resulted in friendships which have kept most of us sane as we struggled towards our elusive goals, and which will undoubtedly withstand the test of time and distance after our respective departures. From this group, I must single out Scott Peaker for special kudos. As a colleague and as a housemate, he has provided suggestions and support, and has provided a tireless ear as I batted about my own ideas about this project. Brent Corkum has also been invaluable as a programming mentor to myself and indeed, the entire Rock Engineering Group over the last several years.

Thanks must also go to David Wood, Jim Wong, Don Grant and Trevor Carter whose inspired, if not often possessed, input into the development of DIPS has been a welcome annoyance.

Just as they have been though every stage of my life, my family has been a endless source of love and support. Eternal thanks to Mum, Sara and Beccy for always being there, and to Dad, whose memory will forever be an inspiration.

CONTENTS

LIST OF FIGURES

LIST OF TABLES

1.0   INTRODUCTION

The study of geological structure is a fundamental component of any study of stability characteristics for rock slopes and underground excavations. It is also an important step in the assessment of general deformation characteristics and fluid conductivity. As well, identification and extrapolation of geological structure often forms a basis for preliminary mineral prospecting.

While scalar properties such as length and separation are often considered, many of the problems which are encountered in these studies are fundamentally problems in three-dimensional geometry, and focus primarily on orientation relationships. Even if the problem involves only a few distinct or representative orientations, it's three dimensional nature leads to difficulties in visualization and in the solution of arbitrary interrelationships. While some "black box" techniques exist for the solution of specific types of three dimensional structural problems, a technique is required which permits the analysis to progress in a non-prescribed fashion as the problem dictates, while allowing simultaneous visualization.

Before analysis can proceed with representative structural orientations, however, simplified models must often be reduced from multiple field measurements. Unless the regional or local structure is already well established, the systematic collection of field data is a key first step in any analysis of three dimensional structural relationships. Because the historical factors such as stress, which contribute to the formation of geological structure are often consistent throughout a volume of rock,

natural discontinuities or rock fabric can frequently be represented by several dominant orientations. The three dimensional nature of the data as well as the natural variance of geological structure make this reduction process difficult unless an appropriate visualization and analysis tool is available.

The most appropriate tool for both stages of orientation analysis is, in the opinion of this author, spherical projection. First used in the second century B.C. by crystallographers for the study of crystal morphology and optics, this technique has been adapted in the last century for use in structural geology (Phillips, 1971).

This technique considers only the orientations of linear or planar features. Planes and lines are assumed to intersect the centre of a sphere. This sphere is often called the *primitive* in crystallography. The term *reference sphere*, however, is used by this author. The circle and point traces formed as the planes and lines intersect the surface of the sphere are projected by means of one of two methods to form the spherical projection which is the basis for this work.

The projection can be used in a time tested manual process, utilizing reference grids and rotating overlays to perform a wide variety of otherwise complex geometrical calculations with relative ease. The method's power lies in its interactive and graphical nature. These techniques are described throughout the literature (Goodman 1976, Hoek and Bray 1974, Hoek and Brown 1980, Phillips 1971, Priest 1985, Ragan 1973) and are summarized in chapter 3 of this work.

Lines plot as points on the spherical projection as do normals to planes, often referred to as poles. This allows large numbers of linear or planar features to be plotted on a projected *stereonet* in a relatively uncluttered fashion. Dominant orientations can be derived from apparent clusters or sets visible on such a plot. The visual impact of this clustering may be further enhanced by a orientation density contour plot. This technique is also described by the above authors as well as by CANMET 1977, Denness 1972, Stauffer 1966 and Zanbak 1977. Since there does not exist a reliable mathematical process to reduce a large multimodal (having more than one dominant orientation) orientation data set to representative features, spherical projection is a unique and vital part of such an analysis.

The process can prove tedious if performed manually, however. The development of computers has not, in turn, led to the development of a replacement for spherical projection. It has, on the other hand, created the possibility of drastically increasing the speed and power of the existing process. There have been many attempts in recent years to adapt the process for use with a computer. Some of these are discussed in chapter 4 of this work. Most of these attempts, however, have focused on generating static output of pole plots, contoured density plots or stereonets with prescribed distinct planes. Further analysis must then be carried out by hand from the computer screen or from paper output. These early attempts, in the opinion of this author, fail to capture the powerful visualization features and interactive nature of the manual spherical projection techniques.

1.1   DIPS - An interactive toolkit using spherical projection

The purpose of this work was to develop a computer package for orientation analysis which would dynamically mimic the original techniques involving spherical projection and cover all phases of the analysis from data reduction to analysis of distinct features. The program was to possess many interactive features in addition to producing high quality graphical output. It was also to accept a wide variety of data formats and conventions. In addition, since orientation data is often associated with other information (spacing, continuity and roughness of rock joints, for example), the program was designed to allow several means of simultaneous processing this additional data. The program was designed to access a data file which could act as a single database with the ability to interactively screen and process data subsets as the analysis warranted.

The resulting package is called **DIPS - Data Interpretation Package using Stereographic projection.** The program disk and user manual can be found appended to this thesis.

The rest of this thesis deals with the design philosophy and rationale for the program DIPS. Chapter 2 of this work discusses a variety of orientation nomenclature and measurement conventions. Chapter 3 summarizes previous work dealing with orientation analysis including the development of spherical (stereographic) projection. Chapter 4 deals with previous attempts at computerization of stereographic techniques. Chapter 5 describes the various features of the DIPS package.

2.0 ORIENTATION NOTATION AND MEASUREMENT

Few aspects of orientation analysis create as many difficulties as the initial recording of the data itself. This arises from the great variety of conventions and methodologies which are in use at present. This chapter outlines common conventions and identifies those used throughout this work.

2.1 ORIENTATION NOMENCLATURE

2.1.1 Vectorial Notation

A vector in three dimensional space can be described using three cartesian coordinates based on some arbitrary origin and three mutually perpendicular (orthogonal) reference axes. The same vector may also be described using independent measures of magnitude, or absolute length, and of orientation. This orientation can be expressed in terms of the coordinates of a collinear unit vector (vector of length 1). It may also be described using a combination of angles in mutually orthogonal planes. The horizontal and vertical angles between a vector and a reference line, for example, uniquely describe an orientation.

The three coordinates of a unit vector, are also termed *direction cosines*. This term arises from the fact that each coordinate represents the cosine of the minimum angle between the unit vector and the axis in question. This form of notation is the most convenient for analytical manipulation of orientations using linear algebra and is

ideal for use in computer programs. It is not, however, the most appropriate means of intuitive visualization for the engineer or geologist. It is often difficult for the human brain to process three dimensional cartesian expressions. The use of two dimensions, however, rarely presents a problem (which explains our attachment to two dimensional forms of analysis and presentation). For this reason, geologists and engineers have traditionally dealt with information in planar sections.

When describing orientations in the field, a reference vector is chosen, such as true or magnetic north, and all orientations or attitudes are expressed in terms of a horizontal angle (*azimuth*) and vertical angle (*inclination*) from this reference. This convention is the most convenient for the surface geologist, for example, who typically treads upon a horizontal plane armed with a bubble level clinometer and a compass which references magnetic or true north. Different reference angles may be adopted in other circumstances, as when surveying in a magnetic ore body (where compasses may prove unreliable and other references must be adopted) or when coring underground with equipment standardized for subvertical drilling (making a vertical reference direction more convenient).

Geological convention and convenience of expression have led to the development of many different terms for describing the orientation of linear and planar features and their interrelationships. Before proceeding with further discussion, it is worthwhile to describe some of the more widely used orientation terminology. These descriptions are based on generally accepted definitions which can be found in a variety of sources (Ragan 1973, Phillips 1971, Priest 1985, Hoek & Bray 1974, Hoek & Brown 1980).

2.1.2   Orientations of Linear Features

BEARING   The acute horizontal angle between a line and a reference direction (usually one of the four major directions N,S,E or W).

AZIMUTH   The clockwise horizontal angle between a line and the north reference direction.

INCLINATION   The angle between a line and the horizontal plane, measured downward.

DECLINATION   The angle between a line and the horizontal plane measured upward. It is important not to confuse this measure with *magnetic declination* which will be defined in the next section.

ZENITH ANGLE   The angle between a line and the vertically upward direction or *Zenith*.

NADIR ANGLE   The angle between a line and the vertically downward direction or *Nadir*.

PLUNGE   This is the term used most often in geological references and by this author to define the downward angle of a lineation measured from the horizontal plane. This term is equivalent to inclination. Negative plunge is equivalent to positive declination.

TREND   This is the term used most often in geological references and by this author to define the horizontal angle between true or apparent (ie. magnetic) North and the direction of positive plunge of a lineation. Nevertheless, if this measure is associated with a negative plunge, the trend is the azimuth of the negative vector described and not of its positive counterpart. Trend is equivalent to the azimuth of a vector.
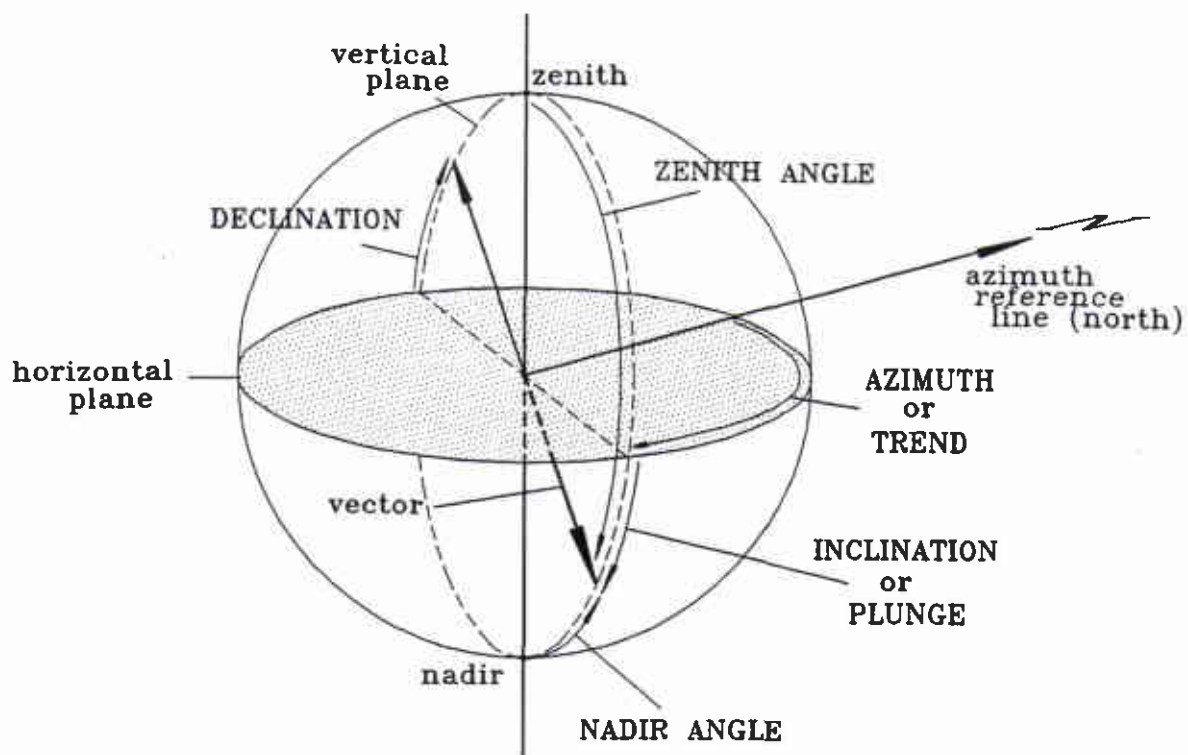
Figure 2.1: Orientations of vectors in 3-D space

2.1.3 Relationship of Trend and Plunge to Cartesian Coordinates

For implementation in analytical analysis or computer processing it is efficient, as discussed, to convert the above angular relationships into cartesian coordinates or direction cosines (the two terms are equivalent if the vector described is of unit length). If a set of axes is adopted, represented by the *north, east* and *down*

directions, then the respective direction cosines, λ , of a vector can be calculated as (Priest 1985):

$$
\begin{aligned}
\lambda_{north} &= \cos(\ trend\ ) \times \cos(\ plunge\ ) \\
\lambda_{east} &= \sin(\ trend\ ) \times \cos(\ plunge\ ) \\
\lambda_{down} &= \sin(\ plunge\ )
\end{aligned}
\qquad\qquad \text{(eq. 2.1)}
$$

Note that only two angular parameters are required to uniquely define an orientation in three dimensions. The same is true for direction cosines since the cartesian coordinates of a unit vector are related by the relationship:

$$
\lambda_{north}^2 + \lambda_{east}^2 + \lambda_{down}^2 = 1 \qquad\qquad \text{(eq. 2.2)}
$$
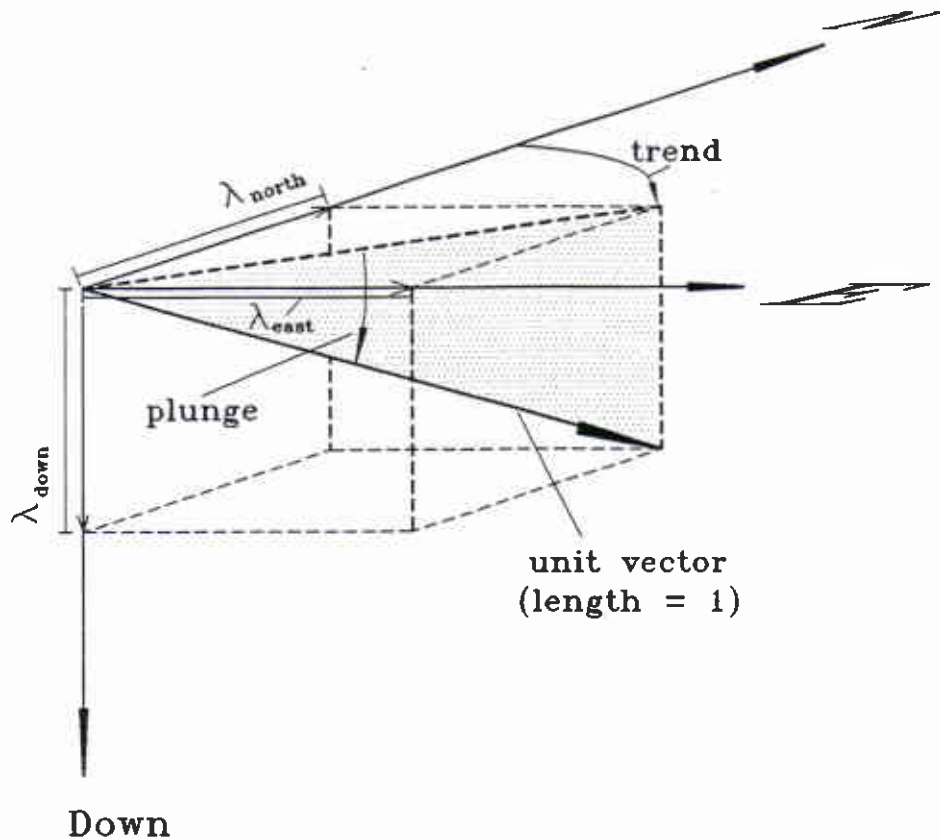
Figure 2.2: Angular and Cartesian expression of vectors

2.1.4 Attitudes of Planes

DIP
: The plunge of a vector representing the maximum downward angle between a plane and the horizontal reference plane. Occasionally the term *hade* may be used by geologists in defining a plane. This is the complement of dip and is the nadir angle of the dip vector.

DIP DIRECTION
: The azimuth of the dip vector. Unless otherwise stated, the two above definitions will be used in this work. Note, however, that the terms dip and dip direction are used occasionally to refer to other relationships. For example, the 'maximum dip' vector or 'core dip angle' of a discontinuity in a drill core is the maximum angle between the plane and the downhole core axis. The 'core dip direction' is then the clockwise angle between the core dip vector and some reference line such as the top of core.

STRIKE
: The azimuth of a horizontal line in a plane. The strike will always be perpendicular to the true dip of a plane.
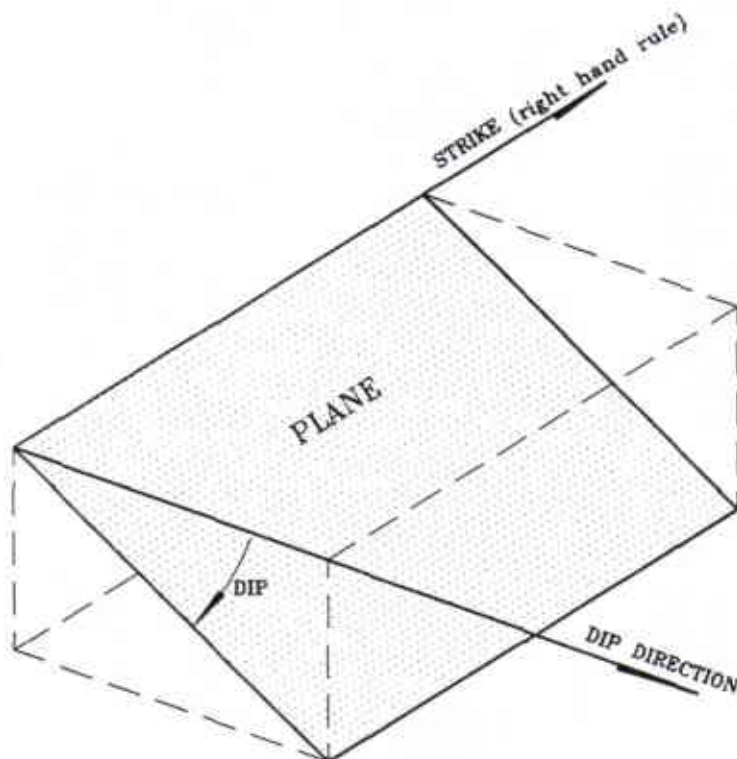
Figure 2.3: Attitudes of Planes (after Hoek & Bray 1974)

2.1.5   Orientations of Plane-Plane and Line-Plane Relationships

APPARENT DIP   The plunge of a line of intersection between a plane and a vertical reference plane not parallel to the maximum dip vector. This value will always be less than the true dip of the plane being measured. In other words this measure is the inclination of a plane measured in a direction not perpendicular to the strike of the plane.

PITCH or RAKE   The angle of a lineation (ie. a slickenside or shear etching on a plane) or of an intersection line as measured in a plane from the plane's recorded strike direction. Note that apparent dip is a special case of pitch where the reference plane is vertical.

SOLID ANGLE   The minimum angle between any two linear or planar features.

CONE ANGLE   The minimum angle between the surface of a cone and its axis of radial symmetry.
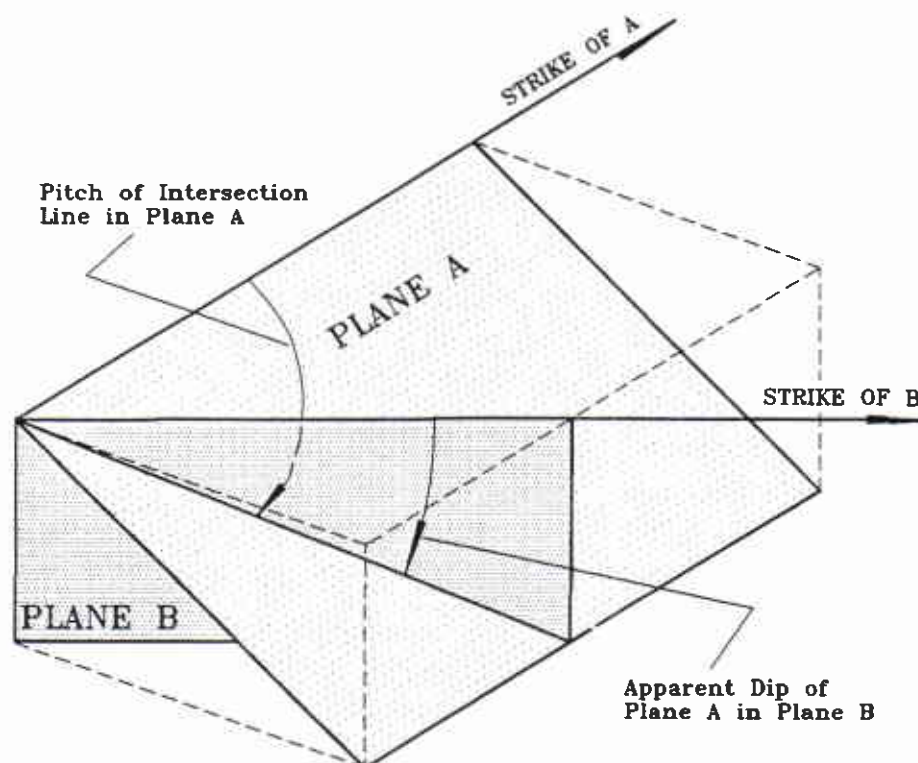
Figure 2.4: Interplane relationships (after Phillips 1971)

2.2   NORMAL VECTOR OR POLE TO A PLANE

While the planar definitions of *strike/dip* or of *dip/dip direction* are sufficient to uniquely define the orientations of planar features, many analysis procedures are more effectively carried out by dealing with *poles* or normal vectors to planes.

The normal or pole to a plane is a line which is perpendicular to the plane. The orientation of this line expressed in *trend* and *plunge* also uniquely define the attitude of its associated plane. While every plane has two associated pole directions (emanating from either side of the plane), it is more common to refer to the downward normal to a non-vertical plane. This is the convention used by the author to define the positive pole or normal.

Pole Plunge = 90° – Plane Dip

Pole Trend = Plane Dip Dir. + 180°
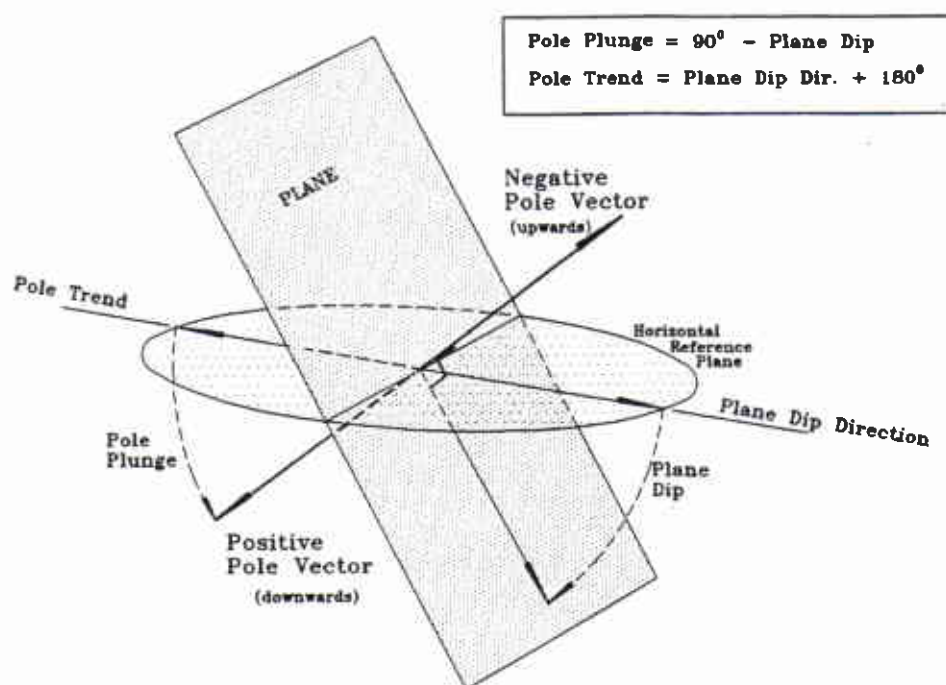
Figure 2.5: Pole - plane relationships

2.3 PLANAR RELATIONSHIPS AND DIRECTION COSINES - DOT AND CROSS PRODUCTS

While the orientation definitions discussed are convenient for measurement and visualization of planar relationships in the field, they do not provide convenient expressions for the analytical calculation of such relationships. Vector analysis of orientation requires an alternative form of expression. The conversion, for example, of a planar orientations, expressed in terms of dip and dip direction, to a triplet of direction cosines for the pole or normal vector to the plane, permits efficient calculation of relationships such as angle of intersection between planes and orientation of their line of intersection (Spiegel 1974, Goodman 1976). It also assists in efficient statistical analysis of orientation trends.

Once the pole vectors for a set of planes have been converted to direction cosines (λ) as discussed earlier, the angle of intersection between any two planes A and B can be determined, for example. This angle is equivalent to the solid angle between the poles. This can be determined graphically or analytically from the following relationship:

Pole to plane $A = \{ \lambda_{Anorth} , \lambda_{Aeast} , \lambda_{Adown} \}$

Pole to plane $B = \{ \lambda_{Bnorth} , \lambda_{Beast} , \lambda_{Bdown} \}$

$A \cdot B = \lambda_{Anorth} \cdot \lambda_{Bnorth} + \lambda_{Aeast} \cdot \lambda_{Beast} + \lambda_{Adown} \cdot \lambda_{Bdown} = \cos \xi$ (eq. 2.3)

where ξ is the solid angle between normals
(and also between planes) A and B.

Notice how this relationship, called the *dot product* of A and B, resembles equation 2.2. Since the angle between a normal and itself is 0, the cosine on the right side of the equation is equal to 1.

The direction cosines can also be used to compute the orientation of the line of intersection between two planes. This formulation is called the *cross product* and is somewhat more involved. The cross product of two vectors (in this case the poles to planes A & B) is defined as follows:

$$A \times B = \{ \lambda_{Aeast} \cdot \lambda_{Bdown} - \lambda_{Adown} \cdot \lambda_{Beast} ,$$
$$\lambda_{Adown} \cdot \lambda_{Bnorth} - \lambda_{Anorth} \cdot \lambda_{Bdown} , \quad\quad (eq.\ 2.4)$$
$$\lambda_{Anorth} \cdot \lambda_{Beast} - \lambda_{Aeast} \cdot \lambda_{Bnorth} \}$$

The above resultant triplet comprises the direction cosines for the line of intersection between planes A and B. If desired, the equations 2.1 can be used to obtain the trend and plunge of this calculated linear orientation.

It is important to note that these relationships are for unit vectors. Vectors with magnitudes greater than one can be dealt with in a similar fashion as would be the case when dealing with vectors representing forces in an analytical rock-wedge stability analysis. The cartesian coordinates in these equations would no longer be equivalent to the direction cosines. The right hand side of equation 2.2 would be equal to the square of the vector magnitude. Similarly, the right hand side of equation 2.3 would become $|A||B|\cos\xi$ where $|A|$ and $|B|$ are the scalar magnitudes of the two vectors.

For complex analysis of geometrical relationships, cartesian vector notation is very useful. It does not, however, easily facilitate intuitive visualization or field measurement.

2.4 ORIENTATION MEASUREMENT

2.4.1 Field Measurement

There are a number of methods for measuring the orientations of linear and planar features in the field. The preferred technique will depend to a large degree on the type of survey and the reasons for performing the survey.

The first stage in measurement is the selection of two reference datums. The first datum will usually be the horizontal plane. This plane can easily be referenced with a bubble level or a plumb-bob. Alternative selections for this datum include the zenith or nadir directions (vertically up or vertically down respectively). An analogous reference for measurement of drill core discontinuities would be the down core axis.

The selection of the second datum can be more involved. True north is the most common reference. Alternatives include magnetic north, mine grid north (an arbitrary reference for mine plans) or a tunnel axis or surveyed lineation. Drill core measurements can be made with respect to a top of core marker line. Selection of this datum will be governed by situation restrictions, convenience and measuring equipment used. It is useful, however, to standardise the notation of an orientation database after the measurements are made.

The reference orientations which will be used in most of this work will be true north and the horizontal plane. A summary of conventional methods for measuring

orientations of planar features is given in Hoek & Bray 1974. Orientations may be obtained from stereoscopic examination of aerial or ground based photographs and computer enhancement of video or still photography (Franklin and Dusseault 1989, Peaker 1990). The experience of this author is primarily with manual mapping using a variety of magnetic compasses or a carpenter's rule (clinorule).

A pocket transit such as the *Brunton* compass is well suited for measurements of lineations. It is composed of a magnetic compass with articulated sighting arms for improved accuracy. It also has a number of bubble levels and a clinometer (dip indicator) with vernier precision. This device is also well adapted for the measurement of plane orientations on a large scale since its operation is very similar to the workings of a complete surveying transit. Measurements of strike can be made by sighting along a horizontal line through the plane being measured. Dip measurements can be made with the clinometer.

When a large number of planar measurements is required, a *Clar* type compass, as described in Hoek and Bray 1974 , is more convenient. It possesses a folding planar back with an angular measure on the hinge. Placing this back against the plane being measured and levelling the compass allows measurement of dip and dip direction in one step instead of the two required with the Brunton or Silva type compasses.

When surveying in magnetic environments, compasses will not give correct azimuth readings. In this case a device called a *clinorule* should be employed. This device is composed of two straight rulers which are joined by a hinge centred on the pivot

point of a protractor or angular measure. One of the ruler units should also have a bubble level. A surveyed reference line of known orientation is marked with a tape or string. Relative strike is measured from this line and compensated later. Dip measures are recorded using the clinorule as a clinometer. It is important to measure dip in a consistent direction such as positive dip in the direction of the recorded scanline trend.

The amount of accuracy and precision inherent in each measurement should be determined by the importance of the individual measure. For example when tracing a fault over the ground surface for the purpose of predicting its position at depth, a very precise and accurate measure with a Brunton type compass is in order. When mapping several hundred joint planes in a mine drift network for statistical determination of dominant trends, quick and numerous measurements, possibly at the expense of accuracy, are more appropriate and a Clar type compass should be used. In general however, selection of the measurement tool may be simply a matter of personal preference.

2.4.1   Magnetic Declination

It is important, when using a magnetic compass for determination of trend, strike, or dip direction (ie. azimuth or bearing measurements), to be aware of *magnetic declination* and its significance. Since magnetic north and true north are not always coincident, a correction must be made to all compass measurements. The convention used in this work is as follows. The magnetic declination can be calculated by subtracting the apparent azimuth (with respect to magnetic north) from the true

azimuth. From this definition, west magnetic declination is positive and is added to all compass readings while east magnetic declination is negative.

2.4.3   Notation for Orientation Measurements

There are numerous conventions for the numerical recording of orientation data. One source of variation is the use of either bearing or azimuth notation for records of horizontal angles such as trend, strike and dip direction. Traditional bearing notation utilizes a combination of reference compass points and numerical values to express relative orientation, while azimuth is usually expressed as a single numerical value (from 0 to 360) representing the clockwise angle from true north. For example, the bearing measure of S40W (read south 40 degrees west) is equivalent to the azimuth measure 220. Similarly the bearing NNW (read north-northwest) is equal to the azimuth 337.5 (halfway between north and northwest compass points). When the user is accustomed to bearing measure, the notation is very effective in facilitating visualization of the oriented features. Azimuth measure, however, is less susceptible to misinterpretation by the unacquainted and is less cumbersome when processing large amounts of orientation data or utilizing analytical methods or computer programs. Azimuth notation will be used throughout this work.

The vertical angles of plunge or dip are usually expressed as a single numerical value between 0 and 90 (angle with respect to the horizontal). There are some

exceptions such as the vertical angle in borehole orientation. This is typically measured from the zenith and ranges from 0 to 180.

The azimuth measure is usually expressed as a three digit integer with leading zeros if necessary (if the azimuth is less than 100). Likewise the vertical angle is recorded as a two digit integer with leading zeros for values less than 10. This notation distinguishes between horizontal and vertical angles in orientation pairs (ie use 073/45 instead of 73/45). Note that the degree symbol (°) is left out in this notation. If a higher degree of precision is required, a division of the degree unit into minutes and seconds may be used as an alternative to decimal expression (ie. either 075° 15′ 36″ or 075.26°). Such precision is only used in very accurate surveying or specific geological analysis. Natural lineations and planar features possess too much spatial variability, however, to make measurement precision greater than $\pm 0.5°$ meaningful. Integer azimuth and integer vertical angle notation will be used throughout most of this work.

Variability in orientation expression arises from differences in the way planar features are measured. While linear features are expressed primarily using trend and plunge in geological work, planar features are commonly measured using dip and dip direction or one of two strike and dip conventions. Table 2.1 describes the different conventions.

ORIENTATION CONVENTIONS FOR LINEATIONS AND PLANES	BEARING NOTATION	AZIMUTH NOTATION
TREND/PLUNGE (Linear features)	S60E/35 (eg. pole to a plane)	120/35
DIP/DIP DIRECTION In this work dip will proceed dip direction in all planar measures to avoid confusion with strike and dip notation. This is, however, only the convention of this author. Other works may use other conventions.	55/N60W	55/300
STRIKE/DIP -generic- In this notation, a plane can have one of two strike measures, independent if the dip orientation. The nearest compass point to the dip direction is therefore appended to the dip to prevent ambiguity.	N30E/55NW -or- S30W/55NW	030/55NW -or- 210/55NW
STRIKE/DIP -right hand rule- The handedness indicated can be interpreted as follows. The hand indicated is held outstretched with the palm down, fingers extended and thumb held at 90 degrees to the fingers. If the fingers point down dip, the thumb indicates the direction of strike. Alternatively, if a compass is held in the palm-up hand with the fingers pointing in the direction of strike, the thumb will point in the direction of dip.	S30W/55	210/55
STRIKE/DIP -left hand rule-	N30W/55	030/55

Table 2.1. In this work, the azimuth conventions of trend/plunge, dip/dip direction, and right handed strike/dip will be used for lineations and planes. Other measurements such as interplane angle, and apparent dip will be expressed as simple degree measures.

3.0   SPHERICAL PROJECTION

3.1   INTRODUCTION

Direction cosines and angular relationships in plan and section both provide effective means for visualization of single lineations and planes in space. Vector analysis using the cosine approach permits more complex analyses of interplane relationships when two or more planes or lines are involved. When many planes are involved, however, or when very arbitrary relationships need to be determined, even vector algebra proves inadequate, particularly when one considers this method's lack of visualization appeal.

Traditional graphical solutions prove useful for resolving certain orientation relationships. Consider the following example solution for determination of a line and angle of intersection between two planes:
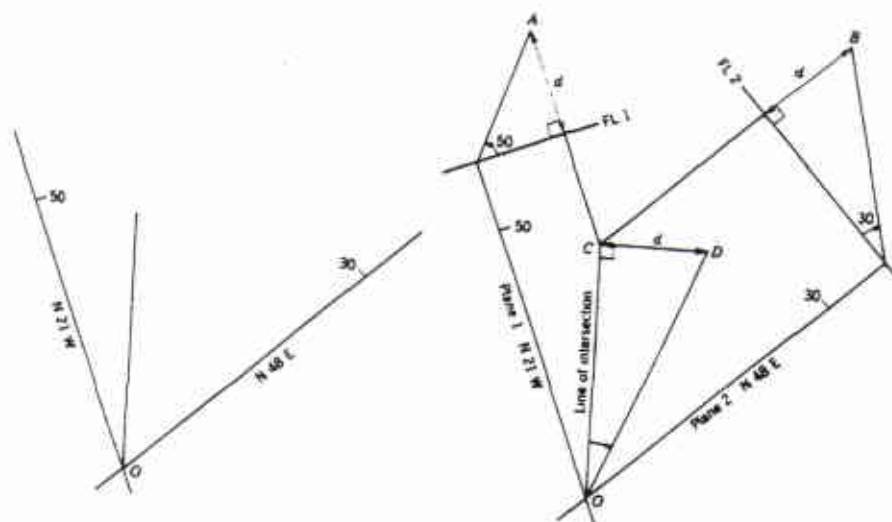
Figure 3.1:   Graphical Determination of Line of Intersection for Two
Planes (after Ragan 1973)

Compare this solution to equations 2.3 and 2.4 using direction cosines. For more complex and arbitrary problems, such graphical solutions are more versatile than analytical methods but can prove to be prohibitively cumbersome. A more adequate two dimensional graphical tool is required for solving three dimensional relationships.

Such a tool was developed in the second century B.C. and revived by modern crystallographers for the study of crystal morphology and optics (Phillips 1971). The method of spherical projection is now a fundamental tool of geoscientists and engineers, who use it for statistical reduction of orientation trends (Priest 1985, Hoek & Bray 1974, Ragan 1973, Zanbak 1977), kinematic and stability analysis for blocky ground (Priest 1980, Priest 1985, McMahon 1971), solution of arbitrary geological relationships (Ragan 1973, Goodman 1976) and studies of in situ stress fields and seismic behaviour (Park 1983, Markland 1974).
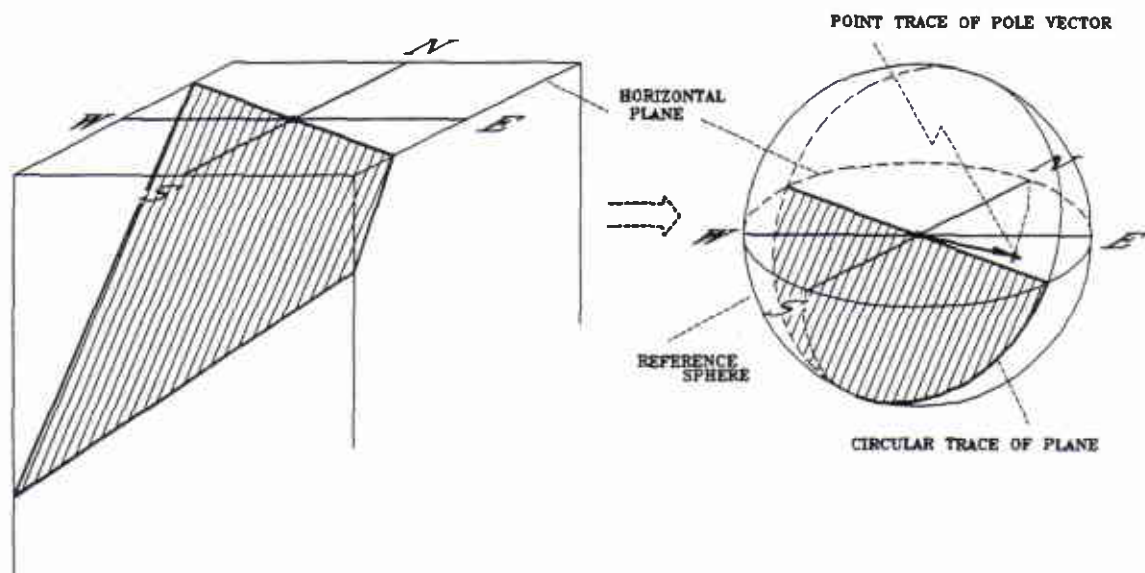
Figure 3.2: Spherical traces of planes and normals (after Phillips 1971)

3.2   PROJECTION METHODS

The general principles of the method are based on the concept of a sphere with a centre point through which all lineations and planes are assumed to pass (remember that it is the orientations which are to be studied and not the spatial relationships). This is called the *reference sphere*. Vectors or linear orientations can then be represented by their points of intersection with the surface of the sphere. Similarly, planes can be represented by the circular traces created as they intersect the surface of the sphere. These traces are called *great circles*. One of two procedures may then be used to transform these points and traces into two dimensional projections.

3.2.1   Equal Angle Projection

This method of projection also known as the *Wulff* projection begins with the arbitrary division of the reference sphere into two hemispheres. Since every vector and plane has equivalent and diametrically opposite traces in each half of a divided sphere, only one half is required to express all orientation information. This work will follow common geomechanical convention and utilize the lower hemisphere. The same general principles apply to any arbitrary hemisphere.

An imaginary ray emanating from the zenith (or its relative equivalent if the lower hemisphere is not being used) traces the points and great circles of intersection on the lower hemisphere. The corresponding points and curves, traced on the horizontal diameter plane as it intersects this ray, form the *equal angle* projection or stereonet.

ZENITH

PLANE

REFERENCE
SPHERE

EQUATORIAL
PLANE

POLE VECTOR

PROJECTION

POLE

GREAT CIRCLE
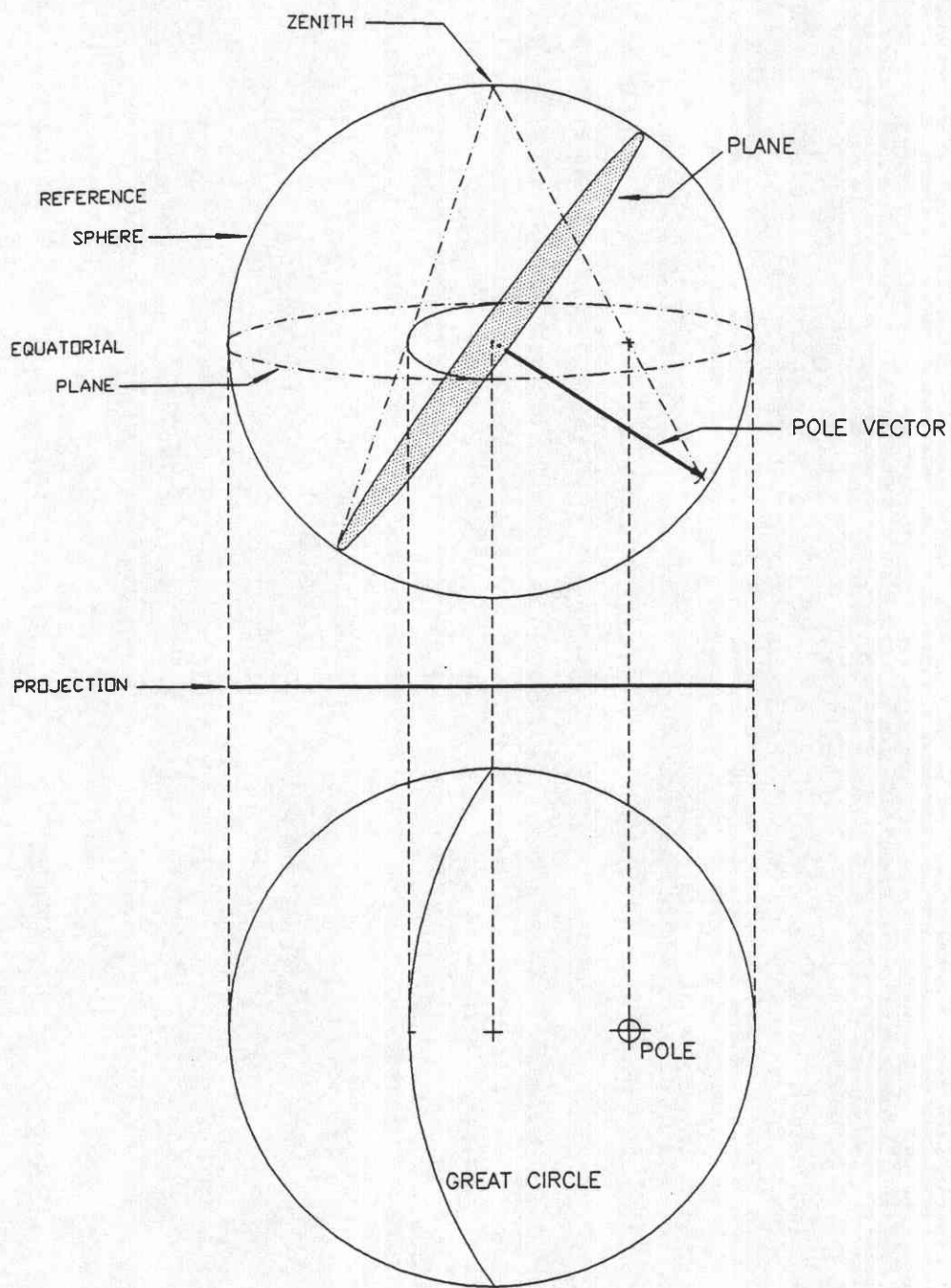
Figure 3.3: Generation of Equal Angle Projections

This process can be expressed mathematically by the following relationships:

Figure 3.4: Equal angle relationships (after Priest 1985)
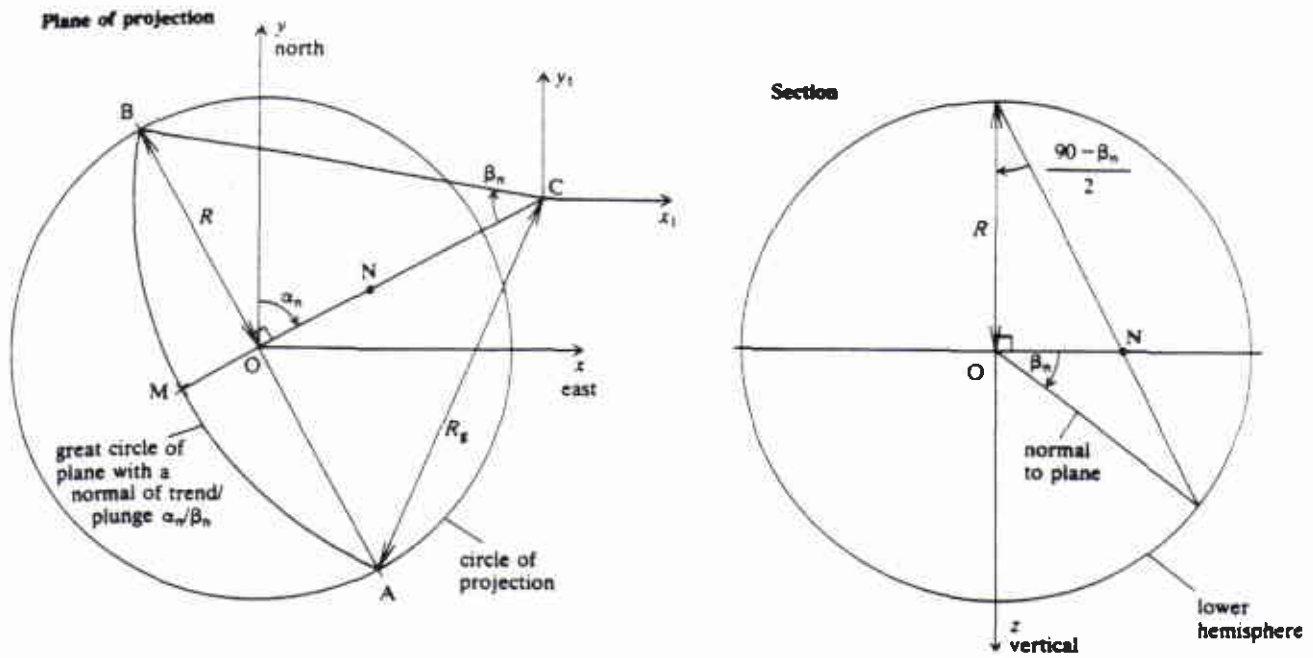
Point	x	y
N	$R \sin \alpha_n \tan\left(45 - \dfrac{\beta_n}{2}\right)$	$R \cos \alpha_n \tan\left(45 - \dfrac{\beta_n}{2}\right)$
M	$-R \sin \alpha_n \tan\left(\dfrac{\beta_n}{2}\right)$	$-R \cos \alpha_n \tan\left(\dfrac{\beta_n}{2}\right)$
A	$R \cos \alpha_n$	$-R \sin \alpha_n$
B	$-R \cos \alpha_n$	$R \sin \alpha_n$
C	$R \sin \alpha_n \tan(90 - \beta_n)$	$R \cos \alpha_n \tan(90 - \beta_n)$

$$R_g = R/\sin \beta_n$$

This term *equal angle* is derived from the preservation of angular relationships which this method ensures. This property is reflected in the fact that a *small circle*, or the trace of a cone on the surface of the reference sphere, is represented by an undistorted circle on the projection. The relative size of the projected circle with respect to is associated cone trace, however, will very depending on the proximity of the circle to the centre of the projection (ie. the angle of the cone axis with respect to the nadir of the sphere). As the small circle's distance from the centre of the stereonet increases, the larger the projected circle becomes with respect to the real cone trace on the reference sphere. It is important to note that the centre of the cone trace on the reference sphere will not plot as the centre of the associated projected small circle unless the cone is centred about the vertical axis. The construction of a projected small circle is described in Priest 1985, along with proof of angular preservation. It should be noted that this specific method was originally called *stereographic projection*. This term has come to describe any form of spherical projection and will be so used throughout the rest of this work.

3.2.2   Equal Area Projection

In this method, pole points, great circles and small circle traces in the lower hemisphere are rotated through a circular arc, centred on the nadir of the sphere, to the horizontal plane tangent to the base of the sphere. The resultant projection is then normalized to the radius of the reference sphere to form the *equal area* stereonet.
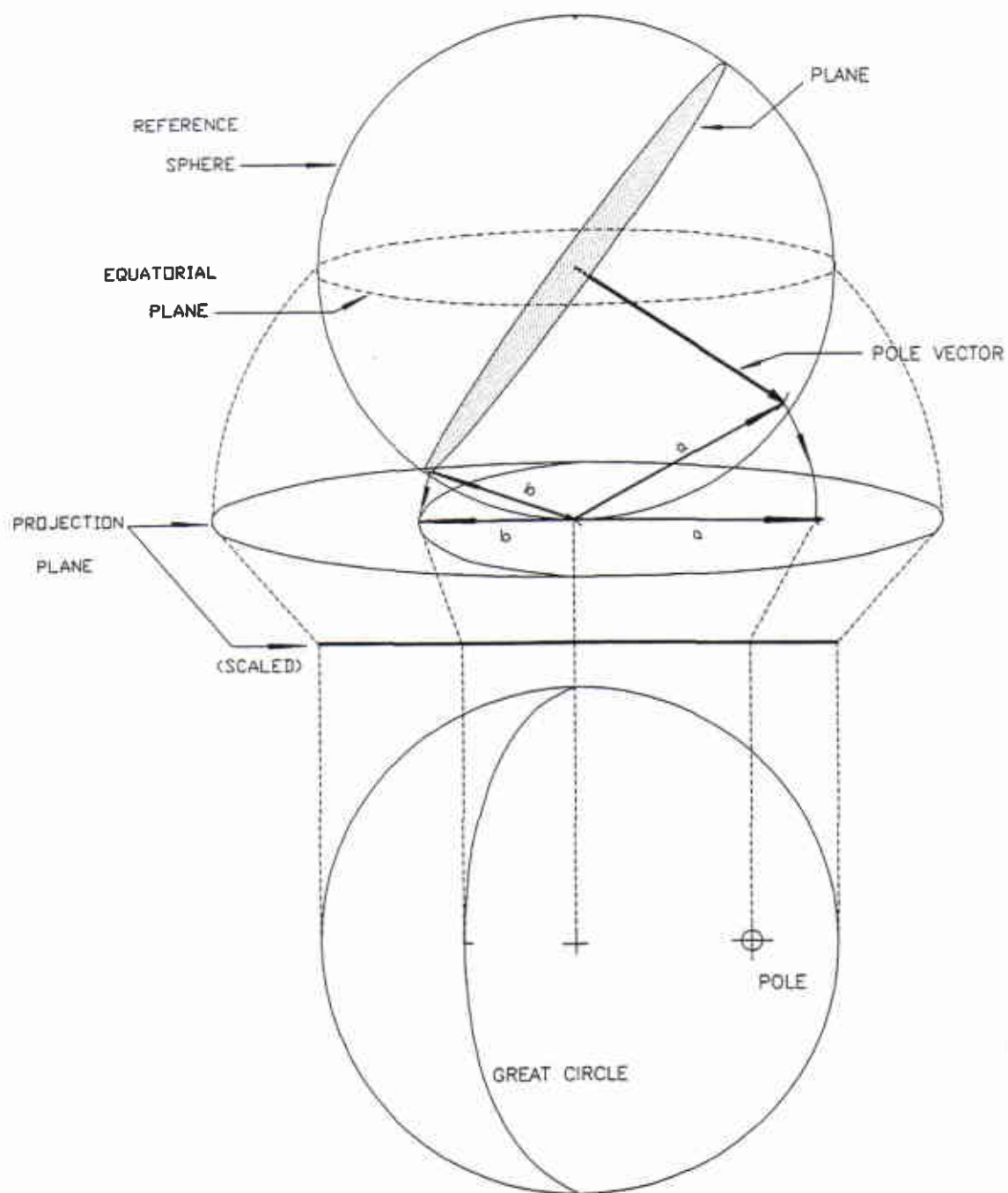
Figure 3.5: The equal area projection

The equal area or *Schmidt* projection follows the following transformation relationships:

azimuth = trend

$$r = R \cdot (\sqrt{2}) \cdot \cos(45 + plunge/2) \qquad\qquad (eq. \ 3.2)$$

where R is the radius of the stereonet

r is the radial distance of the projected point

$\sqrt{2}$ is a scaling factor

The equations for the curve of a projected great circle are more complex in this method. The great circle does not plot as a circular arc in this projection unlike the equal angle procedure. Likewise, cone traces do not plot as small circles except in the case of cones centred on a vertical axis. Both features plot as higher order curves which will not be derived here. The main advantage of this projection method is that it does not suffer from the areal distortion of the equal angle projection. This means for example, that an area such as that enclosed by a circle of constant radius on the projection, represents the same amount of area on the reference sphere regardless of its position. The circle will not however represent a geometrically similar circle on the sphere unless it is positioned at the centre of the projection. In other words, areal relationships are preserved in this method while geometrical relationships are distorted; the opposite is true of the equal angle projection. Attewell and Farmer (1976) give an analytical proof of the areal preservation inherent in the equal area stereonet.

3.2.3   Reference Grids

It is common to plot poles and planes on projections using a stereonet grid overlay. Two main types are used in this case. The first is the polar net. This grid is composed of radial lines representing azimuth increments and a set or concentric circles representing increments of plunge or dip. The second is the equatorial net. This net includes a set of great circles of equal azimuth (ie. strike) and incremented dips. A set of small circles centred about the strike line of the great circles represents increments of apparent dip or pitch in each of the great circle planes. The terms polar and equatorial can be misleading. Both nets are generally used to represent the same hemisphere (the lower hemisphere in this work) and the real equator of the reference sphere is represented by the perimeter of the projected stereonet. The polar net is more convenient for plotting of poles and other lineations, while the equatorial net is useful for the plotting and manipulation of planes. Figure 3.6 shows the graphical origins of the two overlay types.
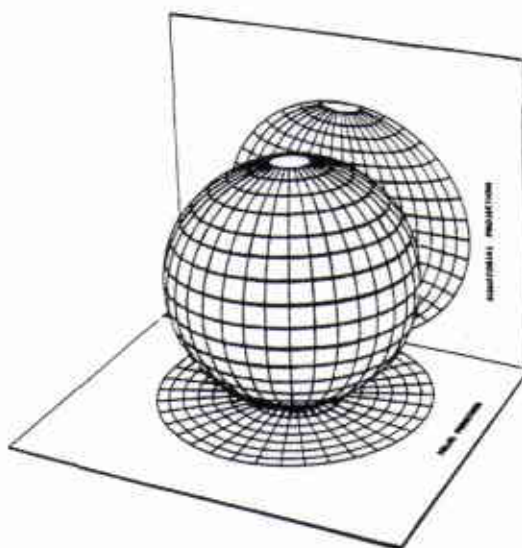
Figure 3.6: Origin of reference stereonets (after Hoek and Bray 1974)

Hoek & Bray (1974) as well as Priest (1985) contain high quality full size reference grids which can be reproduced and used for accurate manual stereonet manipulation. They are shown here reduced for comparison.
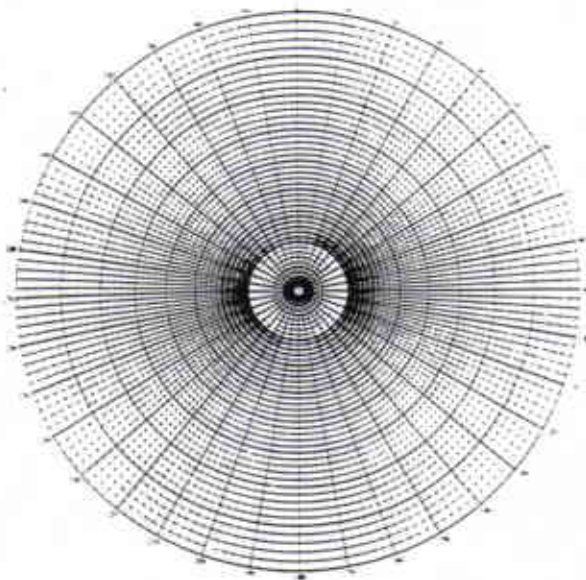
Polar equal-angle net.   Polar equal-area net.
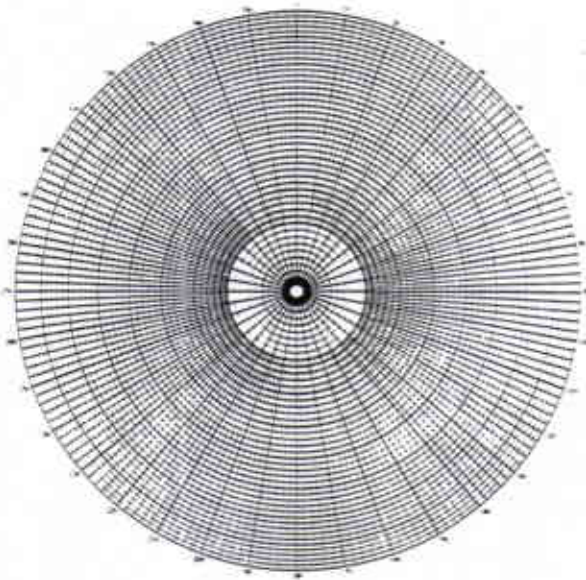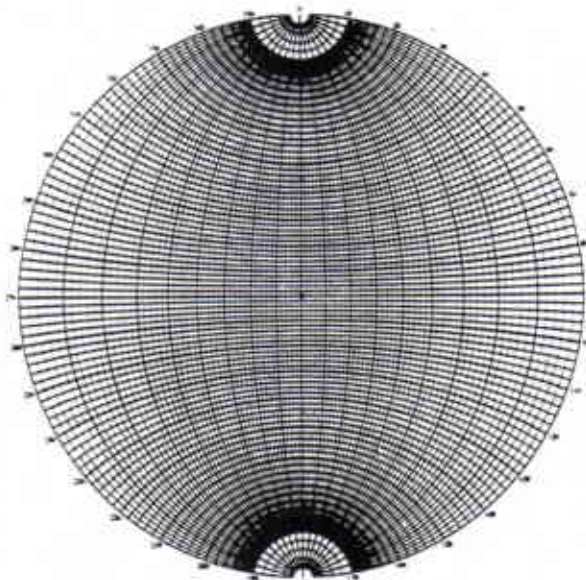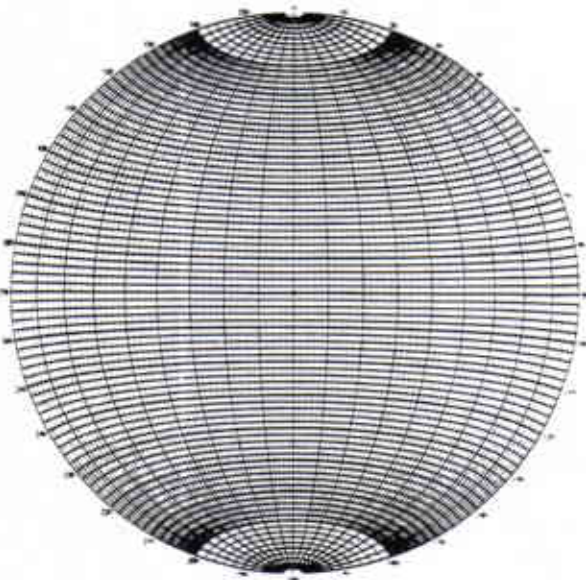
Equatorial equal-angle net.   Equatorial equal-area net.

Figure 3.7: Reference stereonets for manual calculations (after Priest 1985)

3.3   USES OF STEREOGRAPHIC PROJECTION

Stereographic projection can be used to facilitate analysis of any physical problem where orientation is an important factor.

Principle in-situ stresses may be presented as points (vectors) on a stereonet. Where large amounts of measurements have been taken and measurement variability makes analysis difficult, the stereonet may be used to visually resolve principle stress directions (Markland 1974).

Stereographic projection can be used in a similar fashion to resolve orientation trends in the fields of structural geology (Ragan 1973, Hoek & Bray 1974, Zanbak 1977, Priest 1985) or any other field where large amounts of highly variable measurements have been made and where the analytical resolution of multimodal orientation trends becomes prohibitive. The stereonet makes use of the human brain's facility for pattern recognition which is difficult to duplicate even through the use of computer technology. Relationships which can be resolved from the stereonet plots of multiple data units include maximum concentrations of poles or mean poles for clusters of orientations as well as the fold axis determined by the corresponding plane of best fit through joint or bedding poles on the arms of the fold. Contouring methods which aid in the reduction of orientation trends from large samples of highly variable data will be discussed in the next section.

The stereonet can be used in analysis of seismic data. For example, the orientations of the primary slip planes responsible for a seismic event can be resolved by

plotting vector orientations representing the orientation of the epicentre with respect to the recording locations and using symbols to indicate the compressive or expansive nature of the first wave arrival at each location. A pair of perpendicular great circles are then manipulated to separate the regions dominated by either so-called 'push' or 'pull' vectors. These planes then represent the surface of slip and the plane normal to the direction of slip (Park 1983).

Analysis of a number of geological phenomena such as oriented elongation of conglomerate pebbles, oriented clast fabrics in glacial tills, and acicular crystal fabrics in igneous and metamorphic rocks can be carried out using stereographic projection for determination of previous stress and flow histories (Park 1983, Ragan 1973).

Goodman (1976) gives a construction for the direction of greatest compressive strength of a jointed rock mass. A number of poles representing normals to joint planes are plotted on a stereonet. Small circles with cone angles representing the friction angle on the respective joint planes are drawn, centred on the associated pole orientations. The centroid of the region on the projection which is common to all small circles, if such a region exists, represents the direction of maximum compressive strength since full intact strength may be mobilised in this direction without inducing joint slip.

Relationships between distinct planes and lineations which can be analytically complex are graphically simple using the stereonet. The following is an analysis of the relationship between two planes:
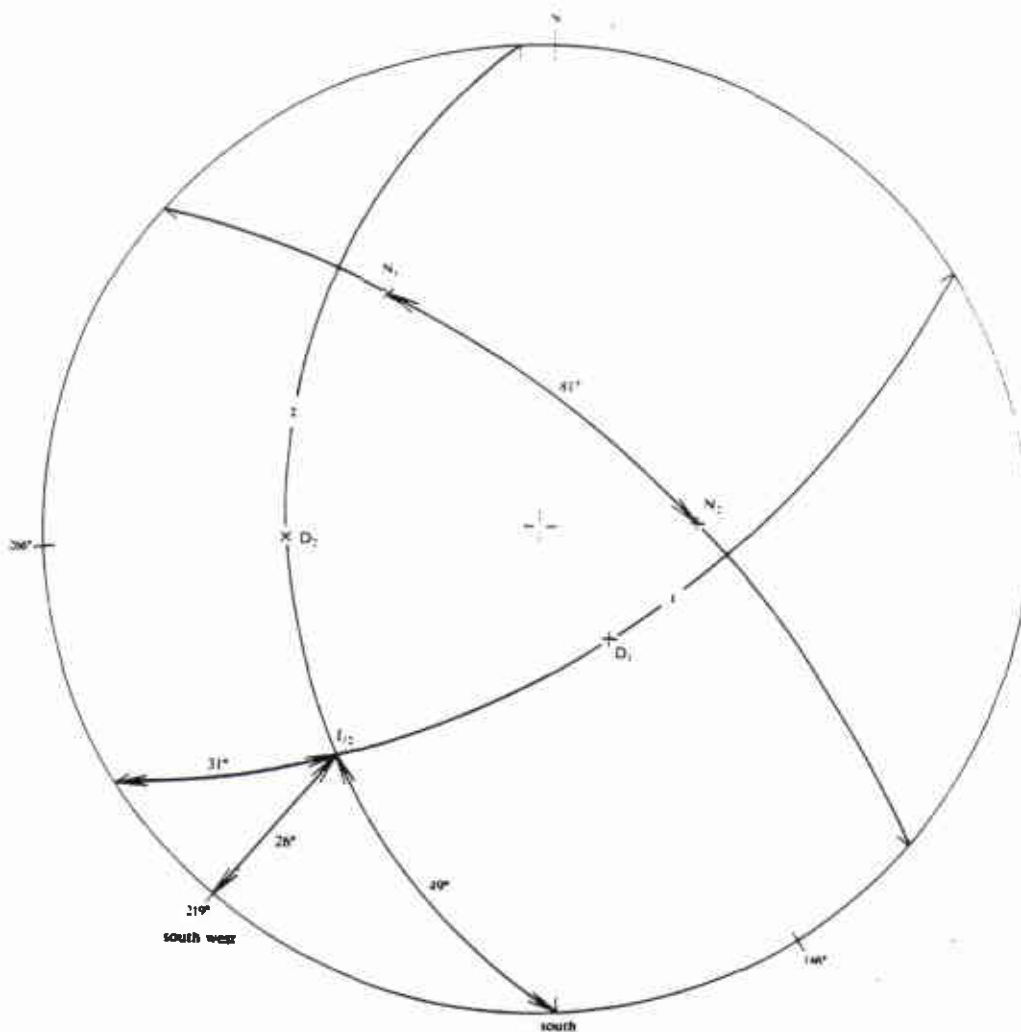
Figure 3.8: Calculation of angle and line of intersection using stereonets (after Priest 1985)

Compare this solution to equations 2.1 - 2.4 and the graphical solution in figure 3.1. The opposite calculation (that is, determination of a planes true orientation from apparent dip or intersection pitch in another plane) is possible with no increase in complexity (Priest 1985, Phillips 1971). The same cannot be said for the analytical solution.

Another example of the flexibility of stereographic projection is illustrated in the following example. A marker horizon such as a consolidated volcanic ash layer is found in two non-parallel and non-oriented drill cores. The true orientation of this bed can easily be derived using the procedures outlined in Ragan 1973 and Priest 1985. These references, as well as, Phillips 1971, Goodman 1976 and Hoek & Bray 1974, all contain many other examples of graphical solutions using stereonets.

One application of stereographic projection of particular interest to rock mechanics and excavation engineering is the method's suitability to multiple plane wedge stability analysis for slope faces or underground excavations (Priest 1980 ,Hoek & Brown 1980, Lucas 1980, McMahon 1971).

The general principle of kinematic assessment of rock wedges above an underground excavation is illustrated in figure 3.9.

The great circles to a group of planes can be plotted on a lower hemisphere projection as shown. If the wedge indicated by the shaded region between the planes encloses the centre of the net, the wedge is free to fall without sliding under the influence of gravity. If the wedge does not contain the centre but possesses a side or edge (vertex of the projected wedge) which falls inside a small circle whose radius represents the compliment of the friction angle, the wedge will fail by sliding along the respective edge or side. If none of the above cases are true, the wedge will be stable (under gravity loading).
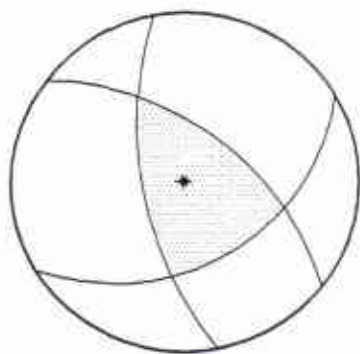
Failure by gravity fall
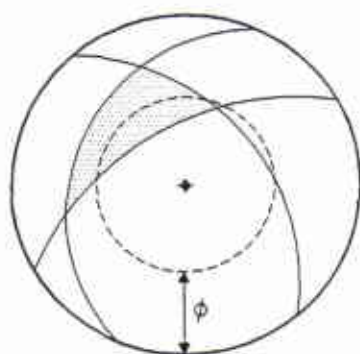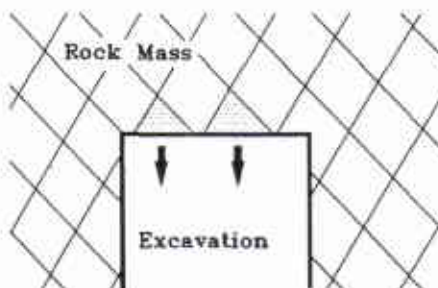
Failure by gravity sliding
(ϕ = FRICTION ANGLE)
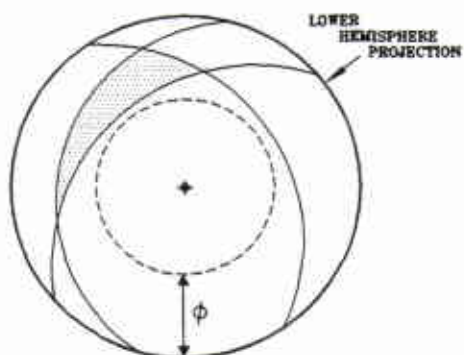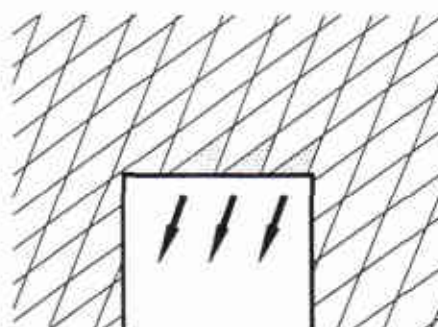
Stable Wedge Conditions
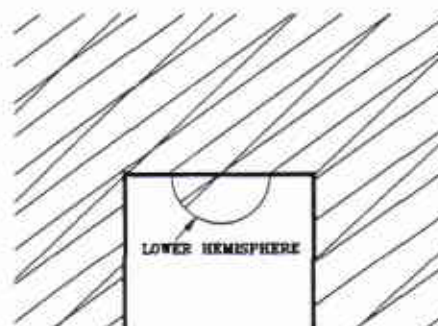
Figure 3.9: Kinematic and stability assessment of rock wedges (after Hoek and Brown 1980)

Similar methods may be used for analysis of sliding and toppling potential in jointed rock slopes (Hoek and Bray 1974, McMahon 1971, Lucas 1980) and on non-horizontal faces of surface and underground excavations. This latter technique utilizes inclined hemisphere projection (the projection uses a hemisphere with a non-horizontal equator) and is discussed in detail in Priest 1980 & Priest 1983.

This construction can be used in conjunction with standard graphical techniques to recreate actual block geometry and properties such as volume and weight (Hoek and Brown 1980).

The combination of graphical stereonets and vector algebra for analysis of stability involving non-vertical loads (eg. cable forces) is discussed in Priest 1985 as well. Examples of problems with more than three planes and complex loadings are also solved in Priest 1980.

3.4 REDUCTION AND ANALYSIS OF MULTIPLE ORIENTATION MEASUREMENTS

3.4.1 Introduction

The previous section dealt with means of analyzing relationships between distinct linear and planar features. On their own, these methods are useful on a very local scale if the features involved are small, or on a regional scale in the case of well defined fault or intrusion features for example. In many cases, however, reliable analysis can rarely be performed using a few isolated measurements due to the variability of in-situ properties and structure found in most natural systems. In the case of in-situ stress determination, many measurements may be required before a reliable estimate of magnitudes and orientation of regional principle stresses can be made. Similarly, the determination of regional or even local structural trends in rock masses may require hundreds of measurements to be statistically acceptable.

Regional orientation trends can be estimated:

- by visual determination on site

- analytically using a number of statistical vector methods

- by visual analysis of stereonet pole plots

- by visual analysis of contoured stereonets

- using a combination of the above techniques

In the case of structural analysis of rock masses, the first approach can be utilised in situations where well correlated joint sets are present and the working space allows for several viewing points in order to objectively assess the dominant orientations. This method must inevitably involve a great deal of subjective judgement. The orientation of an tunnel or mining drift for example will have a profound effect on the frequency of outcrop and the visual dominance of a particular set of similarly oriented planes. This makes objective visual assessment of primary orientation trends difficult and often unreliable.

3.4.2   Analytical Methods

A number of analytical means have been developed for the statistical reduction of orientation data. The methods described in the literature (CANMET 1977, Priest 1985, Markland 1974, Fisher 1953) deal primarily with orientation data which is monomodal or clustered about a single mean direction. Some deal with several mutually orthogonal orientations. In general, no method was found in the literature which seemed capable of resolving multiple independent orientation sets from a single database. Nevertheless, several of these methods prove effective in analyzing single orientation clusters and will be described here.

The simplest computation which can be performed on a cluster is that of mean orientation by vector addition (Priest 1985, Fisher 1953, Golder Ass. 1979). This method involves the conversion of angular measurements to direction cosines

(equation 2.1) and the summation of the respective components ($\sum\lambda_{north}$, $\sum\lambda_{east}$, $\sum\lambda_{down}$) to form a resultant vector. Each component of this resultant is then normalized (divided by the total length of the vector) yielding the direction cosines of the mean vector.

When using the lower hemisphere conventions for orientation measurement (plunge and dip) there is an important point to remember. When the cluster of vectors represents a mean orientation which is subhorizontal, an extra step must be taken before calculating the mean as described above. If, for example, part of the orientation data ranges between trends of 120 and 160 and ranges between plunges of 0 and 20, while the rest of the data ranges in trend from 300 to 340 and in plunge from 0 to 15, one of these two groups of vectors must be reversed (multiplied by -1) before performing a summation of cosines. If this is not done, the mean vector will be directed downwards, midway between the two clusters. To better visualize this problem, imagine a group of subvertical planes striking in the same general direction - north, for example. Some of the planes dip steeply to the east, while others dips steeply to the west. They all, however, represent the same set of discontinuities. If the downward normals are used in the mean vector calculation described here with no conversion, the mean normal will point downwards and the mean plane will be subhorizontal, an obviously incorrect solution. The direction cosines corresponding to the normals of either the east or the west dipping planes must be multiplied by -1 before summation with the rest of the group in order to achieve the correct result. This limitation, which is not mentioned in any of the references listed, makes this method difficult to implement, even for monomodal distributions, in a non-subjective, "black box" analysis.

An alternative and more flexible approach is outlined by Markland 1974. This method employs a procedure called eigenanalysis (Speigel 1974, Watson 1966). Eigenvectors, $[X]_{1xN}$, and their associated eigenvalues , μ , for a general n x n matrix [M] are determined by satisfying the equation:

$$[M]_{NxN} [X]_{1xN} = \mu[X]_{1xN} \qquad \text{(eq. 3.3a)}$$

the three eigenvalues, λ, are therefore the roots of the cubic equation derived from:

$$\det(\mu[I] - [M]) = 0 \qquad \text{(eq. 3.3b)}$$

where *det* is the determinant and [I] is the identity matrix. The eigenvector for each associated eigenvalue can be back calculated from equation 3.3a.

For the analysis of poles clustered about a particular axis, Markland assembles the matrix M:

$$[M] = \begin{vmatrix} \sum l_i^2 & \sum l_i m_i & \sum l_i n_i \\ \sum m_i l_i & \sum m_i^2 & \sum m_i n_i \\ \sum n_i l_i & \sum n_i m_i & \sum n_i^2 \end{vmatrix} \qquad \text{(eq. 3.4)}$$

where l,m,n are the direction cosines of each sample orientation.

The matrix M has three possible eigenvalues and associated eigenvectors. Markland describes the significance of the three eigenvectors in the following way. If each measured pole is assumed to have a particle of unit weight attached to its axis where it intersects the unit reference sphere, the eigenvectors represent the axes

which provide the maximum, intermediate and minimum moments of inertia when the sphere is spun about them. The moment of inertia for a given pole, is calculated by multiplying the mass of the head (which can be one or some representative value for stress, force, etc.) by the square of the distance between the unit pole vectors head and the axis of rotation. The total moment of inertia for the whole data set would be the sum of these values. Markland's analogy is incorrect in that it is implied that the maximum eigenvalue corresponds to the axis of maximum moment of inertia in this system. The opposite is in fact the case.

The eigenvector associated with the maximum eigenvalue, corresponds to the axis of minimum moment of inertia and therefore, represents the mean vector for the cluster. This method should yield the same mean orientation as the vector addition method described earlier. The advantage of this method is that there is no need to convert any vectors to their negative equivalents for subhorizontal data clusters. The moment of inertia of a pole vector with respect to an arbitrary axis is the same as the value for the negative pole vector.

This method also allows for the calculation of a best fit plane through vectors which have a girdle distribution such as the normals to bedding or joints on a fold. The eigenvector associated with the minimum eigenvalue (and the maximum moment of inertia) for such a data set represents the normal to the best fit plane. In the case of a fold, this vector represents the fold axis.

For complete analysis of a pole cluster, the maximum eigenvalue is associated with the mean vector, while the minimum and intermediate eigenvalues correspond to

eigenvectors normal to the planes representing the maximum and minimum axes of the elliptical cone defining an asymmetrical pole concentration. The relative magnitudes of the eigenvalues reveal information about the degree of clustering of the orientation data. Three identical eigenvalues indicate a uniform distribution with no clustering. One small value and two fairly similar large ones indicate pole data distributed about a plane (normals about a fold). One large value and two much smaller ones indicates clustering about a mean vector. In this case equivalence of the two smaller values indicates a symmetrical cluster about the mean while a difference between the two smaller values gives a measure of asymmetry of the distribution.

Once these axes have been determined, then a number of methods may be used to describe the distribution in detail. The most common statistical analysis procedure is based on a radially symmetrical *Fisher* distribution, an adaptation of two dimensional normal distribution to data on the surface of a sphere (Fisher 1953, Priest 1985). Bivariate normal distributions can also be used when the data is asymmetrical (CANMET 1977, Zanbak 1977, McMahon 1971).

Markland discusses other uses for the eigenanalysis method such as the reduction of multiple *in-situ* stress measurements into mean principle stress directions and magnitudes. Although there are three orientations being solved for here, they are assumed to be mutually orthogonal. This method still suffers from the inability to solve for mean orientations in a system with multiple and independent orientation clusters.

It is clear then, that even if these analytical methods are to be used for the analysis of field data, another procedure must first be performed which can group orientation data into clusters of association (about a mean pole or best fit plane as the case may be) and, as will become apparent, rank clusters in order of relative dominance.

3.4.3 The Use of Stereographic Projection in Statistical Analysis of Orientation Data

The use of stereographic projection in the statistical reduction of orientation data relies on the "...powerful human ability for pattern recognition and, therefore, ...has considerable practical advantages over methods based on vector procedures which are purely mathematical and difficult to envisage." (McMahon 1971)

Such analysis begins with the plotting of vectors on a stereonet. For analysis of planar orientations it is convenient to plot the normals rather than the planes themselves. Visual analysis of multiple planar measurements is far too cumbersome when the planes themselves are plotted (figure 3.10).

The poles or normals are used in preference to the maximum dip vectors for reasons of convention. There is another practical reason for doing so, however. Consider a series of similarly oriented subhorizontal planes. The maximum dip vectors will all plot as points near the perimeter of the net but will have widely varying trends between 0 and 360 degrees. This wide variation in azimuth makes visual analysis less effective. If the poles are plotted, however, the pole points will

be tightly clustered about the centre of the stereonet, making visual estimation of mean orientation simple and reasonably accurate. Conversely, consider a set of subvertical planes of varying strike or dip direction. Where the subhorizontal planes could be considered as related family in spite of a wide variation in dip direction, the same cannot be said of the subvertical planes, from a practical point of view. If dip vectors are plotted, however, the resultant clustering about the centre of the net gives the visual impression that such a family exists. The poles would be distributed about the perimeter of the net and would not cause such a confusion.
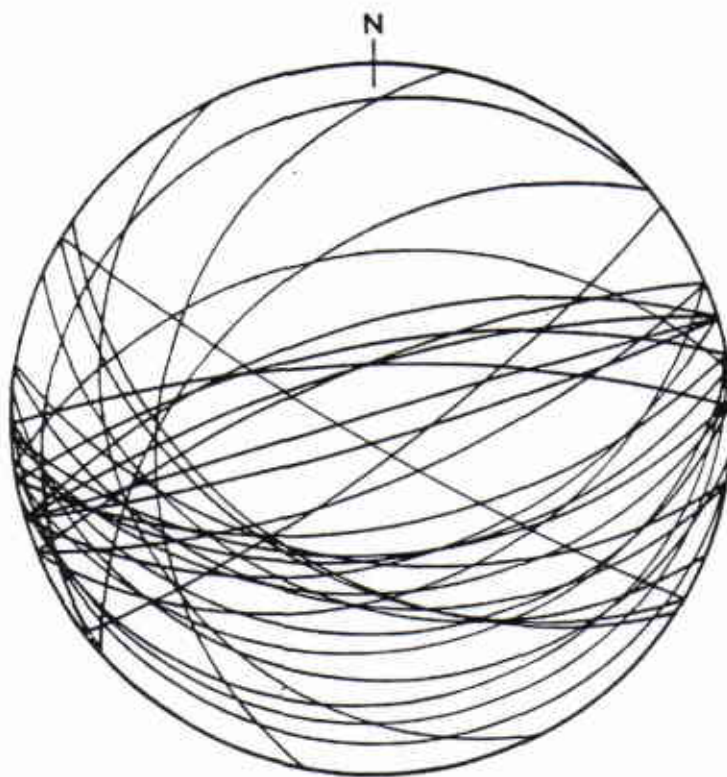
Figure 3.10: Stereographic projection of numerous planes (after Phillips 1971)

A plot of lineations or of normals to planes is termed, simply, a *pole plot*. Additional information may be combined with the plotting of pole orientations. Though the use of symbols or colours, information such as joint continuity, surface type, or, in the case of stress data, magnitudes of stress can be plotted at each pole point. This provides a visual comparison of attributes to supplement or assist in the determination of orientation clusters.

When a large number of data has been taken or when a number of closely aligned orientation measurements have been made, it may become difficult to assess dominant trends from the pole plot alone. Many of the pole points will overlap. A similar plot may be created, using symbols to represent the quantity of similar measurements represented by each pole point. This cleans up the pole plot and reveals multiple measurements otherwise concealed by overlapping pole points. This form of presentation is often referred to as a *scatter plot*.

From these two plots, varying degrees of success can be achieved in visually distinguishing dominant orientation trends.
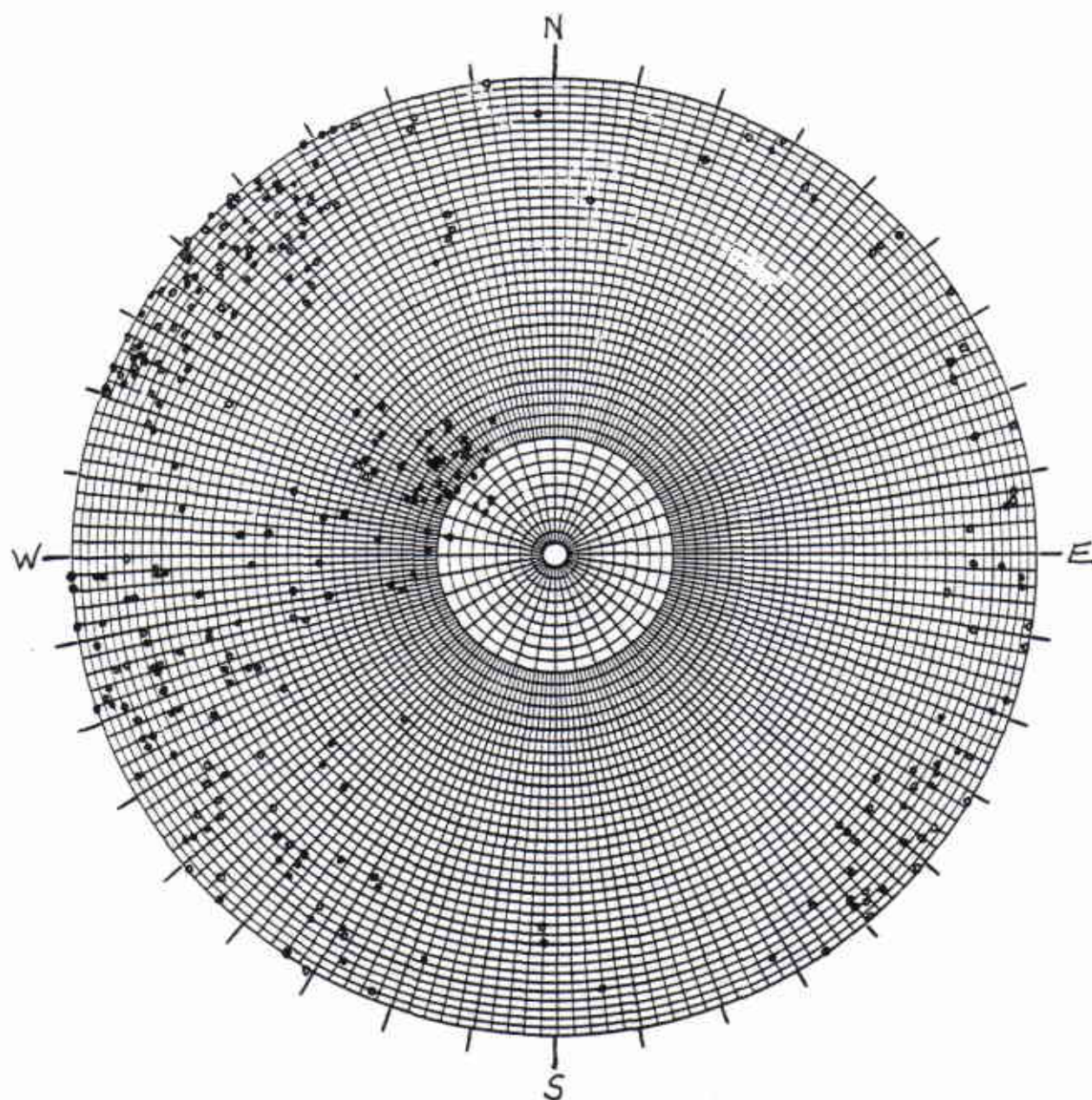
Figure 3.11: Manually generated plot of 304 poles on equal area stereonet

3.4.4: Density Contouring on the Stereonet

If concentrations of poles are well defined on the pole plot or scatter plot, no further processing need be carried out to separate the data into orientation sets and to estimate approximate mean or modal directions. It is often difficult to accurately define dominant pole concentrations from a pole plot if a large quantity of data has been collected or if more than three clusters are present. Such clusters become more clearly defined if the pole concentration is contoured over the stereonet.

The correct interpretation of such contours is as follows. The concentration indicated should represent the probability of pole occurrence within some specified angular distance of the orientation in question. That is to say, if any oriented feature is chosen at random from the data set (and implicitly therefore, from the total population in-situ), this chosen orientation has a probability of lying within a defined region about a reference point on the stereonet, as indicated by the contoured density value at that reference point.

When contouring on a stereonet, it has proven efficient to use a contouring region as defined above, equivalent to 1% of the area of the reference hemisphere (or 1% of the projection area). A number of manual contouring methods have been developed and are outlined in Phillips 1971, Priest 1985, Hoek & Bray 1974, Hoek & Brown 1980, Ragan 1973 and Denness 1972.

The classic method is called the Schmidt method and involves the use of the equal area projection and a movable counting circle. This circle has an area equivalent to 1% of the stereonet. The counting circle can be centred on an arbitrary point on a stereonet containing plotted poles. All of the poles which fall within it are totalled. This number becomes associated with the counting point and when divided by the total number of poles in the data set, represents the pole concentration at that point expressed as 'percentage of poles per 1% area'.

The counting points can be arbitrarily and subjectively determined. This method is called the floating circle counting method. The circle would be used to scan the net until a pole concentration corresponding to one of the predetermined contour intervals is found. 1% concentration intervals are convenient for manual contouring. The concentration is recorded at this point. The counting circle is then moved about the net, following a path which corresponds to this contour interval. The process is repeated throughout the net for different clusters and concentration intervals. This method is very difficult and tedious as a first step in contouring. It is more useful for refining a plot once crude contours have been generated using another method (Hoek and Bray 1974).

A more common method is the counting grid approach. A square grid is superimposed on the pole plot. The counting circle is then centred on each of the grid intersections and the respective concentrations noted. The grid spacing should be no more than half of the counting circle diameter to assure adequate overlap (Priest 1985). The resultant matrix of concentration values must then be contoured. This method is more efficient then the floating circle approach but has some

disadvantages. The grid point concentrations are usually fractional concentration values and contour lines must be subjectively drawn between them. Additionally, this method does not always capture maximum concentrations unless the central pole of a density peak falls on a grid point.

Both counting circle techniques require special attention when counting near the perimeter of the stereonet. Counting circles which extend past the perimeter of the net must partially reenter on the opposite side of the net. This is due to the fact that this procedure is a simulation of a spherical surface counting procedure. Poles near the perimeter of the net (equator of the sphere) have negative counterparts on the opposite side and therefore contribute to counting circle totals on either side of the stereonet.

This problem is overcome through the use of a twinned counting circle pair as shown in figure 3.12. The twin circles are kept at a fixed distance and pivot about the centre of the stereonet. When one circle extends past the perimeter of the net, the area loss outside the net is equivalent to the area of the opposite circle which falls inside the net. There is an loss of area in this case, equivalent to approximately 10 percent of the counting circle area (Attewell and Woodman, 1972) as shown in figure 3.13. In practice, however, this loss of area is not considered significant. The numbers of poles falling inside of both circle are summed and recorded at the counting circle centre which falls inside the net. This value is recorded at both centre points if they fall on the circle perimeter.

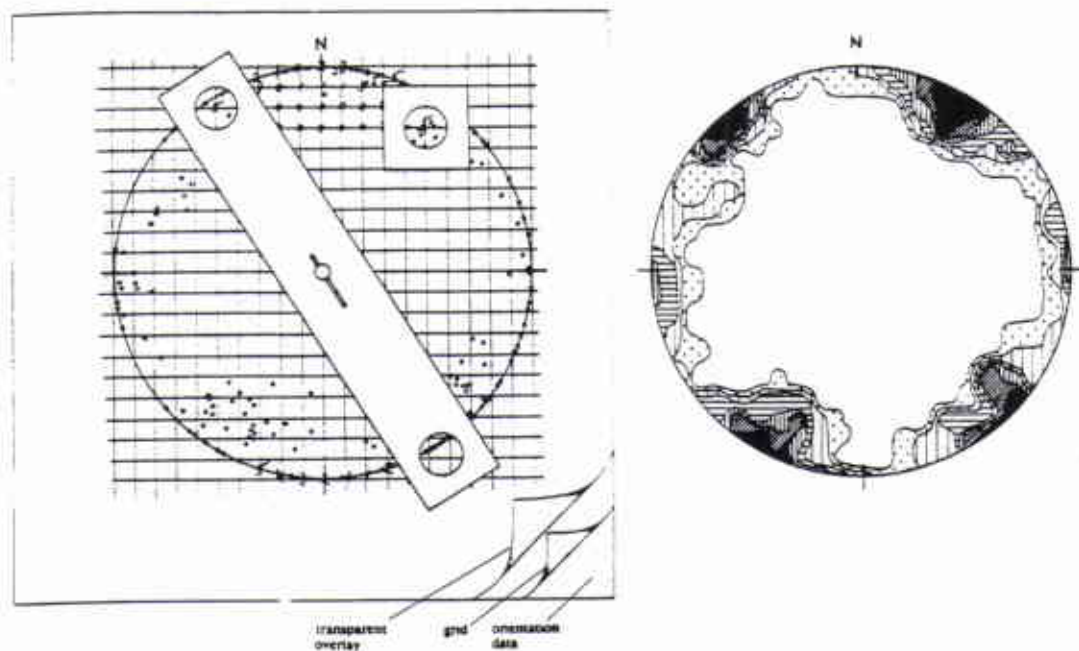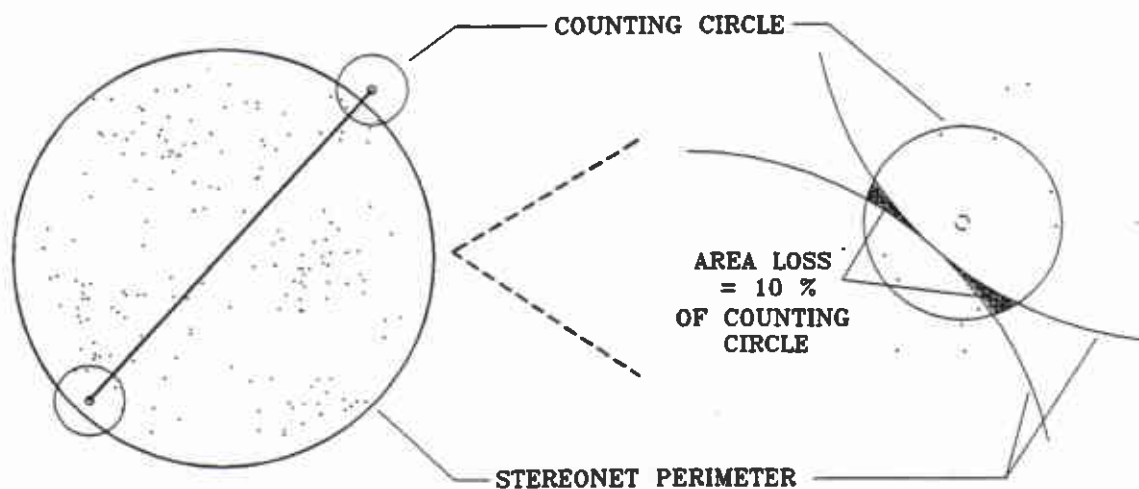**Figure 3.12:** Counting circle method with perimeter counting tool (after Phillips 1971)

Figure 3.13: Loss of counting area near perimeter of stereonet

The following contoured stereonet was generated using the counting grid and circle technique. The data is that shown in figure 3.11.
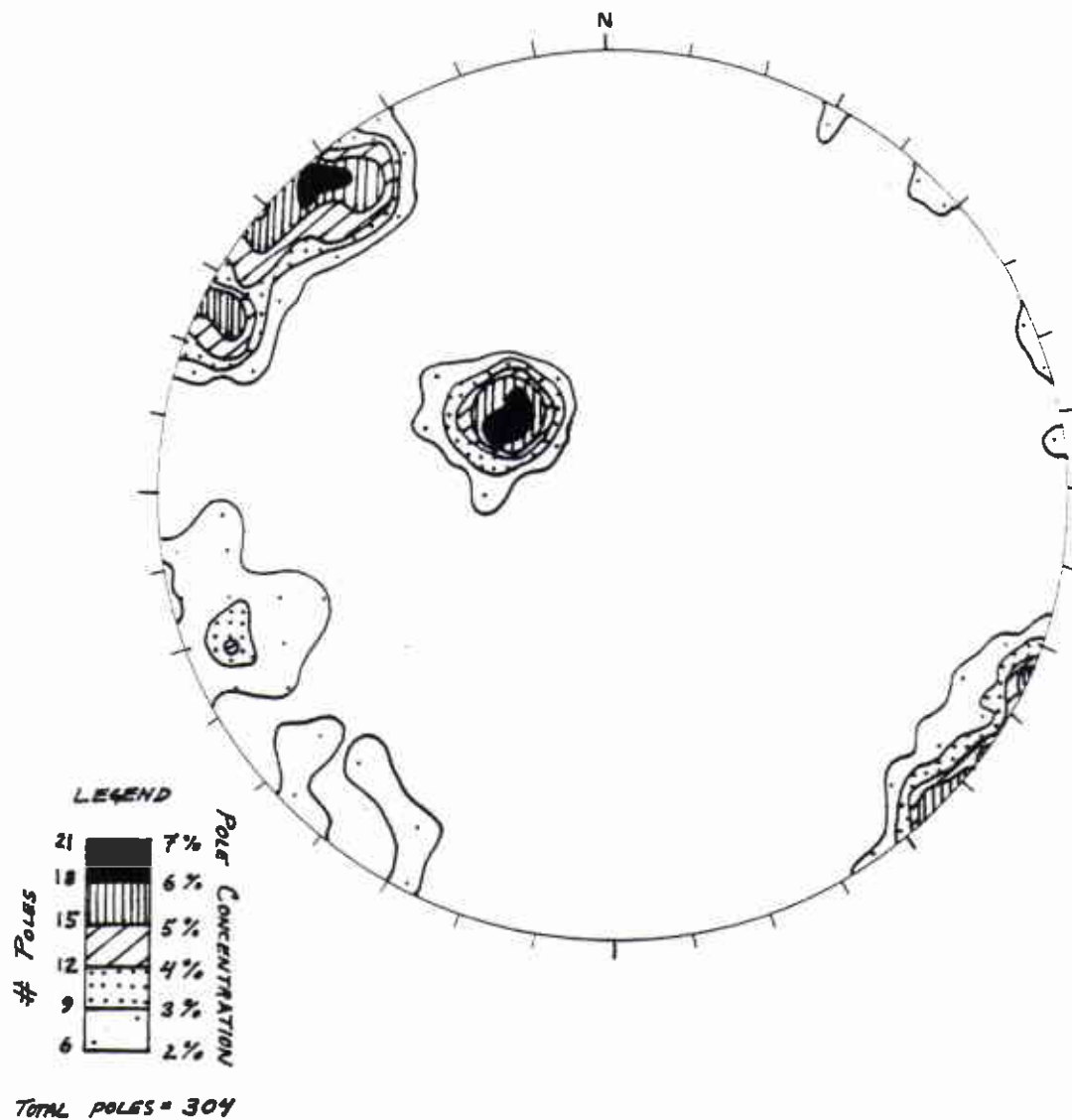
Figure 3.14: Stereonet with pole concentration contoured using 1 % counting circle (data as in figure 3.11)

One disadvantage of either counting circle technique is the areal distortion which occurs due to the use of a counting circle of fixed radius. The radius of a 1% area counting circle is equal to 10 % of the radius of the net from circular geometry. Such a circle at the centre of the equal area projection subtends an angle of approximately 16 degrees. At the perimeter of the net, this same circle subtends an angle of approximately 22 degrees (Priest 1985). The use of an elliptical window near the perimeter would compensate somewhat for this distortion (Stauffer 1966, CANMET 1977). This is an unpopular procedural complication and is rarely done.

The area, however represented on the reference sphere, by a counting circle on the equal area stereonet, is constant regardless of the location of the circle (Attewell and Farmer 1976). The distortion in this case is merely geometrical and means only that a concentration represented on a contoured stereonet correctly describes the probability of pole occurrence within an area surrounding the point in question. The only problem is that for points near the perimeter of the net, the counting point will not represent the centroid of the area described. This will cause an error in location but not in magnitude of the contour lines (Attewell and Woodman, 1972).

The same cannot be said for the equal angle projection. A constant radius circular window subtends an angle of 23 degrees at the centre of the net and only 12 degrees at the perimeter. While this distortion is only slightly greater than for the equal area projection, the areal distortion is directly related to this difference in cone angle. This distortion generates inaccuracies in both location and magnitude of density contours. If a circular counting window is used with equal angle projection, the circle must be made to increase in size near the perimeter of the net and

decrease in size near the centre. This is prohibitively bothersome for manual contouring. The counting circle methods are therefore only efficient when used with equal area projection.

Other variations on contouring methods employing counting circles are summarized in Stauffer 1966. One of particular interest for later discussion is the Mellis procedure in which circles of 1% area are drawn on the net centred on the plotted poles themselves. The concentrations are then determined by the number of circles which overlap at a given point. This method is similar to a reverse Schmidt floating circle technique and the two procedures can be easily shown to be equivalent.

While there may be some statistical validity in the use of circular windows for contouring stereonets, the method can be rather cumbersome. Several researchers have developed other methods for contouring. These generally involve the use of template overlays which are divided into regions of equivalent representative area. These fixed cells are then used in a similar fashion to the circular window to count poles within their areas. One such overlay is the Kalsbeek net described in Ragan 1973. Shown in figure 3.15, it is completely divided into triangles. Six of these triangles form a hexagonal area which is equivalent to 1% of the total area of the net. The total number of poles within each hexagon is recorded at the centre node for later contouring as a percentage of the total. Triangles at the perimeter can be coupled with triangles on the opposite side of the net to form complete hexagons. This method has the advantage that data inside of each triangle is used by three hexagons resulting greater continuity of concentration values from node to node.

This is similar to the overlap achieved in the Schmidt counting grid method if the grid spacing is less than one counting circle radius.
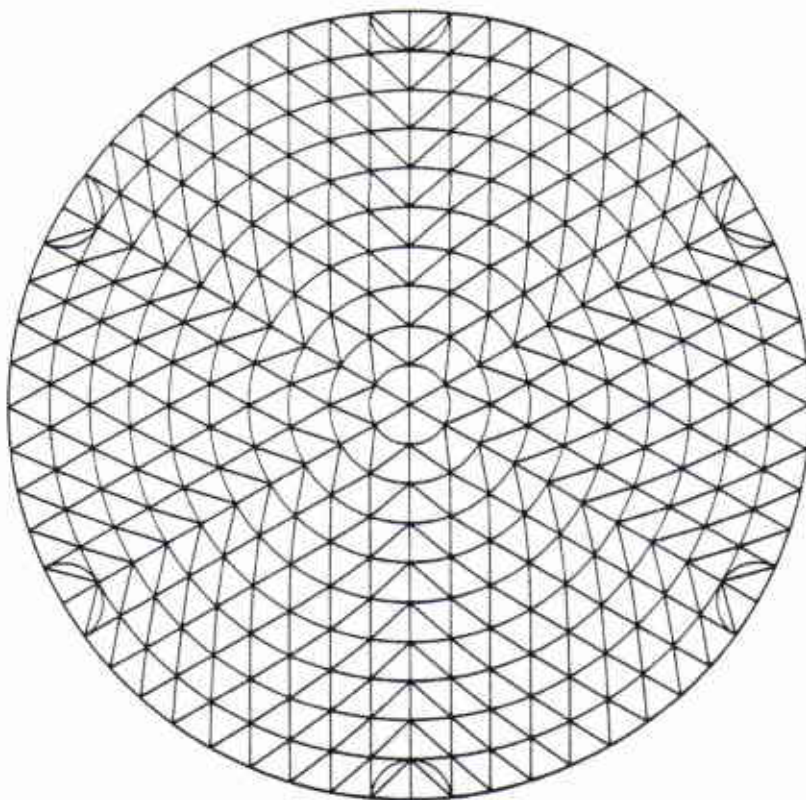
Figure 3.15: Kalsbeek counting net (after Ragan 1973)

For both efficiency and accuracy, the best counting overlays for general field analysis of orientations, in the author's opinion, are the Denness counting grids (Denness 1972). The Denness grids are based on individual cells which vary in shape and size over the stereonet, but which represent areas on the reference sphere of not only constant area, but also of constant shape. The poles inside each cell are totalled and recorded at the centre of the cell for manual contouring. The grids have

the disadvantage that each pole is counted in only one cell reducing continuity of concentration values from cell to cell. For most field applications, however, this deficiency can be overlooked in view of the grids' ease of use and the speed with which contouring can be performed.

The Denness Type A Counting Net is best suited for analysis of subvertical planes or subhorizontal lineations. Notice in figure 3.16 that the outer ring of cells is divided by a ring into equal halves. These outer cells are used as whole cells and the halves outside this ring are used as pairs of opposing half cells to provide detail near the perimeter of the net. The Type B net is designed for efficient contouring of inclined strata. The selection of counting net is governed by an initial subjective appraisal of the data.

Where more accurate contour diagrams are required, Hoek and Bray (1974) suggest using the Denness net as a first approximation and then refining the contours with the floating circle technique. This is an adequate procedure providing the user consider that the inflexibility of the Denness net is compensated for by its lack of areal distortion. The opposite is true for the floating circle method and combining the two techniques may be of dubious value.
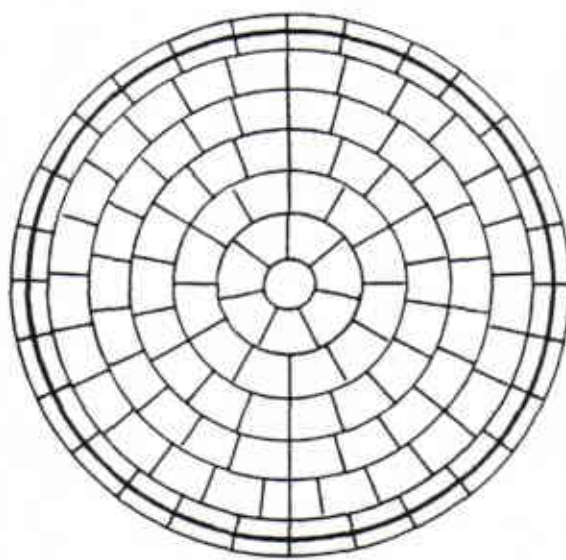
Figure 3.16: Denness Counting Grid A
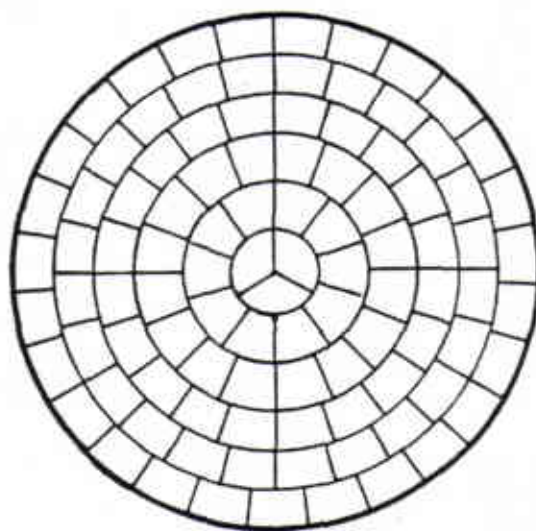
Figure 3.17: Denness Counting Grid B

3.4.5　　　　Interpretation of Stereonets

Once the stereonet has been contoured, the next step should be a purely visual assessment of the clustering which may or may not be apparent. To plunge into further analysis without first qualitatively assessing the distributions is very dangerous. The stereographic technique is ideally suited to this very important stage of assessment.

Figure 3.18 illustrates several idealised pole distributions corresponding to bedding planes and their appearance on a contoured stereonet. The shape of a concentration indicates the nature of the cluster as either a centralised distribution corresponding to a set of lineations or planar surfaces which can be approximated by a single mean orientation, or a girdle distribution corresponding to a folded regional geometry. The contoured stereonet also facilitates the ranking of dominant concentrations. In some cases many peaks will be visible on the stereonet and a decision must be made regarding which if any will be reduced to distinct representative features for further analysis. In other cases, no dominant trends will be visible causing a great deal of conflict in the mind of the geologist who has gone to all the trouble of collecting the data. Stauffer (1966) discusses some guidelines for fabric analysis of contour plots and the definition of dominant clusters. His conclusions are summarised as follows by Hoek and Bray (1974).

1. First plot and contour 100 poles.

2. If no preferred orientation is apparent, plot an additional 300 poles and contour all 400. If the diagram still shows no preferred orientation, it is probably a random distribution.

3. If step 1. yields a single pole concentration with a value of 20% or higher, the structure is probably truly representative and little could be gained by plotting more data.

4. If step 1. results in a single pole concentration with a contour value of less than 20%, the following total numbers of poles should be contoured.

    12 - 20 %   add 100 poles and contour all 200
    8 - 12 %   add 200 poles and contour all 300
    4 - 8 %   add 500 to 900 poles and contour all
                                              600 to 1000
    less than 4 % at least 1000 poles should be contoured

5. If step 1. yields a contour diagram with several pole concentrations, it is usually best to plot at least another 100 poles and contour all 200 before attempting to determine the optimum sample size.

6. If step 5. yields 1% contours less than 15 degrees apart and with no pole concentrations higher than 5%, the diagram is possibly representative of a folded structure for which poles fall within a girdle distribution.

7. If step 5. yields a diagram with smooth 1% contours about 20 degrees apart with several 3-6% pole concentrations, then an additional 200 poles should be added and all 400 poles contoured.

8. If step 7. results in a decrease in the value of the maximum pole concentrations and a change in the position of these concentrations, the apparent pole concentrations on the original plot were probably due to the manner in which the data were sampled and it is advisable to collect new data and carry out a new analysis.

9. If step 7. gives pole concentrations in the same positions as those given by step 5, add a further 200 poles and contour all 600 to ensure that the pole concentrations are real and not a function of the sampling process.

10. If step 5. yields several pole concentrations of 3 and 6% but with very irregular 1% contours, at least another 400 poles should be added.

11. If step 5. yields several pole concentrations of less than 3% which are very scattered and if the 1% contour is very irregular, at least 1000 and possibly 2000 poles will be required and any pole concentration of less than 2% should be ignored.

These guidelines were developed during a study of statistical significance of pole concentrations and are somewhat impractical for field analysis. The basic procedure of stepwise refinement described is nevertheless sound. The numbers of poles suggested in each step may not be realistic and can be reduced accordingly. For the experienced user, it is usually sufficient to analyze whatever data is available within reason, which is usually much less comprehensive than Stauffer suggests. The important thing to note is that the origin of the data should never be forgotten in the analysis process and that interpretations should never be made more detailed than the data warrants. Similarly, if a very accurate and statistically sound selection of representative orientations is critical to the problem at hand, a more detailed analysis with larger quantities of data may be required. One rule of thumb used by this author is that if an apparent dominant concentration, once delineated with the help of a contoured stereonet, does not visibly stand out in the original pole plot or at least in a scatter plot, it is ignored altogether or used with caution in any further analysis. This is a major advantage of the stereographic procedure for reduction of orientation data collected from a natural environment. The visualization inherent in the method is a vital ingredient lacking in purely analytical or statistical analysis.
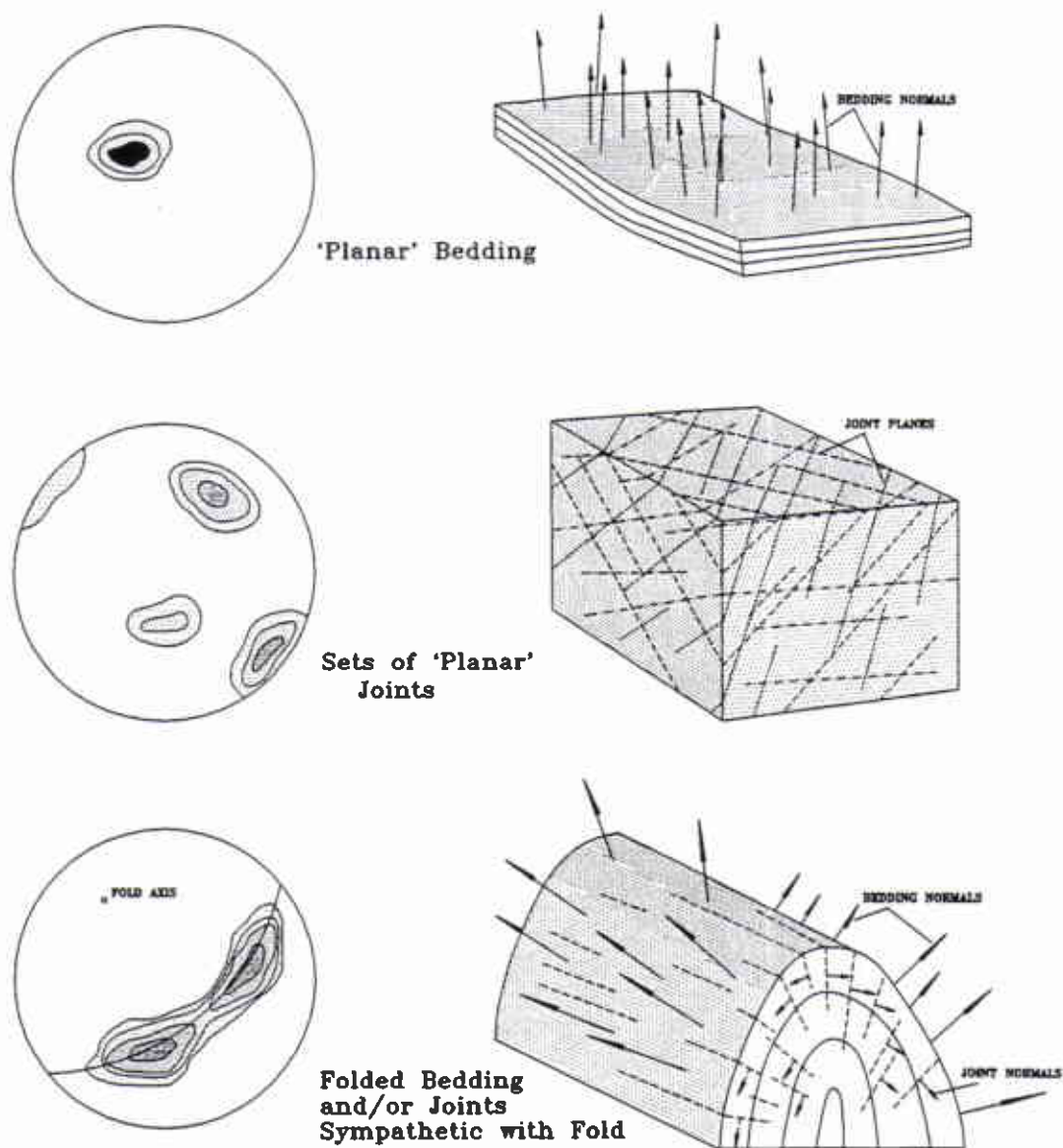
'Planar' Bedding

Sets of 'Planar' Joints

Folded Bedding and/or Joints Sympathetic with Fold

Figure 3.18: Interpretation of contoured clusters

3.4.6   Sampling Bias in Orientation Data Collection

In the preceding discussions, the orientation data has been assumed to be collected without bias in a perfectly objective manner. In the case of data collection for assessment of structural geology measurement error and data biasing can be introduced in a number of ways. Terzaghi 1965, and Einstein and Baecher 1983 summarize a number of sources for error and bias in joint surveys. Several of the principle sources of bias are described here. Most of the errors inherent in an individual measurement will average out to zero over an entire survey and will not be discussed.

1.   Open joints, a phenomena often governed by localised stress directions, are more likely to be recorded than tightly closed joints. This problem can be overcome by a purely objective scanline survey. A tape line is stretched across a face of a slope or along a drift underground and all planar features are recorded which intersect this scanline. This will remove visual bias based on aperture. It could be argued, however, that open joints indicate more important features than closed joints, just as persistent discontinuity planes are more important than those which are impersistant. This view would make these forms of bias beneficial. This is a case where judgement is required based on field stress data and whether or not the data is being collected for local design or regional assessment. A useful rule of thumb for practical joint surveys for engineering design is "...If it is longer than [the geologist] and wide enough to insert a thin knife blade, measure it. Otherwise, ignore it."(Bawden 1989)

2.   Magnetic ore bodies in the vicinity will cause incorrect measurement of strike or dip direction. This problem is dealt with through the use of the clinorule.

3.   Measurement variation due to waviness of the feature being measured may cause a dispersion of the recorded poles. It may be necessary to estimate an average orientation of the surface, or in the case of stability surveys, to quantify this waviness separately (Barton et al. 1974).

4.   Measurement on a flat surface such as a slope face or along a linear scanline or tunnel introduces a measurement bias in favour of those features which are closer to being perpendicular to the survey orientation. Features which are subparallel to a tunnel or slope face are less likely to be recorded than those perpendicular to it. On an irregular rock face, enough variation in measurement surface may be present to allow outcrop of all features present. Over flat traverse planes or in borehole core, this bias can be quite severe. If possible, joint surveys should be performed locally on two or three approximately orthogonal traverse orientations. This procedure should reduce the overall bias in the survey. If this is not possible, Terzaghi (1965) proposed a correction for sampling bias as outlined in figure 3.19.
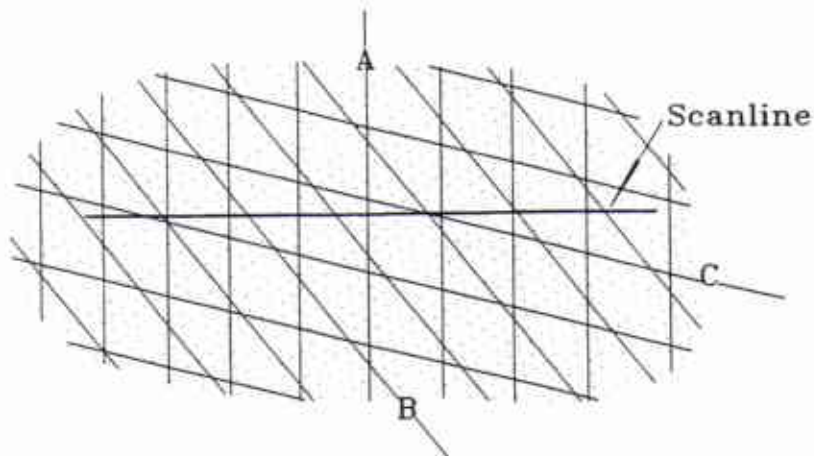
WHEN ORIENTATION MEASUREMENTS ARE CONDUCTED, A BIAS IS INTRODUCED IN FAVOUR OF THOSE FEATURES WHICH ARE PERPENDICULAR TO THE DIRECTION OF SURVEYING (A LINEAR TRAVERSE OR A PLANAR ROCK FACE). IN THE ABOVE SCANLINE EXAMPLE, THREE JOINT SETS WITH IDENTICAL SPACINGS ARE SHOWN. MEASUREMENTS ALONG THE SCANLINE WILL RECORD FAR MORE JOINTS IN SET A THAN IN SET C. THIS WILL BIAS THE DENSITY CONTOUR PLOT HEAVILY IN FAVOUR OF SET A.

TO COMPENSATE FOR THIS BIAS, A GEOMETRICAL WEIGHTING FACTOR CALCULATED BELOW IS APPLIED TO EACH MEASUREMENT BEFORE CONTOURING OR MEAN VECTOR CALCULATION.
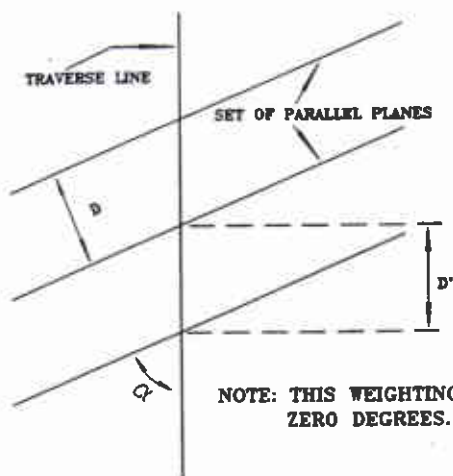
α = Minimum angle between plane and traverse

D' = Apparent spacing along traverse

D = True spacing of discontinuity set
= $D' \sin \alpha$

R' = Apparent density of joint population
= $1/D'$

R = True density of joint population
= $1/D = 1/D' \sin \alpha = D' \operatorname{cosec} \alpha$

W = Weighting applied to individual pole before density calculation
= $(1) \operatorname{cosec} \alpha$

NOTE: THIS WEIGHTING, W, TENDS TO INFINITY AS α APPROACHES ZERO DEGREES. A WEIGHTING LIMIT MUST BE SET.

Figure 3.19: Terzaghi correction for sampling bias

This weighting ,w, is applied to each pole before contouring. A weighting of 2.7, means that a given pole is interpreted as representing 2.7 measurements during contouring. Otherwise the contouring procedure is the same in all of the methods described. When expressing pole counts as a percentage of the total population, the total used must be the weighted population, N_w:

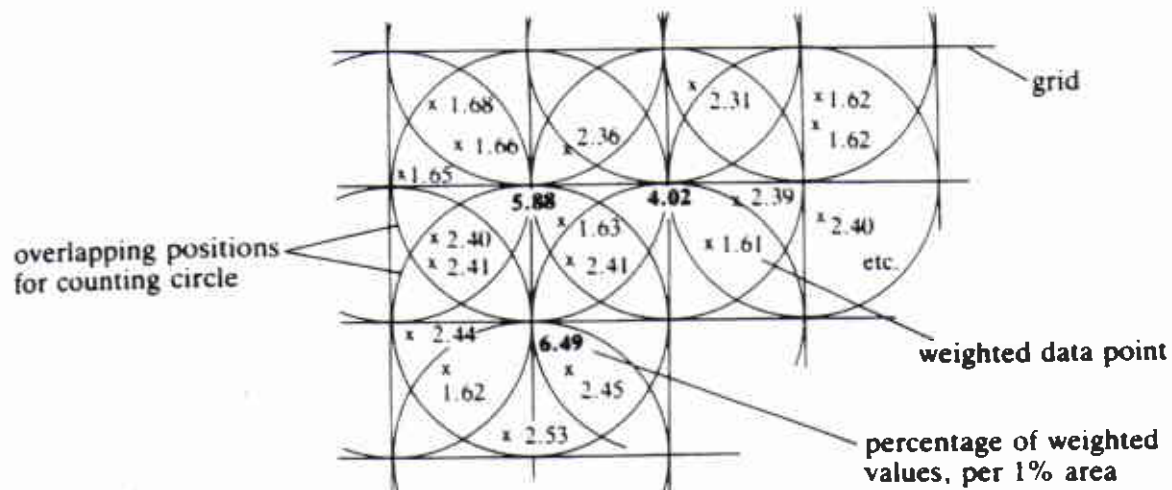$$N_w \quad = \quad \sum_{j=1}^{N} w_j \qquad \qquad (eq.3.5)$$

Figure 3.20: Weighted pole density contouring with counting circle (after Priest 1985)

When computing mean vectors this weighting may be taken into account by multiplying the direction cosines for each pole by the weight for that pole before performing vector addition or eigenvector analysis.

3.4.7   Combination of Stereographic and Analytical Procedures

Once a stereonet has been contoured it may often be sufficient to define representative orientations corresponding to directions of primary concentration peaks on the diagram. This technique is usually sufficient if the dominant concentrations are reasonably symmetrical and normally distributed. In this case the direction of maximum concentration will be approximately equivalent to the mean orientation. For field analysis of data, this approximation will usually be sufficient.

If the orientation is skewed or if a more statistically valid description of dominant orientations is required, analytical post-processing of contoured clusters may be necessary.

Zanbak (1977) describes a method for statistical description of orientation mean and variance which is performed primarily on the stereonet itself and graphically on cartesian orientation - frequency plots. Two orthogonal great circles are overlain on the contour plot corresponding to the major and minor axes of an elliptical distribution. These planes are selected such that they intersect at the point of maximum concentration for the cluster being analyzed. Concentration (probability of occurrence) values are taken directly from the stereonet along these axes and two frequency plots are generated corresponding to each axis. Standard statistical analysis can then be used to determine means and variance along these two axes assuming any form of distribution. *Normal* or *Poisson* are suggested by Zanbak. In this reference Zanbak then uses these statistical parameters for a probabilistic slope

stability analysis. McMahon 1971 uses a similar approach. This method is often called a *bivariate distribution* analysis.

More rigorous methods using vector addition or eigenanalysis can be performed on the original data if the poles are first grouped into clusters based on the stereonet contours. Such a combined procedure is described by Priest 1985. Once the poles are grouped into sets or clusters, each cluster is then analyzed separately. The pole orientations are converted to cosine triplets and the mean is calculated using vector addition. A symmetrical spherical normal distribution (Fisher) is assumed and goodness of fit parameters are calculated. Fisher's constant K, for example is calculated as:

$$K \ = \ (\, N - 1 \,) \, / \, (\, N - R)$$ (eq.3.6)

where N is the total length of pole vectors and R is the length of the resultant.
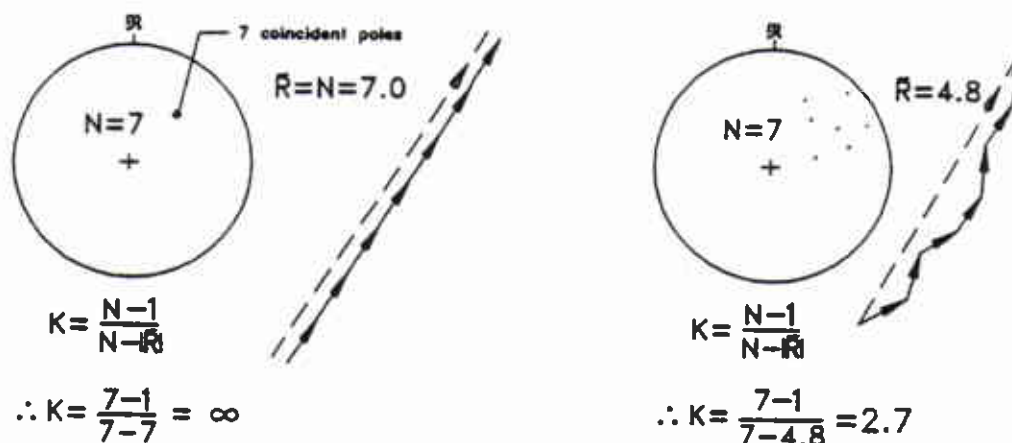

Figure 3.21: Significance of Fisher constant K (after Peaker 1990)

If weighted vectors are used to correct for sampling bias, R must be calculated by summing normalized weighted vectors with w_j':

$$w_j' \quad = \quad w_j N / N_w \qquad\qquad \text{(eq.3.7)}$$

such that:

$$\sum_{j=1}^{N} w_j' \quad = \quad N$$

It can be seen then from equation 3.6 that if the orientations within a set are tightly clustered, that is approximately parallel to the mean, R will approach N and K will tend to infinity. If the data is widely scattered, Fisher's constant K will become very small.

This constant can then be used to generate a probability function for a symmetrical spherical distribution known as a Fisher distribution:

$$P(\theta) \quad = \quad \upsilon^{K \cos \theta} \, d\theta \qquad\qquad \text{(eq.3.8)}$$

where: $\upsilon \quad = \quad (K \sin \theta) / (e^K - e^{-K})$

A complete discussion of this method is found in Priest 1985, based on the original work by Fisher 1953.

A method is outlined in the Pit slope Manual (CANMET 1977) which utilises a special overlay, permitting a direct computational procedure for Fisher parameters from pole plots. The grid, called a Braitsch overlay, closely resembles the Denness

nets described earlier. The cells are identified by codes which relate to a chart of corresponding direction cosines. Each set of cosines is multiplied by the number of poles falling in the respective cell and summed for a given cluster. The summed triplet is then normalized to give the direction cosines of the mean vector. Fisher's constant can then be directly determined and a distribution specified.

Vector components for fitting of spherical normal distribution to measurements of orientation with Braitsch overlay

$$k = \frac{N - 2}{N - R}$$

$$R = \sqrt{[(\textstyle\sum X)^2 + (\textstyle\sum Y)^2 + (\textstyle\sum Z)^2]}$$

(N = number of observations)

Figure 3.22: Braitch overlay (after CANMET 1977)
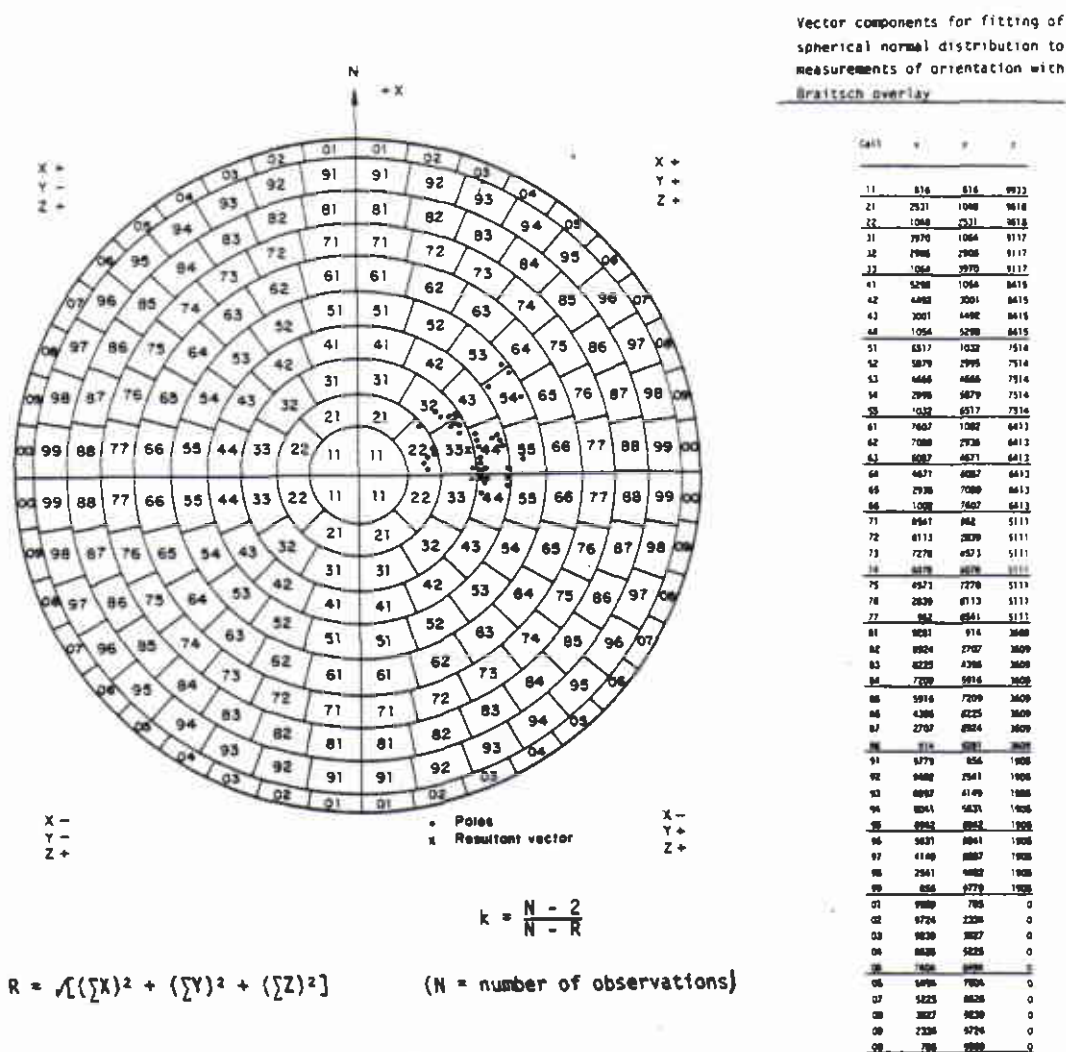
Complex statistical and analytical analysis may be performed on orientation data using a number of methods as described here. The common starting point, however, in most analysis procedures for data measured in the field, is the stereonet and its various flexible applications. The next chapter will discuss the computerization of stereographic projection techniques, the logical progression for orientation analysis.

4.0 COMPUTERIZED STEREOGRAPHIC PROJECTION

4.1 COMPUTER GENERATION OF STEREONETS

The development of computers and, in particular, microcomputers has prompted the development of numerous computer programs involving stereographic projection. Computers permit the rapid calculation of complex analytical problems. As shown in the previous chapter, however, most available analytical techniques for processing of three-dimensional orientation data suffer from an inability to reliably handle multiple arbitrary clustering of data and do not easily facilitate visualization. The most logical alternative, therefore, is to use the computer's computational and graphical power to streamline the process of orientation analysis using stereonets.

The fundamental equations for the computerized generation of stereonets are the mapping functions ,converting trend and plunge values for a vector to a projected x and y coordinate pair on the stereonet. These functions are outlined by Priest (1985) and described in sections 3.2.1 and 3.2.2 of this work. Priest (1983) also describes plotting functions for great circles in the equal angle projection as described in figure 3.4 in the previous chapter.

The improvement in programmable computer graphics in recent years permits the rapid generation of computerized plots of poles and great circles as illustrated by Priest (1983,1985).
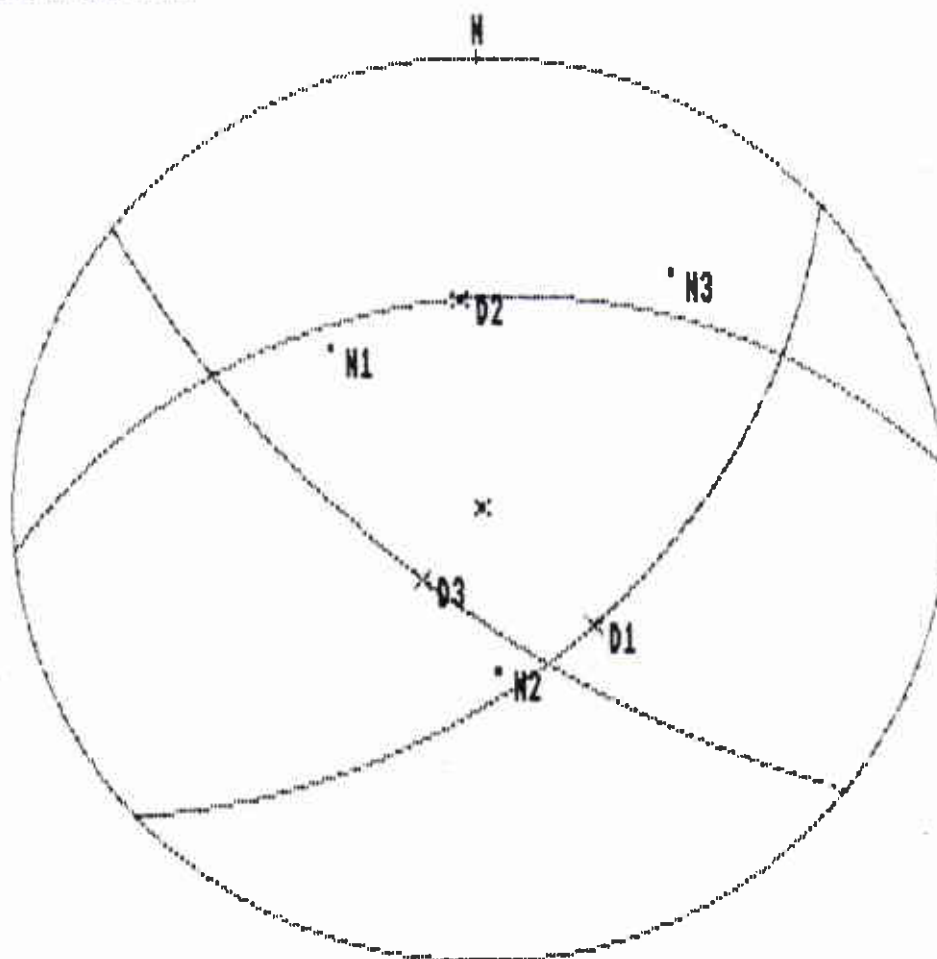

Figure 4.1: Computer generation of projected poles and planes (after Priest 1983)

4.2 COMPUTERIZED DENSITY CONTOURING

A number of other groups have developed computer programs which perform pole density contouring using a number of different methods.

Most of these existing programs allow for input of orientation pairs for each data unit and possibly one other identifying label such as discontinuity type. Static pole plots are then produced along with plots of contoured pole density. Dominant orientations can then be selected visually from the screen or printer/plotter output and input separately into a great circle plotting routine as described in section 4.1. Improvements in subsequent efforts in computerized pole contouring have come as a result of improved computer graphics.
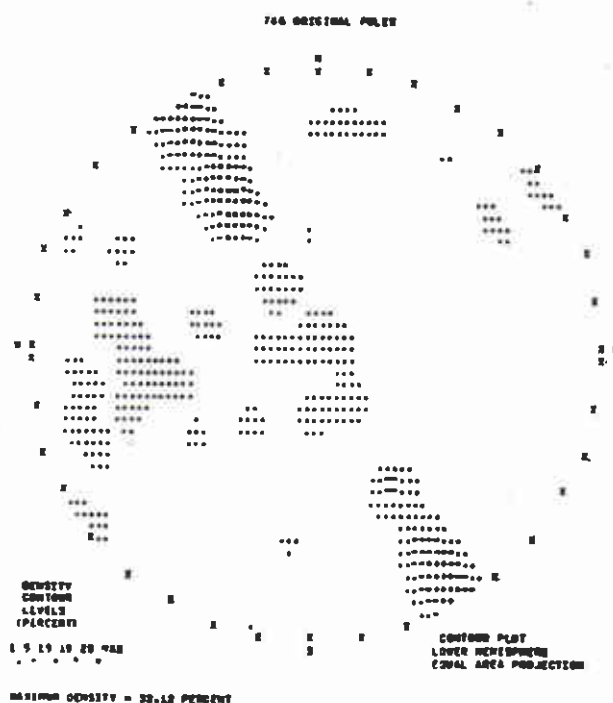

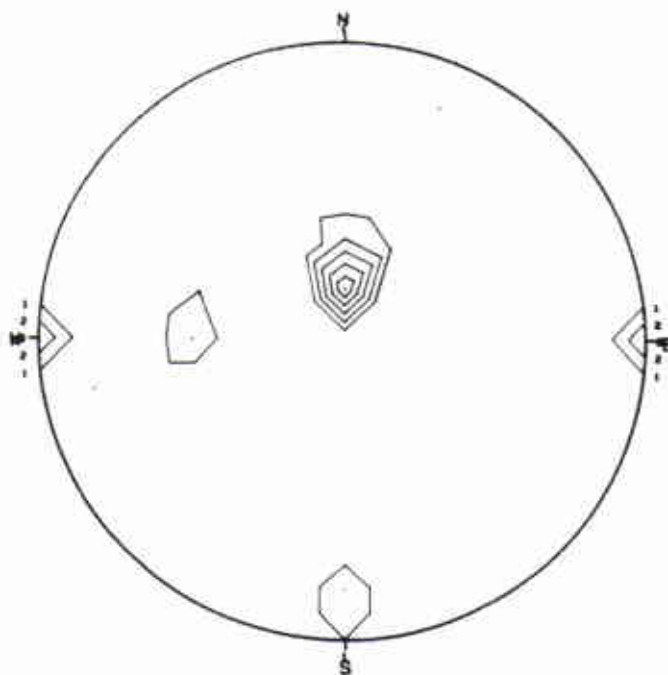**Figure 4.2**: Computerized contouring example (after Golder Ass. 1979)

Figure 4.3: Computerized contouring example (after Shi & Goodman 1989)
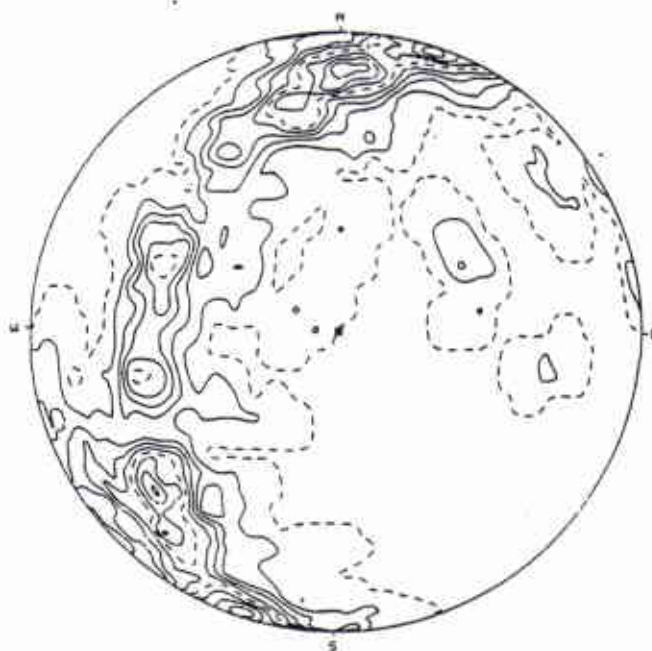

Figure 4.4: Computerized contouring example (after Tocher 1978)

Another improvement has been in the contouring method itself. Early attempts at computerized contouring utilized the fixed grid counting circle approach. Poles were located on a two dimensional projection using equations 4.1 and 4.2. These projected pole positions were then used in the contouring algorithm which was simply a computerized version of the manual technique. This method involves some very complicated logic and calculation, particularly around the perimeter of the stereonet (Zhang & Tong 1988, Tocher 1978). Calculation of concentrations near the perimeter require duplication of either poles or counting circle on the opposite side of the projection (just as in the manual approach) to correctly incorporate subhorizontal poles.

Data loss due to the two dimensional nature of the problem also occurs near the perimeter. This loss is acceptable in the manual approach as described in the previous chapter but would seem to be avoidable in a computerized approach. Tocher 1978, proposes a compensation technique to deal with this problem.

The computer approach also permits the use of a variable counting circle to deal with the angular distortion on the stereographic projection. Separate mapping functions for this counting circle must be adopted depending on which projection is being used (equal area or equal angle). Zhang & Tong (1988) describe such a method for equal angle projections.

All of the above problems are eliminated entirely, however, if density contouring is performed on the surface of the sphere instead of on the projection. This approach

is obviously impossible to utilize manually. This is, however, the easiest method to computerize.

Spherical contouring employs the mapping functions described for either projection method (equations 4.1 and 4.2) as well as the inverse of these functions for mapping from the projection back onto the sphere. A grid is first mapped onto the surface of the sphere, either directly as regular spherical coordinate intervals, or indirectly. The latter approach would involve a regular grid overlay on the projection. Each grid intersection would then be transformed to an equivalent vector point on the sphere (using the inverse of the appropriate projection equations).

A floating cone is selected such that its circular intersection on the surface of the sphere encloses an area equivalent to 1% of the area of one hemisphere. This circle (or cone) is then centred on each grid vector and the pole vectors falling within the cone are counted and each grid total is divided by the total population. The resultant concentration values are then associated with the corresponding grid point on the stereonet plane and contoured accordingly.

This method will be described in more detail in the next chapter. This methods has the advantages of eliminating any distortion and data loss since the counting circle is used on the sphere and not on the projection.

Near the horizontal equator of the sphere, grid vectors just below the horizontal plane have negative counterparts just above this plane on the opposite side of the sphere. Poles vectors falling inside of cones centred on these negative grid vectors

are included in the totals for the associated positive grid vectors. In this way, there is no data loss at the perimeter, another advantage over contouring on the projection.

From a programming point of view, this method has one very major advantage over two dimensional contouring. The counting circle radius can be equated to a cone angle by the following relationship:

$$a = \pi r^2 \qquad \text{area of counting circle}$$
$$A = (4 \pi R^2)/2 \qquad \text{area of reference hemisphere}$$

$$\text{if } n = \frac{a}{A} :$$
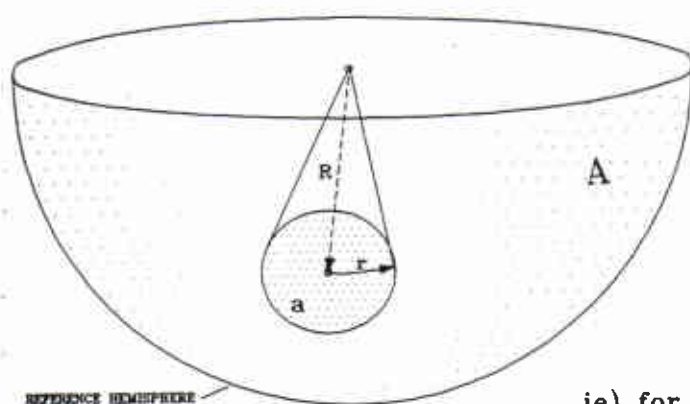
$$n = \frac{2 \pi r^2}{4 \pi R^2}$$

$$\text{since } R = 1 :$$

$$n = \frac{1}{2} r^2$$

$$r = \sqrt{2n}$$

ie) for $n = .01$ (1 % circle) :

$$r = \sqrt{.02} \quad \text{(cone angle in radians)}$$

Figure 4.5: Calculation of cone angle for spherical counting circle

If pole and grid vectors are expressed as direction cosines (equations 2.1), then the dot product (equation 2.3) of a grid vector and a pole vector can be calculated. Remember that the dot product of two unit vectors yields the cosine of the angle between them. If this value is greater than the cosine of the counting circle cone angle, then the pole is inside the counting circle and is included in the counting total for that grid vector. This is a much simpler relationship than that which must be used to determine the relationship between a pole and grid point on a two dimensional projection. This dot product is also used directly in more complex statistical contouring methods which will be discussed in detail in the next section.

Several recent contouring programs utilize spherical contouring (Golder Ass. 1979, Diggle and Fisher 1985). Both of these programs utilize some form of probability distribution associated with each pole. In the Schmidt method on the sphere, as on the projection, a pole is counted as having full influence on a grid point (grid total is incremented by one or the full weight of the pole if corrected) if the pole falls anywhere inside a counting circle centred on the grid point. The pole has zero influence on the grid point if it falls immediately outside the circle. In a more sophisticated statistical approach as employed by these and other authors, the influence of the pole on a grid point decays continuously with angular distance from the grid vector. These influence functions produces smoother and more statistically valid contours, and better reflects the degree of measurement error inherent in each measurement (Golder Ass. 1979). These functions are easily implemented in a spherical contouring algorithm since they are usually a direct function of the dot product of the grid and pole vector.

A number of different approaches can be used to determine the function used in this type of density calculation. Diggle and Fisher (1985) describe one method in detail. A different derivation is used by this author and will be described in detail in the next chapter.

4.3   CURRENT DEFICIENCIES IN COMPUTERIZED STEREONETS

All of the programs evaluated as part of this study were found to be deficient in several areas.

Computer graphics, particularly for the personal computer have improved immensely in the last few years. Programs written several years ago are not up to date in their graphical presentation.

Use of these programs was seen to be very cumbersome. Development focus was placed on internal procedures and statistical validity and very little emphasis placed on usability.

Most current programs are static. That is, they do not reproduce the flexibility and interactive nature of the original manual stereonet. Most programs provide simple pole plots of data and then provide contour diagrams for this data. Alternatively,

stereonet programs permit visualization of discrete planes in horizontal or inclined projections. The paper output can then be used manually to perform stability assessments, for example (Priest 1983).

It was apparent to this author, that a real need existed for a computer package which could duplicate as much as possible the interactive nature of the manual stereonet, utilize modern graphical techniques to produce report-quality output, and provide a direct bridge between statistical reduction of large data sets and the use of dominant orientations in further analyses.

Other features which were seen as important in a comprehensive stereographic toolkit, were the incorporation of an easily accessible data base from which data could be selectively plotted and analyzed, as well as the ability to process and visualize data attributes other than orientation such as discontinuity spacing or seismic amplitude. These features are present in some existing packages (CANMET 1977, Golder Ass. 1979, Noranda 1989) but were found by this author to lack an acceptable degree of flexibility and ease of use.

The decision was made by this author, based on these deficiencies, to develop a comprehensive package for stereographic analysis of orientation based data. The resulting program, DIPS, will be described in the next chapter.

5.0   A NEW APPROACH TO COMPUTERIZED STEREOGRAPHIC ANALYSIS

5.1   REQUIREMENTS FOR EFFECTIVE COMPUTERIZATION OF STEREOGRAPHIC ANALYSIS

After examining previous attempts at computerized stereographic analysis as presented in the previous chapter and after discussions with practising engineering geologists (Carter 1989, Wood 1989, Noranda 1989, Bawden 1989), some mandatory requirements were established by this author for an effective software tool for data processing. These requirements can be summarized as follows:

-the program must utilise effective graphics.

-the program must be interactive both in preprocessing, and in data manipulation. This would enable the program to effectively mimic the time tested manual process of arbitrary analysis using stereonets.

-the program should support several processing, projection and presentation conventions in order to suit the diversified preferences of practitioners.

-the program should permit progressive analysis of data at a number of stages from plotting of poles, to cluster analysis and manipulation of selected distinct orientations.

-the program should include tools for both the interactive visual processing and analytical analysis of orientation clusters.

-the program should accommodate processing of qualitative and quantitative non-orientation data.

-the program should be as portable and hardware insensitive as possible without sacrificing efficiency.

-the program should include a flexible data base to permit quick screening and selection of data as the analysis progresses.

-program input should be as free-form as possible to allow analysis of data from a wide variety of applications. It should use primarily a row-column entry format and should accept an ASCII data file which would permit file creation by other software packages such as data collection programs or industrial databases.

-the program should generate report quality hardcopy output.

5.2   PROGRAMMING PHILOSOPHY

The Turbo - C programming language from Borland-Osborne was selected for this project due to its superior graphics capabilities and data handling features.

Turbo - C also includes compilation modes which creates one executable program capable of running on an XT, 286 or 386 system with or without an associated math coprocessor. A wide variety of video graphics drivers are supported by Turbo - C, including Hercules, CGA, EGA ,VGA and others. Again these can be included in the executable program to permit autodetection and initialization of many graphics system configurations. When designing software for field use, such system portability is critical for the acceptance and usage of the product.

Many previous engineering software packages require specific system configurations or require lengthy and complicated setup and initialization procedures. One major goal of this project was to provide a single program, "load and run", package which would be as system independent as possible. Turbo - C permits this form of programming.

Concurrent with the development of this author's stereographic analysis package, the Rock Engineering group at the University of Toronto was developing a Turbo - C graphics interface library, which it intended to incorporate into all subsequent interface software. In order to be consistent with future programs, the system drivers, screen layout routines and menu functions from this library (Corkum 1990)

which were available at the time of start-up of this project were used as a base for development. These permitted the support of multiple video modes, mapping of real coordinates to screen device coordinates for a variety of video configurations, mouse support, and the generation of the basic screen design including a prompt and input bar, drawing region, status line, and a flexible cursor key or mouse driven menu system (Figure 5.1).
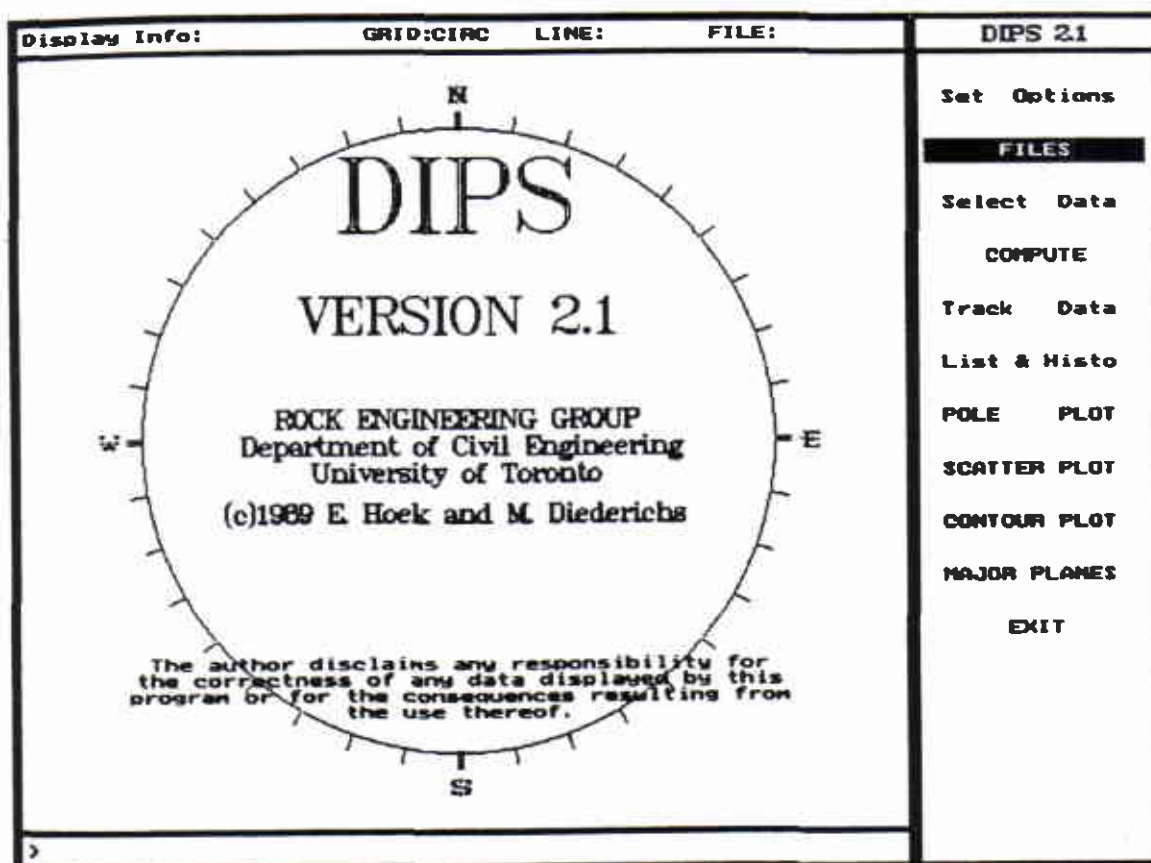

Figure 5.1: Basic Screen Layout for the DIPS package

5.3   **DIPS   2.1**
Data Interpretation Package
Using Stereographic Projection

The software package which resulted from this work is called DIPS. All of the requirements outlined in the beginning of this chapter have been satisfied in this authors opinion. DIPS is viewed as an interactive toolkit containing a wide variety of features enabling the user to customize the analysis process to accommodate the needs of the problem at hand and the user's personal preferences regarding analysis methodology. It was found that it was difficult, if not impossible, to find one particular data processing format that would satisfy the requirements of enough individual applications where orientation analysis is required. As mentioned, it was therefore decided to provide as broad a range of analysis tools as practical in one interactive package while maintaining the program's ease of use.

The basic layout of the program and the basic programming methodology will be described in this chapter.

5.3.1   Data Input

Data input is, at present, performed by creating an ASCII text file which contains some header information and the data in column format. This format was designed to allow easy file creation by another program such as a data collection or database

system (Noranda 1989, CANMET 1977) and to allow file creation and editing using spreadsheet packages, word processors or text editors. At the time of this writing, a customized data file creation utility written in Turbo - C is planned.

The header information contains several pieces of information:

-Project titles for use in hard copy output

-Traverse information for data organization and for bias correction

-Several flags concerning the setup of the data portion of the file

-Magnetic declination data for automatic data correction

-Information regarding the number of data columns and their physical layout (order, column title and column width).

-Comments are allowed throughout the data file if the line begins with an asterisk or if the comment follows required information in a line.

More detailed information on the data file makeup can be found in the program manual in appendix B. This header section contains enough user specified information to completely customize the format of the data portion of the file to fit the user's requirements. Only three columns are mandatory - one numerical identifier for each row of data and two orientation parameters. Traverse identifiers for each data unit must also be present if traverse information is to be used in the file. A quantity column for multiple orientation measurements can be turned on or off using a flag in the header file.

The data file can then contain up to twelve additional columns of data in qualitative or quantitative form. For structural analysis these columns could be used to specify

spacings, roughness, discontinuity type, etc. (figure 5.2) For seismic data these extra columns might contain information on intensity, and directional sense of first arrival for focal mechanism studies.

This data can be processed in a number of different ways in DIPS. It can also be used for data subset selection and screening. These features will be discussed in a later section.

The column widths are user specified in order to allow file creation from fixed format column editors. The only limits on the quantity of data in a file are imposed by system restrictions. DIPS is currently configured for a system with 640 kilobytes of random access memory (RAM). With average concurrent RAM use (mouse driver, DOS shell and screen save utility) 7000 - 9000 rows of data may be processed. A row of data will hereafter be termed one data unit.

In addition, since no real consensus exists on proper data notation, DIPS permits data input using one of five formats:

-TREND/PLUNGE may be used for direct plotting of pole vectors of lineations. No further processing is required.

-DIP/DIP DIRECTION , STRIKE/DIP (left hand rule), and STRIKE/DIP (right hand rule) may be used for input of planar measurements. Internal processing is required to convert these data units to pole orientations. (See table 2.1).

The desired input format is specified using a global orientation flag in the data file header section. For data in a particular traverse as identified by its traverse number, a traverse orientation flag may be used to override the global flag for the traverse involved. This is useful when combining data in DIP/DIP DIRECTION format with data from another source which may be in STRIKE/DIP format , for example.

-BOREHOLE DIP/ BOREHOLE DIP DIRECTION may be used when inputting data from oriented core measurements. This data is identified by its traverse number which references a traverse type specified as BOREHOLE. The data is rotated using the borehole reference directions and the real orientation is calculated and specified in the global orientation format. The rotation technique is the matrix transformation equivalent of the procedure outlined in Golder Ass. 1979. A description of input parameters is given in the manual in appendix B.

It was intended to include a clino-rule input format. However, since the notation and datum conventions used when measuring with a clinorule vary greatly, it was decided that clino-rule data conversion is best done by the individual taking the measurements in order to avoid serious error.

DIPS permits the creation of several types of output files containing information about the original data (after processing), as well as calculated features such as mean or representative orientations. The original data file, however, is never altered within the DIPS program. This allows the data to be stored in a stable data base which can not be altered by careless errors during the use of the program.

```
•DIPS 2.1 DATA INPUT TEMPLATE
•PROJECT TITLES ( 2 lines ) :


          STRUCTURAL SURVEY - DEVELOPMENT LEVELS 2000 - 2050
          University of Toronto     Dec.7/1988


•NUMBER OF TRAVERSES :

         7

•TRAVERSE INFORMATION (1 line for each traverse) in the form...
•traverse #;(opt.trav orient);traverse type;orient. 1;orient. 2;title


          1;LINEAR;325;00;28 Level,Dec7/88,N.D.,chainage 2026+0 to 12
          2;LINEAR;325;00;28 Level,Dec7/88,N.D.,chainage 2022+0 to 23
          3;LINEAR;062;00;28 Level,Dec7/88,N.D.,chainage 2022+23 to 33
          4;LINEAR;174;00;25 Level,Dec7/88,N.D.,chainage 2011+0 to 22
          5;LINEAR;154;00;2050 Level,Dec7/88,N.D.,chainage 2028+0 to 15
          6;LINEAR;164;00;2050 Level,Dec7/88,N.D.,chainage 2013+0 to 30
          7;LINEAR;070;00;2050 Level,Dec7/88,N.D.,chainage 2013+0 to 7


•The next line is 'data orientation type flag' , choices are;
•DIP/DIPDIRECTION (of plane)
•TREND/PLUNGE (of pole to plane or of linear structure)
•STRIKE/DIPL  (of plane - left hand rule)
•STRIKE/DIPR  (of plane - right hand rule)

          DIP/DIPDIRECTION

•MAGNETIC DECLINATION (west positive) :

         0

•QUANTITY COLUMN FLAG:
•if the flag is QUANTITY, then the 'quantity' column must be present
•if the flag is NO QUANTITY do not include a 'quantity' column

          QUANTITY

•NUMBER OF EXTRA DATA COLUMNS (0-12):

         9

•COLUMN TITLE LINE:
```

number	dip	dipdir	quantity	traverse	type	rock	persist	aperture	infilling	strength	roughness	shape	spacing
1	79	81	1	1	joint	ore	3	0	clean	medium	smooth	curved	5
2	86	137	4	1	joint	ore	2	0	stain	medium	smooth	planar	0.2
3	90	159	1	1	joint	ore	1	0	clean	medium	smooth	planar	0.5
4	70	166	2	1	joint	ore	3	0	stain	medium	smooth	planar	0.3
5	65	330	2	1	joint	ore	1	0	clean	medium	smooth	planar	0.2
6	65	56	2	1	joint	ore	2	0	clean	medium	smooth	planar	0.1
7	69	243	1	1	joint	ore	2	0	clean	medium	smooth	planar	2
8	44	239	5	1	joint	ore	1.5	0	clean	medium	smooth	planar	2
9	70	158	2	1	joint	ore	2	0	clean	medium	smooth	planar	0.6
.													
.													
.													
39	80	155	3	3	joint	ore	3	0	clean	medium	smooth	planar	0.05
40	84	151	1	3	joint	ore	1	0	clean	medium	smooth	planar	0.05
41	38	206	2	3	joint	shist	1	0	clean	medium	smooth	planar	10
42	77	155	2	3	joint	shist	1	0	clean	medium	smooth	planar	0.1
43	80	147	10	3	joint	shist	3	0	calcite	medium	smooth	uneven	5
44	80	147	5	3	joint	felstuff	3	0	clean	medium	smooth	planar	0.2
45	64	266	1	3	joint	felstuff	3	0	clean	medium	smooth	planar	6
46	81	227	5	3	joint	felstuff	3	0	clean	medium	smooth	planar	0.3
47	86	62	1	3	joint	felstuff	4	0.001	quartz	high	rough	uneven	0.2
.													
.													
.													
101	49	240	3	6	vein	ore	2	0.002	quartz	high	rough	irregular	1
102	80	298	6	6	joint	ore	2	0	stain	medium	smooth	planar	0.3
103	85	258	1	6	cleavage	ore	3	0	clean	medium	rough	planar	0.1
104	53	342	6	6	vein	ore	4	0.005	quartz	high	rough	wavy	0.1
105	49	266	3	6	vein	ore	1	0.005	quartz	high	rough	irregular	0.5
106	76	36	1	6	cleavage	ore	3	0	clean	medium	smooth	planar	0.1
107	19	99	2	6	joint	ore	1	0	clean	medium	rough	planar	0.3
108	81	143	5	6	joint	ore	3	0	clean	medium	smooth	planar	0.2
109	85	246	4	6	cleavage	ore	3	0	clean	medium	smooth	planar	0.2
.													
.													
.													
143	70	161	1	7	joint	shist	1	0	clean	medium	smooth	planar	1
144	85	133	6	7	joint	shist	2	0	clean	medium	rough	planar	0.1
145	10	134	5	7	vein	shist	2	0.1	calcite	medium	smooth	planar	0.2
146	89	57	1	7	cleavage	shist	4	0.001	calcite	medium	smooth	planar	0.3
147	29	296	3	7	vein	shist	2	0.05	calcite	medium	smooth	planar	0.1
148	68	272	1	7	vein	shist	3	0.1	calcite	medium	smooth	planar	0.5

```
          -1     (end of file flag)
```

Figure 5.2: Example of DIPS data file (data for figures 5.4, 5.23, 5.24, 5.28 & 5.29)

5.3.2   Projection Options and Spherical Mapping

The heart of the DIPS computation and presentation algorithms is the set of mapping routines which convert world coordinates to angular measures of trend and plunge and vice versa. The conversion from device (ie. screen pixel) coordinates to world coordinates is handled by the basic interface routines.

The angular to cartesian mapping functions are based on those outlined in Priest, 1985. The two functions WORLDTORADIAL and RADIALTOWORLD are outlined on the following page. Note that both EQUAL AREA and EQUAL ANGLE projections are supported. The projection type is selected from an options menu in the DIPS package. A flag is toggled and the appropriate functions are executed by these two routines. Since all operations involving projections and user interaction with the screen are directed through these two routines, this is all that is required to support both projection methods in the program.

Priest and others have outlined functions for the computer generation of other features such as great and small circles. These involve analytical routines for calculation of the circle centre and then the generation of arc segments for the great circle and small circle curves. These routines are for equal angle only and are difficult to program in a flexible fashion. The equivalent two dimensional curves for equal area projection require complex fourth order functions to generate.

The alternative is to map all pole points and vertices of polygon approximations of great and small circles from the reference sphere to the projection and then connect the vertices as required to form the projected features. The following routines from DIPS are the mapping functions which form the basis for all projections in DIPS:

```c
#define   PI        3.141592654
#define   ROOT2     1.414213562
#define   rad(x)    ((x)/57.29577951)  /*degrees to radians*/
#define   ang(x)    ((x)*57.29577951)  /*radians to degrees*/


/*Global flags toggled in main program*/

extern int project_type;    /*(EQUAL ANGLE or EQUAL AREA)*/
extern int gridradius;      /*(radius is 100)*/


/*WORLDTORADIAL                     converts world coordinates (worldx,worldy) on projection
                                    to (trend,plunge) vector orientation*/

void worldtoradial(float worldx,float worldy,float *trend,float *plunge)
{

        double angcheck;

        if (project_type==EQANGLE){
                angcheck=(sqrt(worldx*worldx+worldy*worldy)/(gridradius));
                *plunge=(float)(rad(90)-atan(angcheck)*2);
        }
        else if (project_type==EQAREA){
                angcheck=(sqrt(worldx*worldx+worldy*worldy)/(gridradius*ROOT2));
                if(angcheck>1.0)angcheck =1.0;
                *plunge=(float)(acos(angcheck)*2-rad(90));
        }
        if (worldy!=0){
                *trend=(float)(atan2(worldx,worldy));
        }
        else{
                if (worldx>=0)*trend=rad(90);
                else *trend=rad(270);
        }
        if (*trend<0) *trend=(float)(rad(360)+*trend);
}



/*RADIALTOWORLD                    converts (trend,plunge) vector orientation to world
                                   coordinates (worldx,worldy) on projection*/

void radialtoworld(float trend,float plunge,float *worldx,float *worldy)
{

        float length;

        if (project_type==EQANGLE){
                if(((90-ang(plunge))/2>89.5)&&((90-ang(plunge))/2<91.5))length=1000.0;
                else length=tan((rad(90)-plunge)/2)*gridradius;
        }
        else if (project_type==EQAREA){
                length=(gridradius*ROOT2)*cos((rad(90)+plunge)/2);
        }
        *worldx=(float)(length*sin(trend));
        *worldy=(float)(length*cos(trend));

}


/*NOTE   that world coordinates are converted to screen pixel coordinates ( and vice versa ) by a
         second set of conversion routines in the interface (Corkum 1990)*/
```

The two mapping routines on the previous page, however, eliminate the need for the projection-specific and feature-specific functions outlined by Priest 1985. The plane and cone intersections on the surface of the sphere can be calculated by vector rotations in 3 dimensional space using direction cosines, matrix transformation, and conversion to angular measurements for a number of interval points on the curve. These points can then be assigned world coordinates using the mapping routines described and a polygon approximation can then be drawn on the screen. This method is then projection independent and is very flexible. All great circles, small circles and cluster definition windows are generated this way in DIPS.

The windows described do not require matrix rotation since they are defined by plunge and trend limits and can be mapped directly to the screen using the conversion routines. These are used to interactively surround pole clusters for set definition and mean vector calculation for a given set. They can be moved and stretched with the cursor keys or mouse in an interactive "rubber band" fashion. These will be discussed in more detail in a later section.

Both polar and equatorial reference grids can also be generated directly by drawing great circles and small circles at appropriate intervals using the methods described above. If adequate angular resolution is used when generating the polygon approximations to the great and small circles, the results are indistinguishable from the results obtained using the arc functions outlined by Priest 1985. Since the computer excels at tedious but simple iterative calculation, there is no real need for computational elegance if the results are compatible.
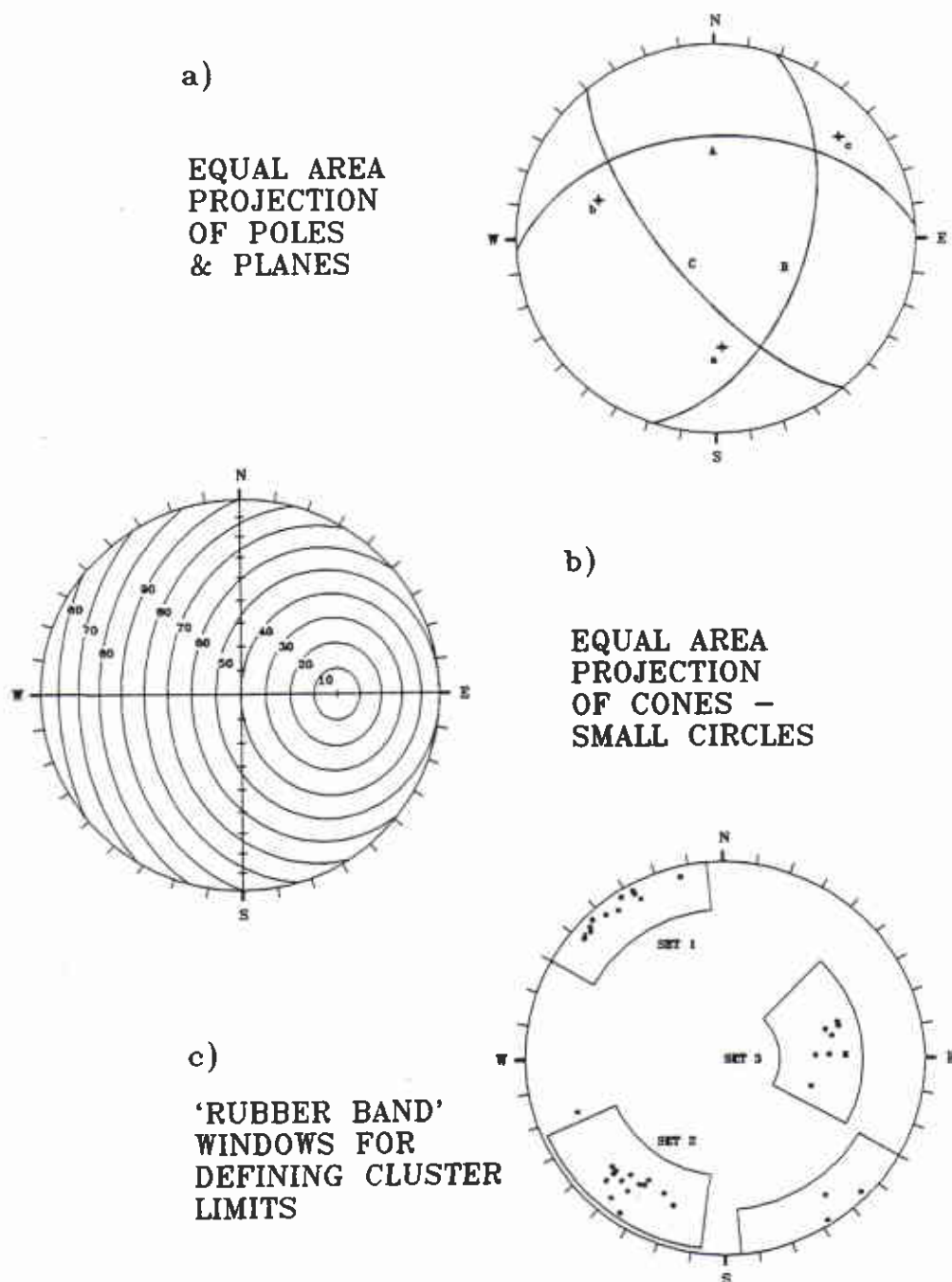
Figure 5.3: Examples of projected a) poles & planes, b) cones (small circles) and c) trend/plunge windows for defining cluster limits

5.3.3   **Presentation of Multiple Data Measurements**

The Pole Plot

The simplest form of presentation in DIPS is the basic POLE PLOT. Data is read from the file in a form specified by the global orientation flag or the traverse orientation flag, and converted to equivalent pole orientations specified by trend and plunge. These orientations are then directly mapped onto the projection using the RADIALTOWORLD routine. The default plotting method involves the generation of a simple pole symbol at the projected location of the pole. This would normally represent the first step in analysis and reduction of multiple data measurements.

The database in DIPS can also be utilised at this stage to provide additional information. Any one of the columns in the data file can be used to generate a plot with symbols at the pole locations representing particular feature attributes such as surface type, roughness or strength, or ranges of values for spacing, continuity or seismic intensity, for example. The symbols and colours used have been chosen to create a gradient in colour (cold to hot) and in symbol complexity. For quantitative data, the legend defining these symbols and colours can be modified to highlight either greater or smaller values, and to accentuate linear or log distributions. Likewise, for qualitative data such as roughness evaluation, the symbols can be interactively selected to highlight desired properties. The combination of pole plotting and symbol representation permits a double purpose plot (Tufte, 1983) where visual dominance can result either from closely spaced data points or high intensity symbols representing undesirable properties such as high continuity. Both
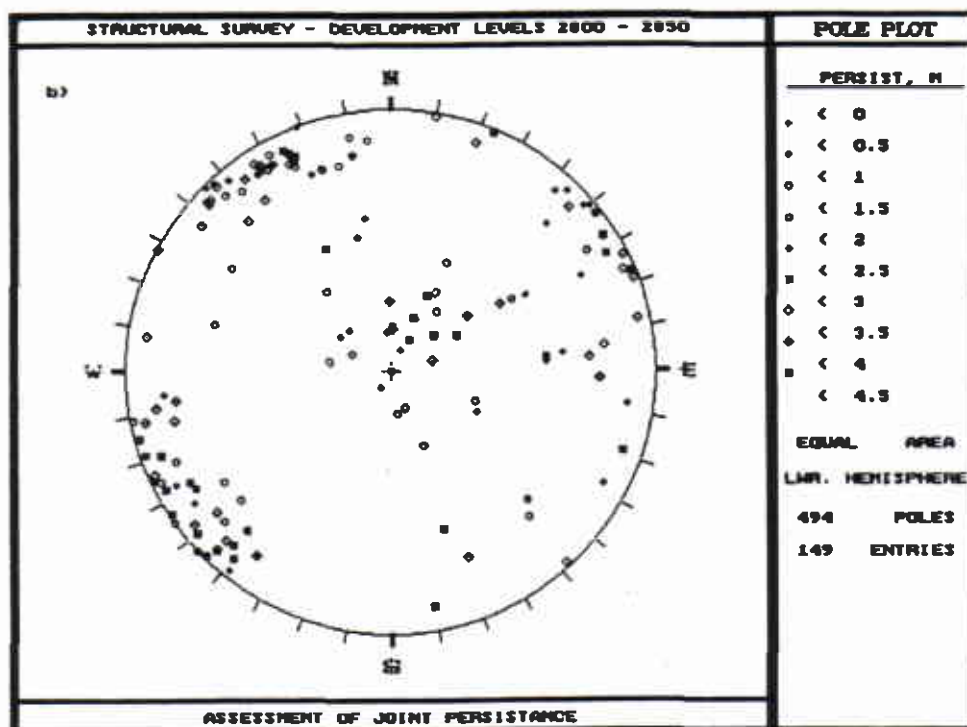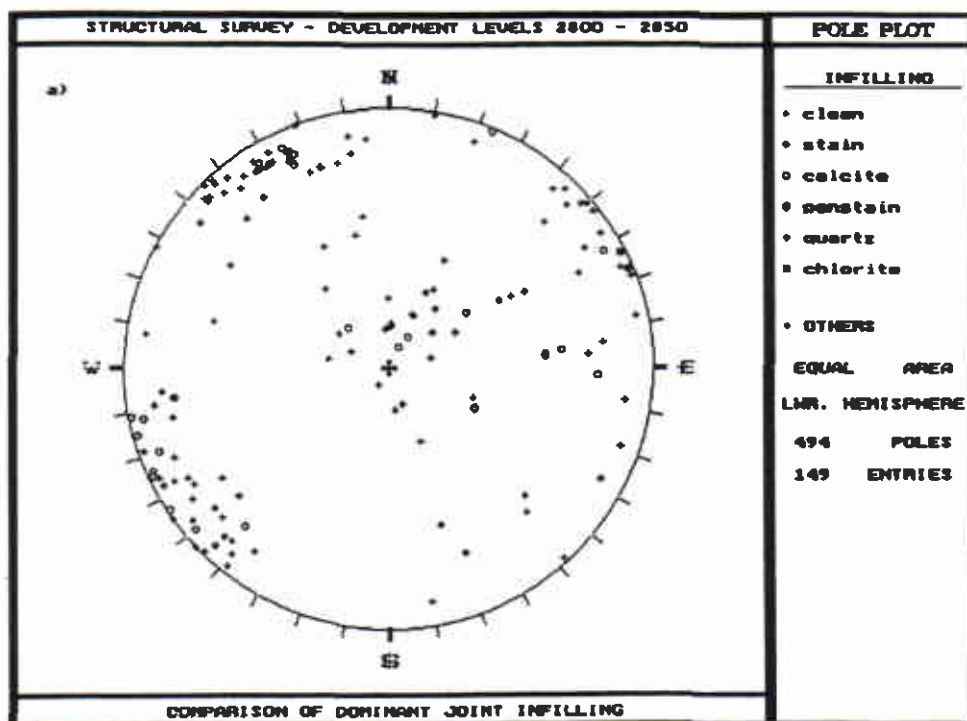
Figure 5.4: Symbolic pole plots illustrating a) qualitative and b) quantitative attributes

factors must be considered in assessing critical surfaces for slope stability, for example.

Non-orientation data, loaded using the TRACK DATA option in DIPS, can also be presented using a histogram option in the program. This can be useful when a more rigorous examination of the data is warranted as in the case of joint spacing evaluation. This histogram can be generated for all data plotted or for data enclosed by a set window. This can be useful for examining, in detail, the attributes of a particular joint set as required when performing a Q rock mass classification (Barton 1974), for example. The operation of windows will be discussed later.
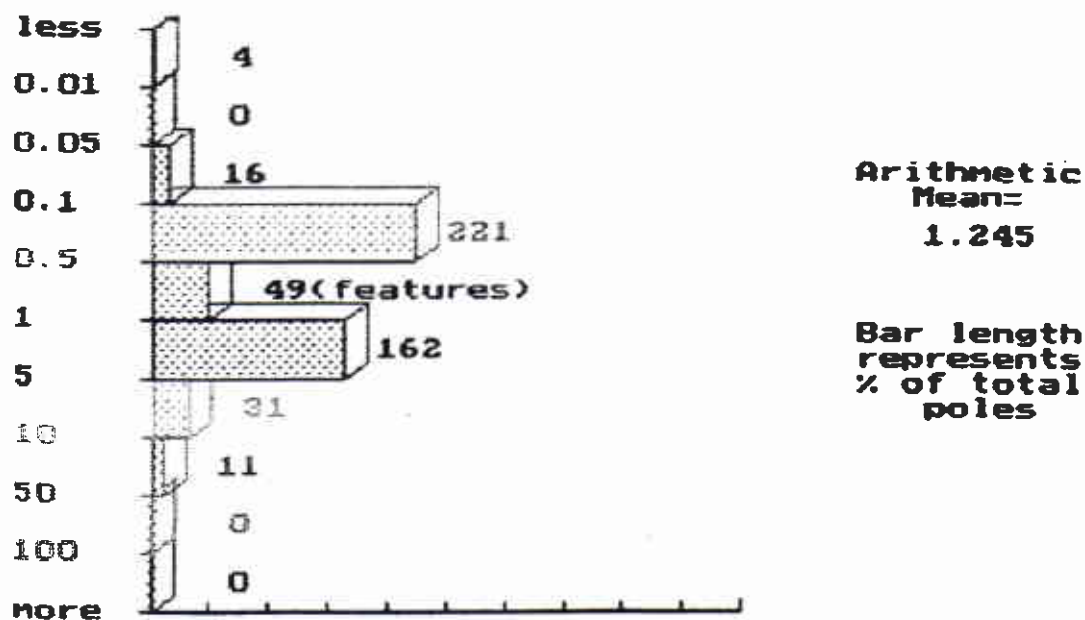
Figure 5.5: DIPS Histogram of data attributes

5.3.4   Visual Clarification of Pole Distribution

The Scatter Plot

When multiple data measurements have been taken (one data unit representing more than one similar feature) or when a large number of data measurements has been taken, a single pole symbol in the pole plot may conceal many actual measurements. A second plot is then needed to identify the number of collinear or similarly oriented pole vectors at a given location on the stereonet.

This plot is called a SCATTER PLOT. This plot uses a square grid pattern superimposed on the stereonet. This is the same grid which is used for contouring pole density as described in the next section. All poles which plot within one half grid spacing (with a square region centred on the grid point) are tallied and the total assigned to that grid point. A symbol plot is then generated which shows the number of poles in the immediate vicinity of each grid point. This plot gives a clearer picture of the pole distribution.

It is important to note, however, that the symbol positions in the scatter plot are determined by the grid point locations. Consequently, the scatter symbol positions will differ from the pole positions in the pole plot. The scatter plot should not be used for determination of exact orientations of features. It is only intended to clarify the quantity distribution. The accuracy of the symbol positions in the scatter plot can, however, be improved if a finer computation grid is selected through the options menu in DIPS.
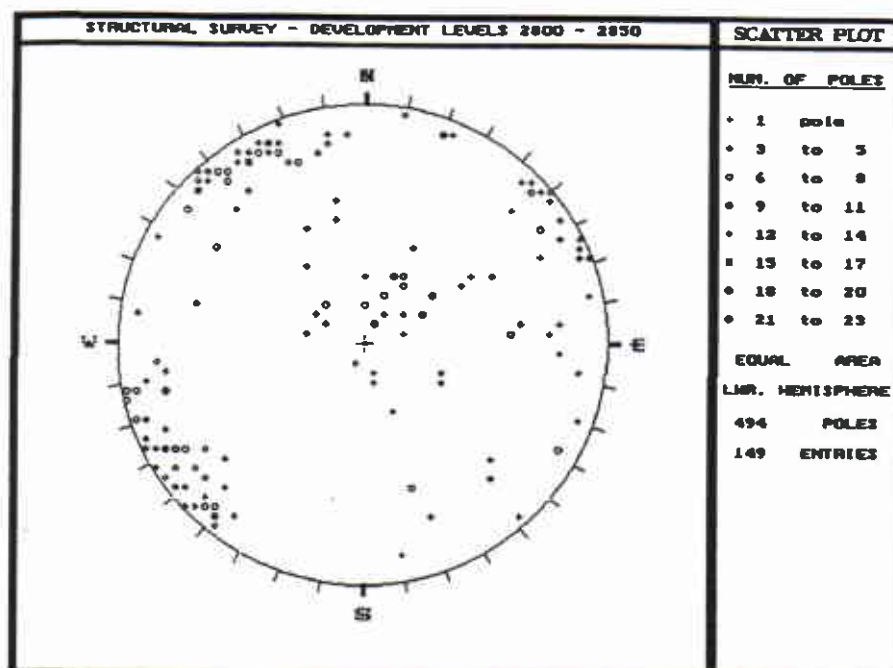
Figure 5.6: DIPS Scatter Plot
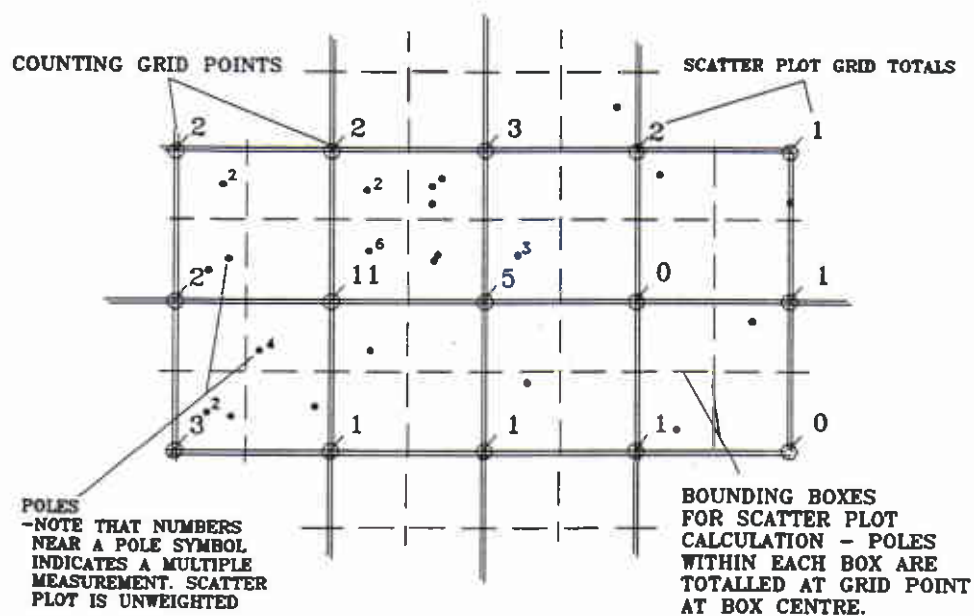
Figure 5.7: Grid point approximation method for Scatter Plot

5.3.5 Contoured Pole Concentrations

The Contour Plot

A more statistically valid assessment of pole distribution is obtained using a contour plot of pole density. The interpretation of such a plot is discussed in section 3.4. The contours represent intervals of probability (in percent) of pole occurrence within a specified angular distance of a given orientation.

DIPS features two options for contouring pole density on the sphere. The so-called SCHMIDT method is similar to the manual grid counting circle approach and assumes 100 percent confidence in each orientation measurement. Each data unit contributes either 100 or 0 percent of its value to a grid point depending, respectively, on whether or not it falls within defined angular limits of the grid vector. In the FISHER method (so-named by this and other authors because of its use of the probability function described in Fisher, 1953) each pole possesses an bell shaped distribution which contributes a fractional influence on a grid point which decreases with increasing angular distance between pole and grid vector.

Contouring in DIPS occurs on the surface of the sphere. A grid of user specified resolution is generated which is square when projected in two dimensions. This is to facilitate efficient generation of the continuous interpolated screen contours. These grid points are converted to unit grid vectors in three dimensional space using the WORLDTORADIAL mapping routine. The angular distances between grid vectors and pole vectors in the data set are then used to calculate concentrations. In order

to optimize the computation process, DIPS calculates grid contributions at all grid points for each successive pole in the data list, rather than cycling through the pole list for each grid point. The DIPS approach is optimized by processing only those grid points within an angular distance as specified by the counting circle radius. Only a small row/column defined cluster of grid points needs to be considered for each data unit. This greatly reduces the computation time required.

After mapping the grid points onto the sphere, the next step is to compute the cone angle, β, represented by the radius of the counting circle. Figure 4.5 *illustrates this* relationship. The default area of the counting circle is 1 percent of the area of one hemisphere. The user may alter this area if desired.

Each pole vector is converted to equivalent direction cosines. Each grid vector is also expressed as direction cosines. The dot product of the pole vector with each successive grid vector yields the cosine of the angle between them.

In the Schmidt method, if this cosine is greater than $\cos \beta$, the grid vector is within the cone corresponding to the counting circle centred on the pole vector. The grid point concentration is therefore incremented by the value of the pole (unity or greater if multiple measurements are represented or if a weighted contour is being calculated as described later in this section).

If the pole is within an angular distance β of the stereonet perimeter, it will have an influence on grid points on the other side of the net. DIPS must then repeat this process using the negative pole vector.
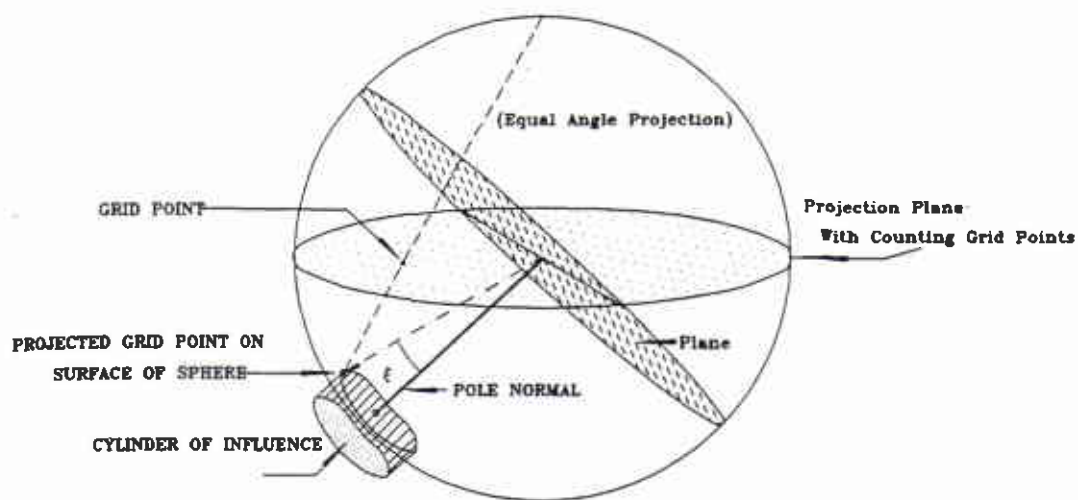
ℓ = small angle between pole normal and projected grid vector

Figure 5.8: DIPS Contouring on the sphere (Schmidt method)
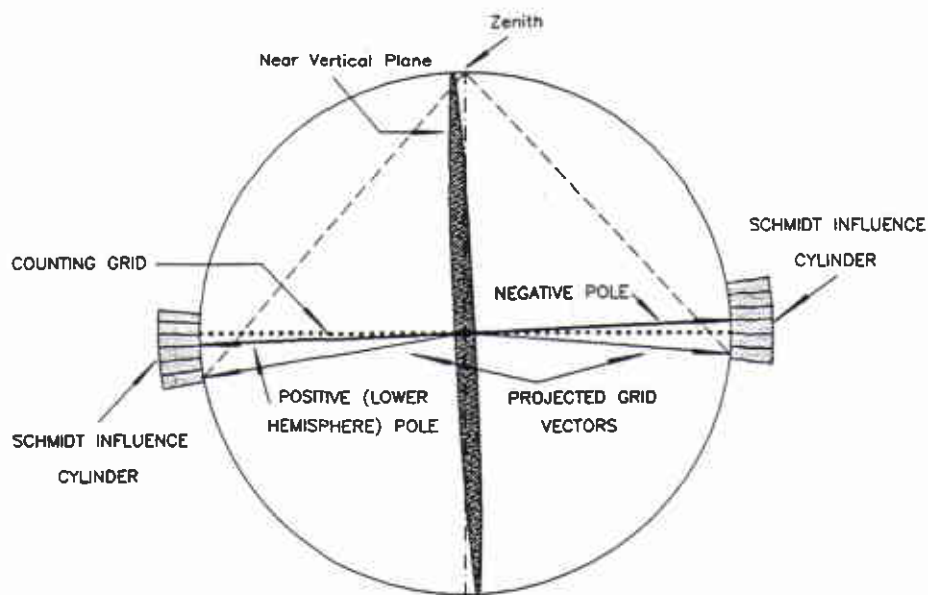
Figure 5.9: Method for contouring near perimeter

In DIPS, for greater memory and computational economy, only one quadrant (north-east) of grid information is stored in an array. Each grid point has four concentration values corresponding to the symmetrically associated grid locations in the other three quadrants. There are also redundant grid points in the upper right corner of the grid array which are an artifact of the row-column indexing of the grid. Since only neighbouring grid points are processed for each pole, these redundant grid points pose no extra computational overhead.

The user can select between SCHMIDT and FISHER distributions for density contouring. As discussed, the Schmidt distribution is analogous to a cylinder on the surface of the sphere and centred about the pole vector. The density contribution to each grid point inside the cylinder's radius is given by the height of the cylinder. This height is unity for a single unweighted pole but can be a greater integer or rational value. The same analogy applies to the FISHER method used in DIPS, though in this case the height of the distribution surface above each grid point varies with angular distance from the pole. This distribution is based on the equation for a normal distribution on a sphere:

$$P(\theta) \quad = \quad \upsilon^{K \cos \theta} \, d\theta \qquad\qquad (eq.5.1)$$

where:

$$\upsilon \quad = \quad (K \sin \theta) / (e^K - e^{-K})$$

This equation can be thought to represent an assumed distribution of probable error inherent in the measurement of the orientation in question. In this context, the above equation expresses the probability that a measured orientation actually represents a

true orientation which is an angular distance of between θ and $\theta + d\theta$ of the measured (recorded) vector.

In DIPS, the constant K is calculated such that the value of the probability function has a value equivalent to 5% of its maximum at a distance β corresponding to the cone angle of the counting circle. In other words, the counting circle represents the 95% confidence limit of the Fisher distribution. The function is truncated outside this limit.

If this truncated function defines a distribution over the surface of the reference sphere, the volume under the surface, enclosed within an equivalent and partially overlapping counting circle centred on a grid vector, can be calculated by numerical integration. The ratio of this volume compared to the total volume under the distribution curve defines the contribution of the pole to the concentration total for the grid point. It can be seen that while the new distribution, formed by plotting these integrated and normalised volume ratios with respect to the distance between pole and grid vectors, extends to an angular distance of 2β from the pole centre, the total volume is equivalent to a Schmidt cylinder (radius=β) of influence for the same pole.

Since the grid totals are now normalized with respect to the total volumes under each pole distribution, the grid totals are merely divided by the total number of poles (or total quantity or weighted total represented by all the poles in the data group) to calculate the densities in percent. The derivation of the FISHER method used in this program is outlined in appendix A.

This volume (common to overlapping counting circles) is calculated using numerical integration for a range of ξ values to generate the influence surface in bottom figure

Fisher Distribution

REFERENCE SPHERE

Pole Vector

Grid Vector

Schmidt Influence Cylinder

Fisher Influence Dome

β ξ
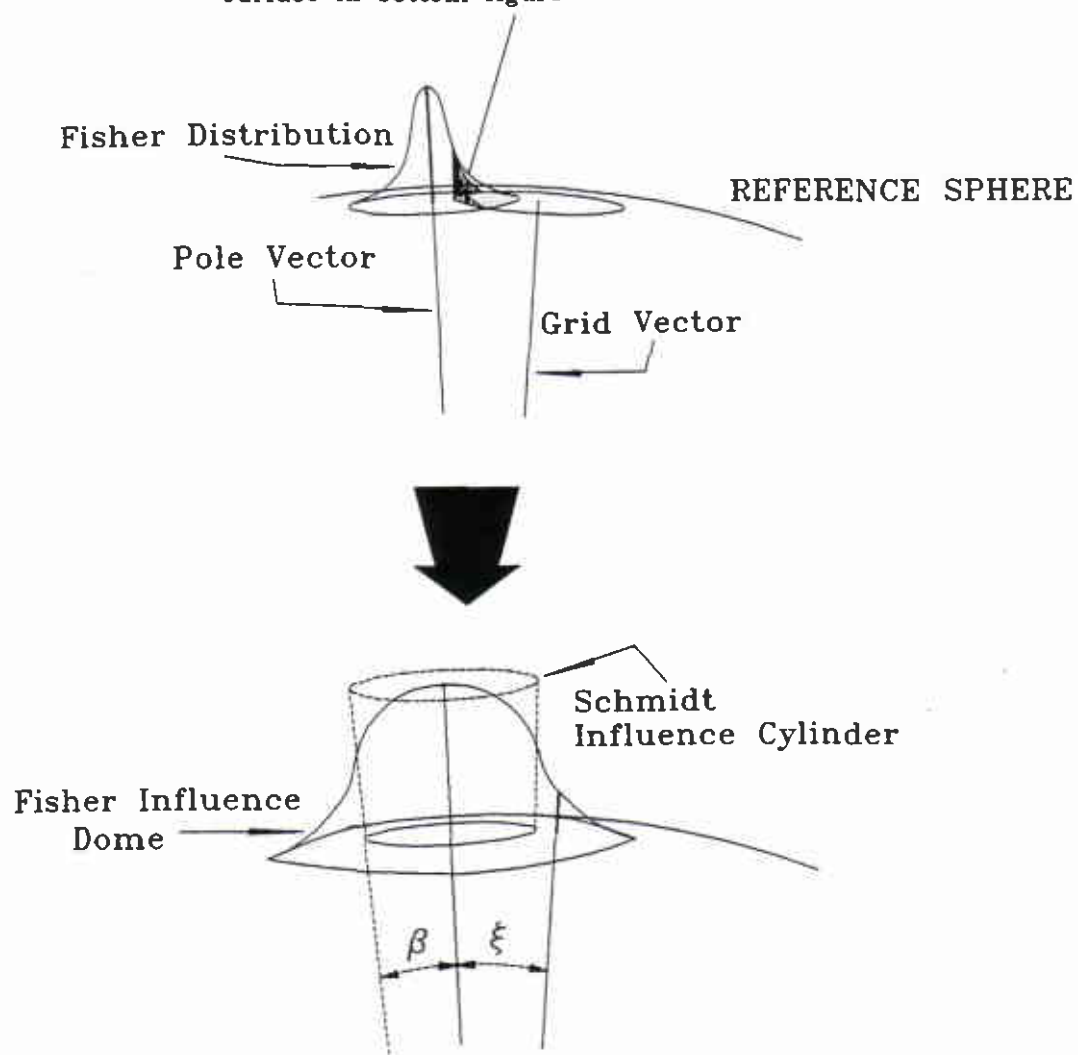
Figure 5.10: Derivation of Fisher influence function in DIPS
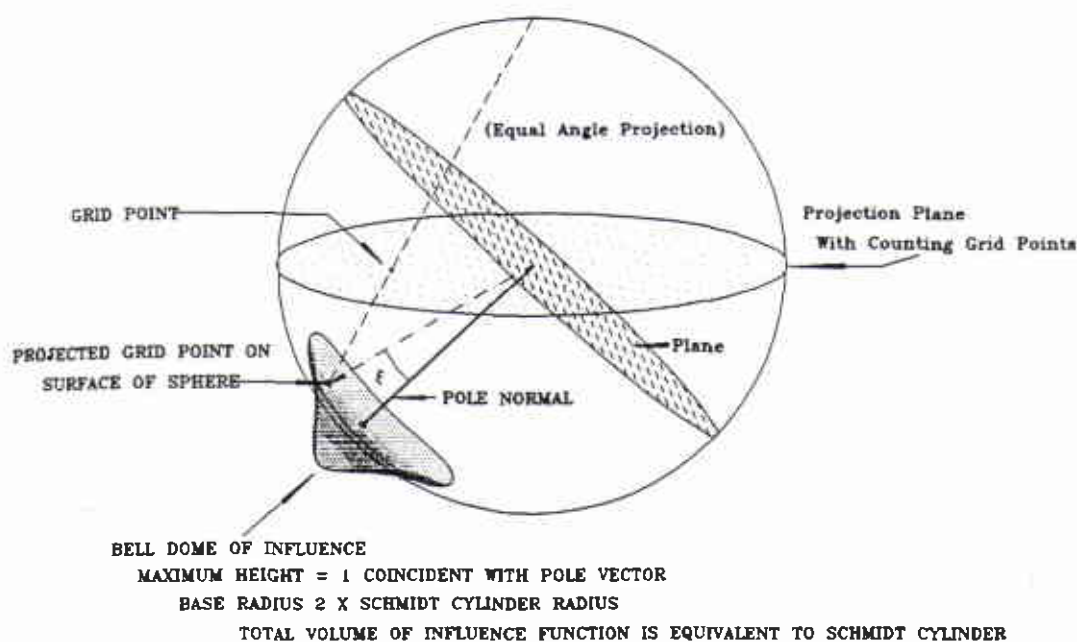
Figure 5.11: Calculation of influence contribution on sphere

The repetitive calculation of the influence contribution for each pole - grid combination would be extremely expensive. Fortunately, it was found that the ratio of contributing volume (for a given grid - pole separation ,ξ) to total volume for a pole was independent of counting circle size when compared to the associated ratio of the dot product, $\cos \xi$, of the grid and pole vectors, to $\cos \beta$ (where β is the cone angle of the counting circle). This permitted the calculation, in advance, of influence ratios for a set of 50 intervals of $\cos \xi$ / $\cos \beta$. This list is then stored in an array, and the actual values as required are interpolated from this list. This greatly improves the efficiency of the Fisher counting algorithm without sacrificing measurable accuracy.
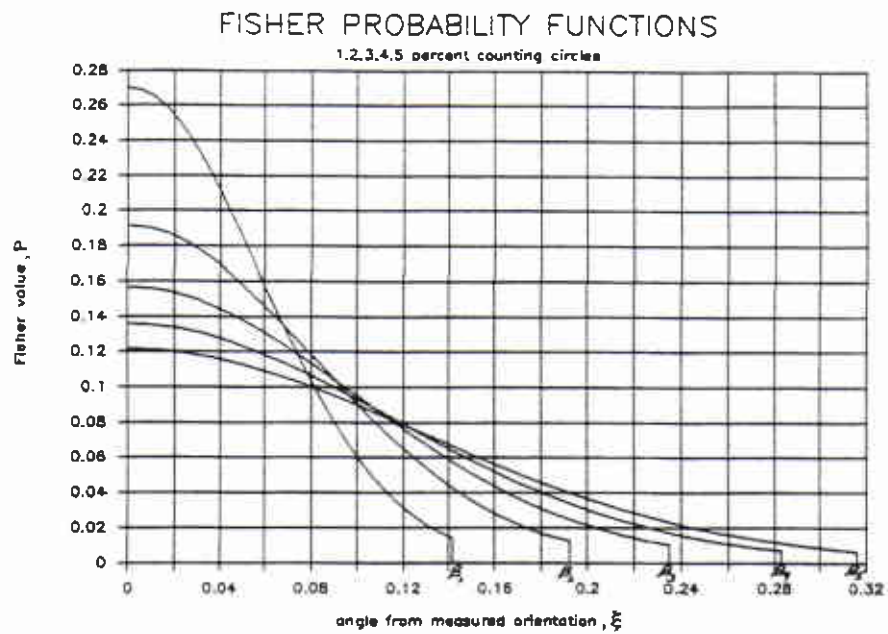
Figure 5.12: Fisher probability functions for varying counting angles, β
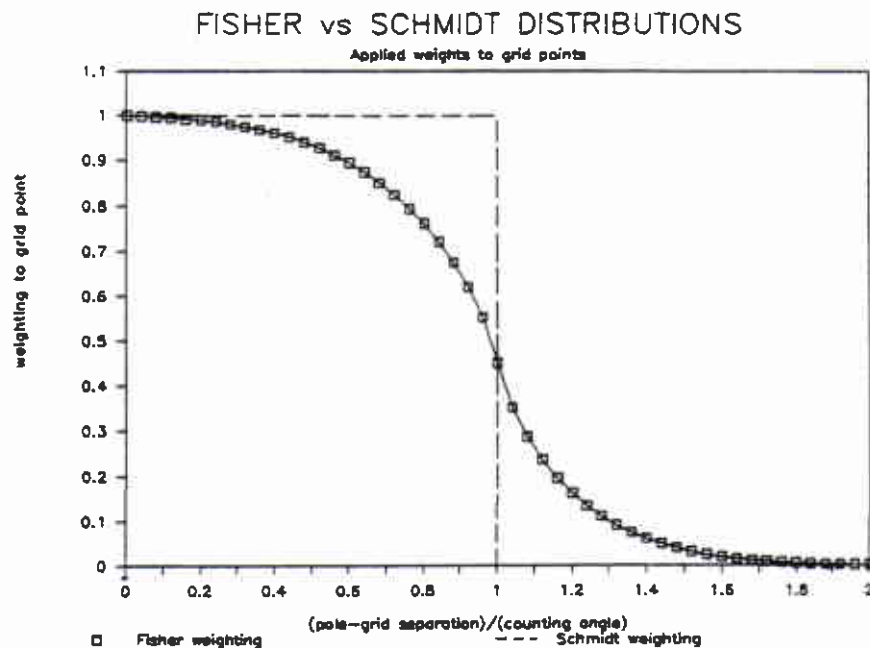
Figure 5.13: FISHER influence function in DIPS as compared to SCHMIDT cylinder

FISHER DENSITY
CONTOURING

1 % counting area

SCHMIDT DENSITY
CONTOURING
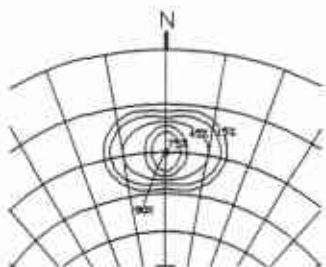
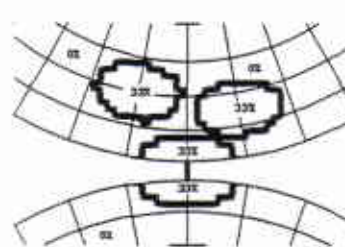EQUAL ANGLE
TWO POLE TEST

POLE SEPARATION
≃ 10 degrees
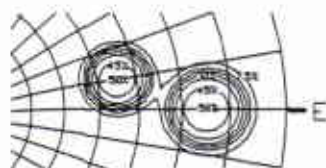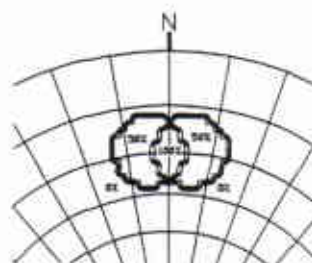
EQUAL ANGLE
TWO POLE TEST

POLE SEPARATION
≃ 22 degrees
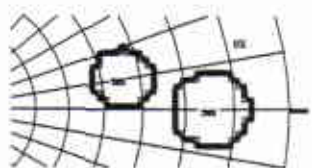
EQUAL AREA
TWO POLE TEST

SAME POLES AS
PREVIOUS TEST
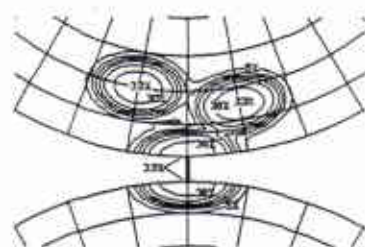
EQUAL AREA
THREE POLE TEST

WITH ONE POLE ON
EQUATOR
(plunge = 0)

NOTE: These plots were created with DIPS 2.1 DXFOUT option
and edited with AUTOCAD Release 10. (See section 5.3.11)

Figure 5.14:Two & three pole testing and comparison of Schmidt and Fisher
density calculation.

5.3.6   Terzaghi Weighting

When performing the contouring calculations described the resultant influences are multiplied by a quantity value for a given pole. This value can be unity for a single unweighted pole, or a user specified value, corresponding to a number of similar features represented by one measurement. This quantity can also be multiplied by a weighting factor to compensate for measurement bias against planar features which are subparallel to the outcrop surface where the measurements were made.

These weights are calculated when the data file is loaded. The traverse number for each data unit references a particular traverse orientation. The angle between the line or surface of the traverse and the feature in question is calculated in one of two ways and used to calculate an appropriate weighting factor.

The weighting is calculated as:

$$\lambda_{pole-north} = \cos(\text{pole trend}) \cdot \cos(\text{pole plunge})$$
$$\lambda_{pole-east} = \sin(\text{pole trend}) \cdot \cos(\text{pole plunge})$$
$$\lambda_{pole-down} = \sin(\text{pole plunge})$$

For LINEAR traverses:

$$\lambda_{trav-north} = \cos((\text{traverse trend}) + \text{declination}) \cdot \cos(\text{traverse plunge})$$
$$\lambda_{trav-east} = \sin((\text{traverse trend}) + \text{declination}) \cdot \cos(\text{traverse plunge})$$
$$\lambda_{trav-down} = \sin(\text{traverse plunge});$$

For PLANAR traverses:

$$\lambda_{trav-north} = \cos((\text{traverse normal trend}) + \text{declination}) \cdot \cos(\text{traverse normal plunge})$$
$$\lambda_{trav-east} = \sin((\text{traverse normal trend}) + \text{declination}) \cdot \cos(\text{traverse normal plunge})$$
$$\lambda_{trav-down} = \sin(\text{traverse normal plunge});$$

$A =$ cosine of angle between pole and traverse orientation or traverse normal (dot product)

$$A = \textit{pole} \cdot \textit{traverse} = \lambda_{trav-north} \cdot \lambda_{pole-north} + \lambda_{trav-east} \cdot \lambda_{pole-east} + \lambda_{trav-down} \cdot \lambda_{pole-down}$$

w =   weighting applied to the pole for weighted contouring
and mean calculation

For LINEAR traverses:

$$w = 1 / A$$

For PLANAR traverses:

$$w = 1 / \sqrt{(1 - A^2)}$$

NOTE that in the above cases, $w \rightarrow \infty$ as $A \rightarrow 0$ for a LINEAR traverse and as $A \rightarrow 1$ for a PLANAR traverse. This is avoided by specifying a lower or upper limit, respectively, on A. For a LINEAR traverse in DIPS this limit corresponds to the sine of a user specified minimum angle. For a PLANAR traverse, the maximum A is equivalent to the cosine of this minimum angle.

Density contributions calculated by the Schmidt or Fisher method for given pole - grid vector combinations are multiplied by this weighting, w, and added to the grid point total. The individual grid point totals are then divided by a weighted total for the whole population to obtain the percentage density values plotted.

Because the weighting tends to infinity as the traverse and planar feature become parallel, a limit can be set by the user for minimum angle and therefore, for maximum weighting factor. In addition, since judgement and care is required when using a weighted plot, both unweighted and weighted concentrations are calculated at the same time. Both plots can be instantly generated and compared. If a high concentration appears in the weighted plot, but is totally absent in the unweighted plot, it is advised that the user interpret this cluster with caution. A single measurement which closely parallels the traverse can take on an exaggerated importance in the weighted plot (figure 5.19). The user must decide whether such a measurement warrants serious consideration without the backing of other similar measurements.

5.5.7   Contouring the Grid Values

Once the weighted and unweighted grid point densities have been calculated, the grid values are assigned to the associated projected points on the stereonet overlay. This square array of values is then contoured using linear interpolation in two dimensions to generate the continuous contours shown in figures 5.14 - 5.15. A simple line contouring routine (Bourke 1987) is also used to generate line contour plots if desired. The line contour plot is shown in figure 5.16.
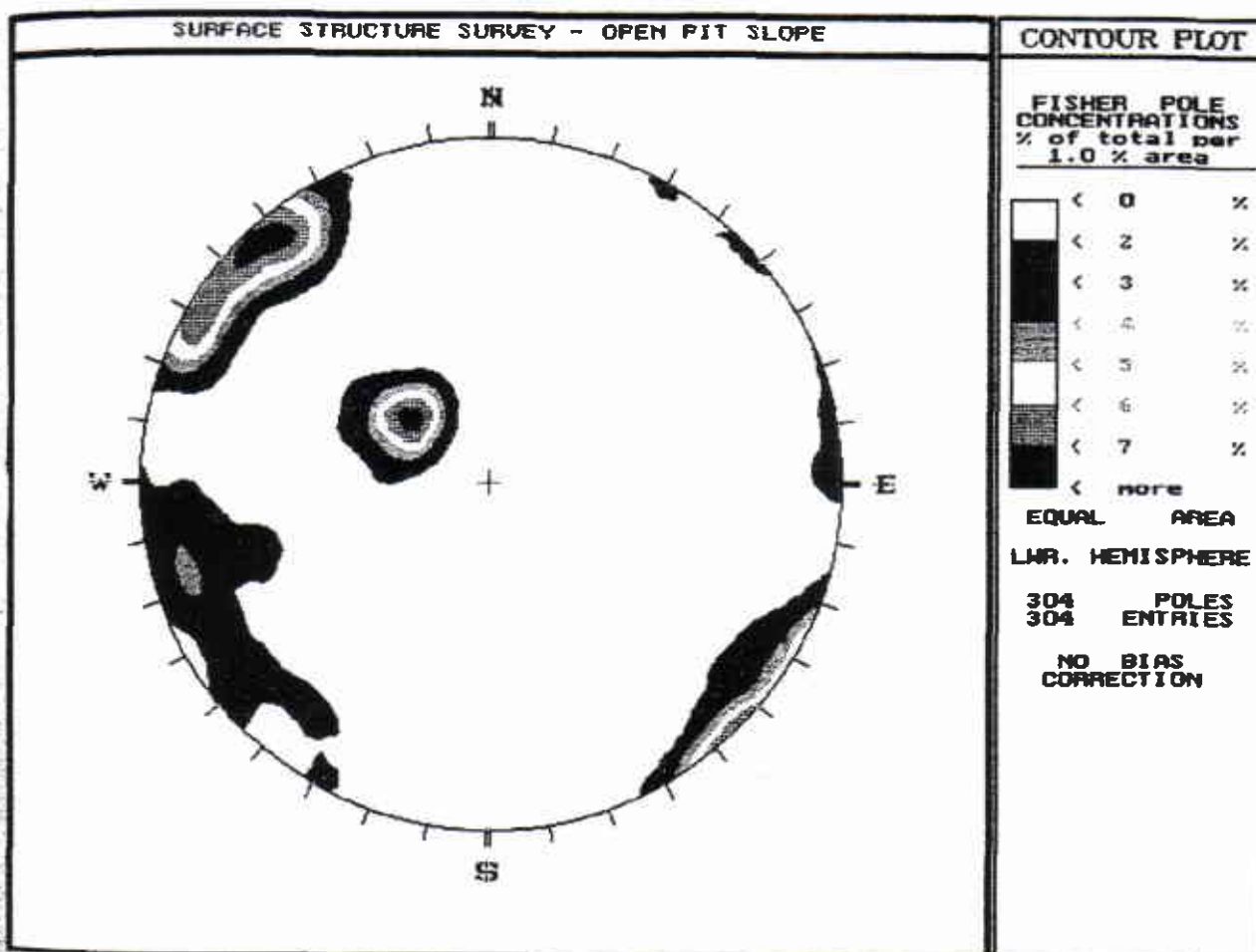

Figure 5.15: DIPS colour contour plot (same data as manual plot in fig 3.14)
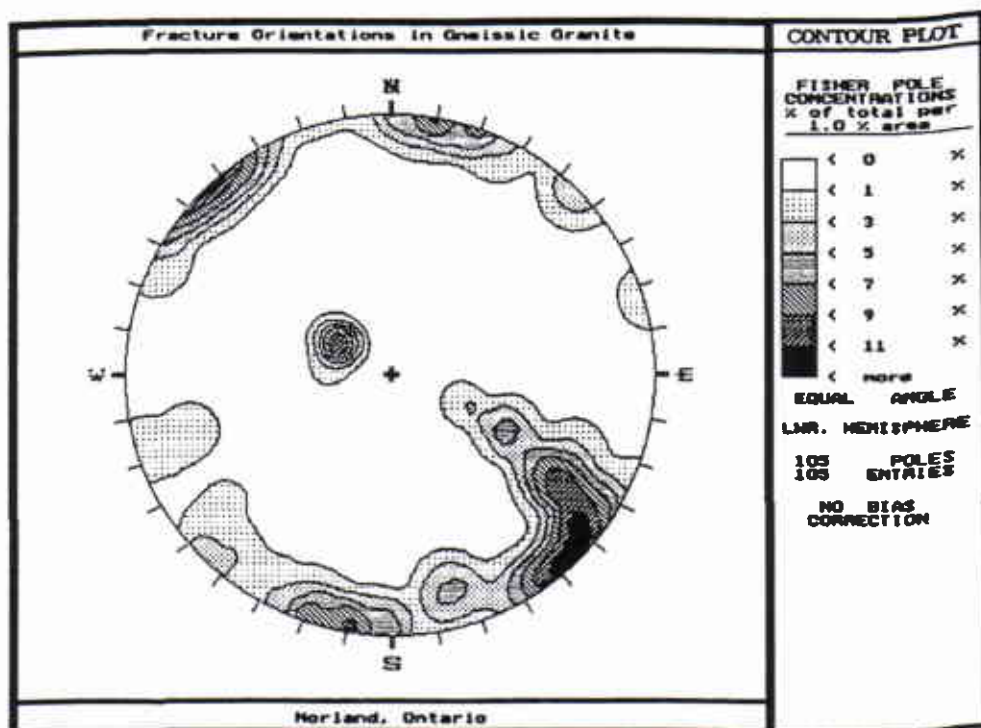
Figure 5.16: Stippled contour plot (data from Wallach 1990)
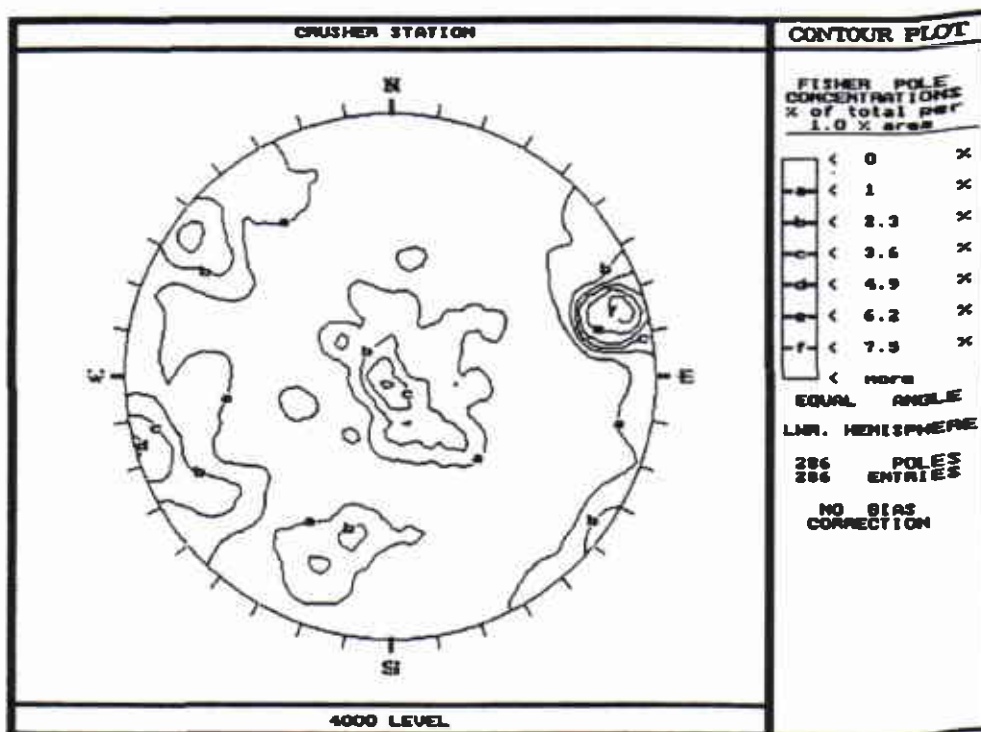
Figure 5.17: Line contour plot (data from De Azevedo 1990)
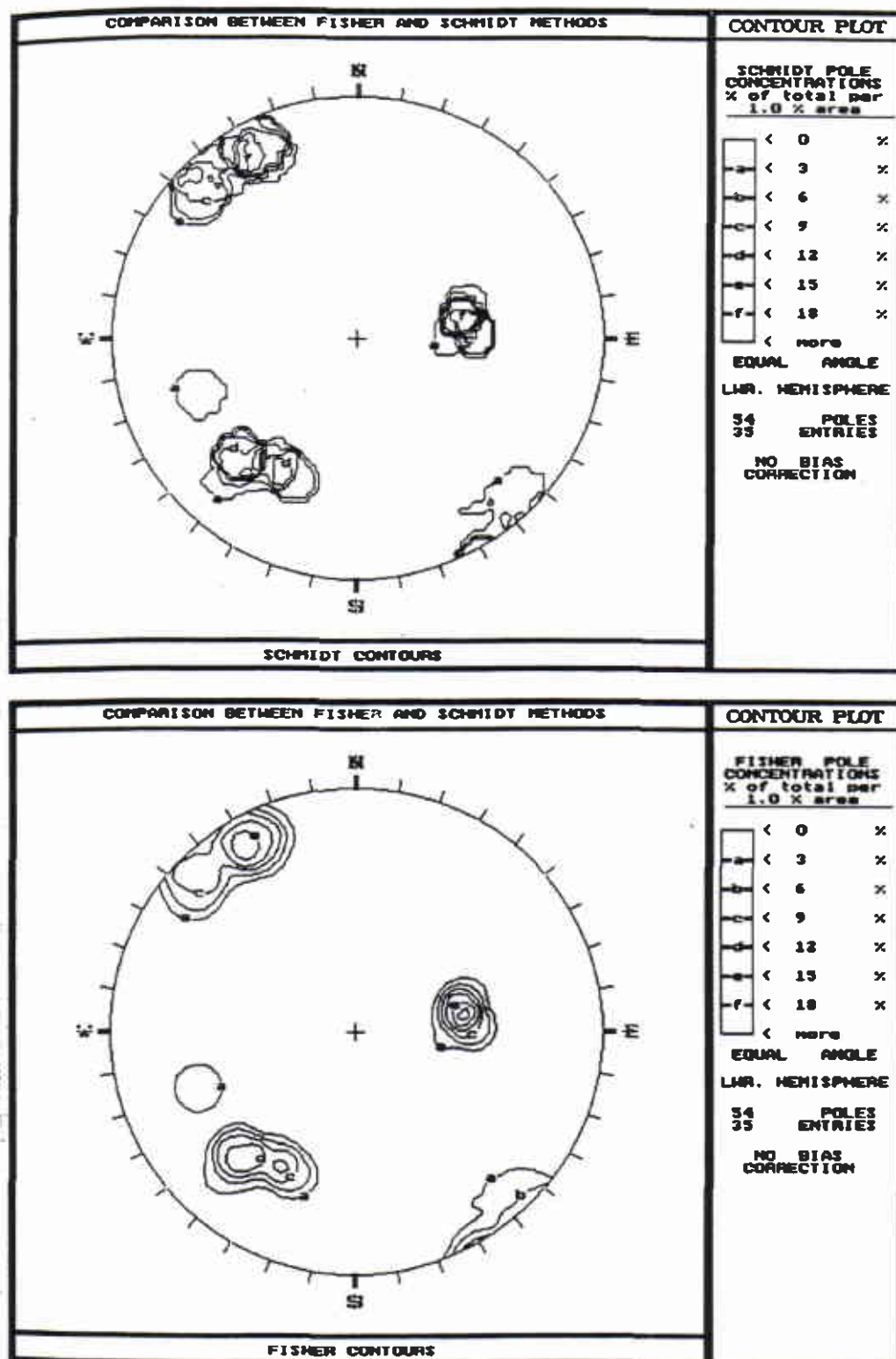
Figure 5.18: Comparison between Schmidt and Fisher density contours
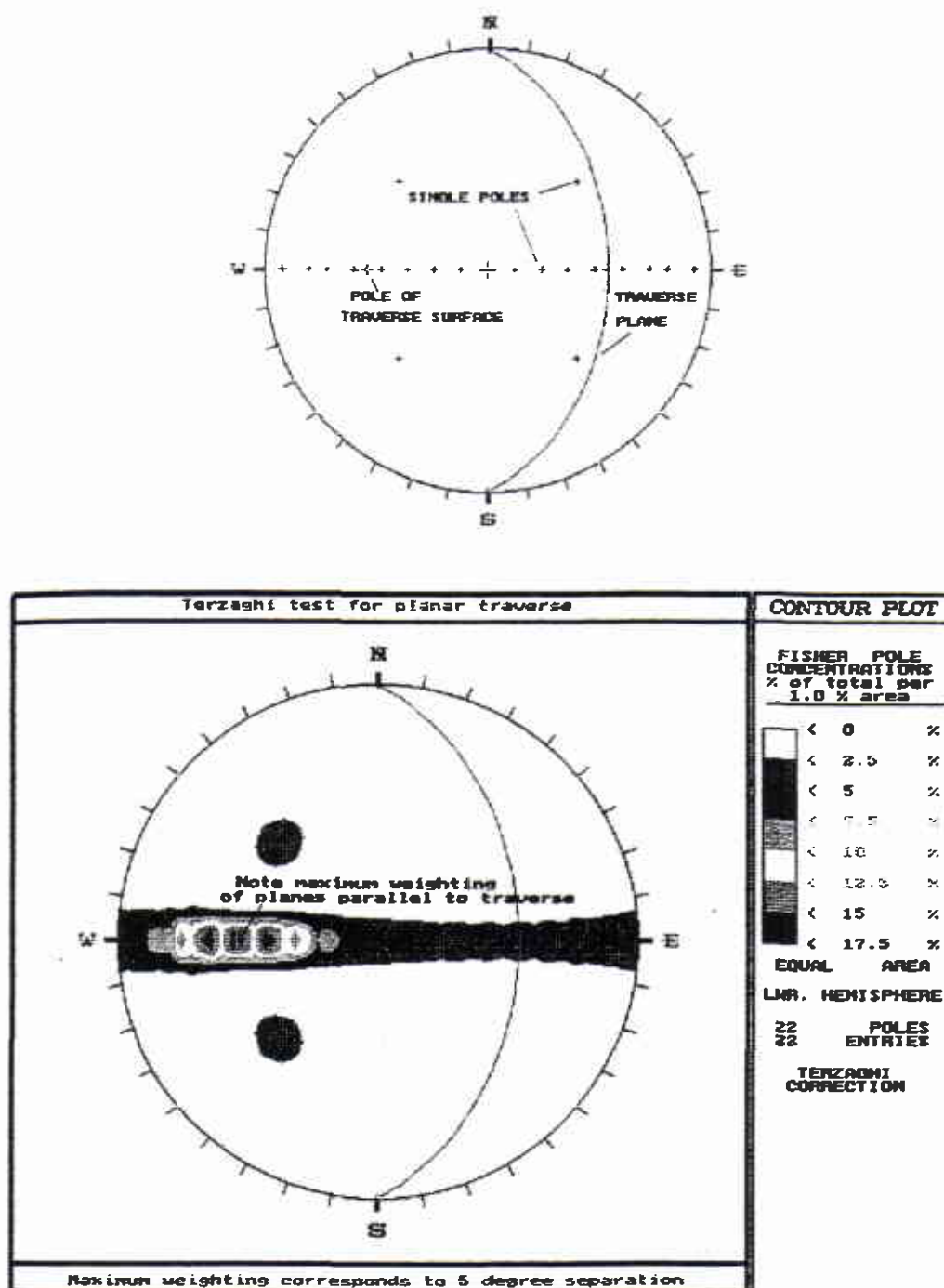
Figure 5.19: Effect of Terzaghi weighting

5.3.8   **Reduction of Data to Dominant Orientations**

The DIPS contour plot permits effective visual analysis of orientation patterns. Once clusters of data have been identified, DIPS provides two methods of reducing these to representative orientations. The first follows a methodology similar to the manual method.

The LOCATE POLES option allows the user to select with a cursor (using the cursor keys or the mouse), distinct orientations from the stereonet. The density contours can be used, for example to select the direction of maximum pole density within a cluster as the representative orientation. Certain individual features such as continuous faults can also be singled out in this way for special consideration. The orientations of any features can be interactively resolved using this cursor. As the cursor moves about the screen, the corresonding orientation is instantaneously displayed on the upper status line (fig 5.20).
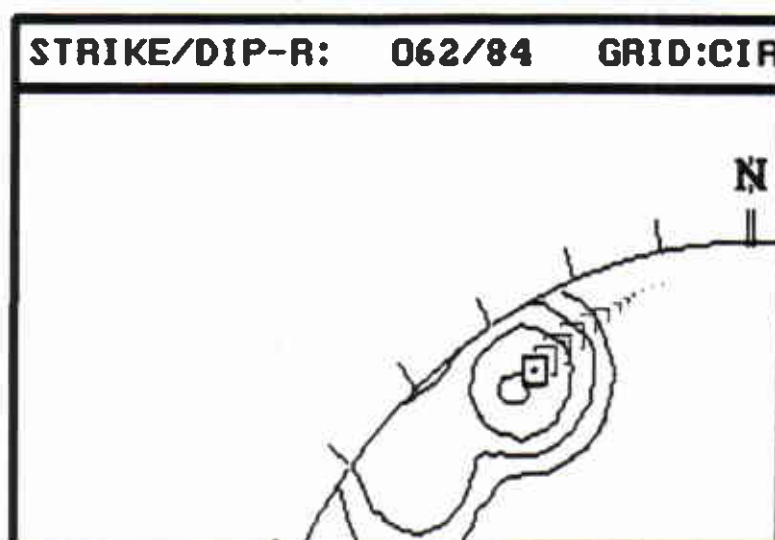
STRIKE/DIP-R: 062/84   GRID:CIR

Figure 5.20: Screen cursor and orientation readout in DIPS

The SET WINDOWS option in DIPS is somewhat more sophisticated. Using the cursor, the user can interactively enclose an entire data cluster within a 'rubber-banding' window. Once the window limits are confirmed, the data within the window limits (specified as a ranges of trend and plunge) are assigned a set number. The mean pole within the window is calculated automatically. Both weighted and unweighted poles can be calculated and plotted, along with their equivalent planes.

The method used in DIPS involves simple vector addition of all pole vectors within the window. The resultant vector (calculated from the component sums of pole direction cosines) is then normalized with respect to its magnitude to yield a mean unit pole vector. For weighted means, the scalar weight for each pole is multiplied by each of the pole's direction cosines before inclusion into the vector summation.
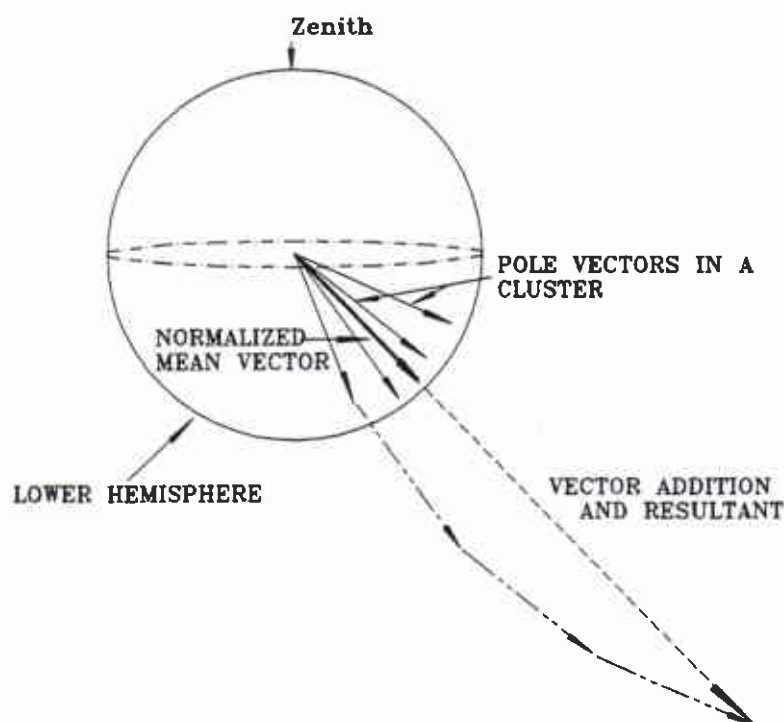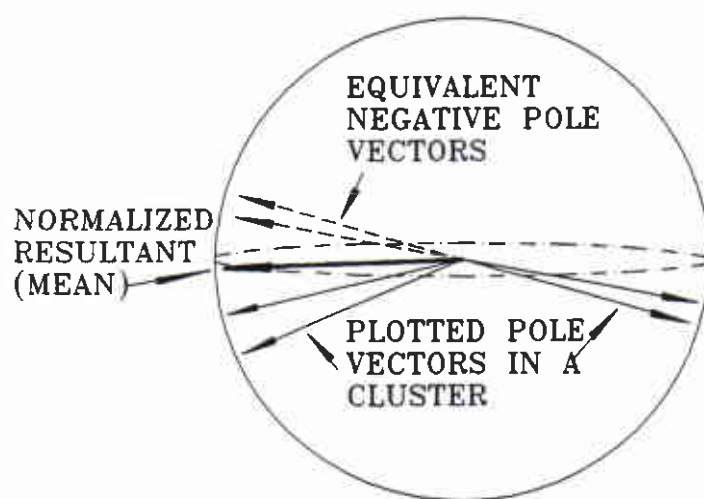

Figure 5.21: Mean vector calculation

Figure 5.22: Mean calculation near equator

The 'rubber' window in DIPS is allowed to wrap around to the other side of the stereo net as required. Poles in this wrapped portion of the window are assigned a negative indicator flag. When calculating the mean vector for a wrapped window, these flagged vectors must be converted to their negative normal counterparts (ie. their direction cosines must be multiplied by -1) before summed with the rest of the vectors. This insures a correct mean for a set of sub-horizontal poles.

The vector addition method was chosen for its simplicity and ease of user application. In the future, an external post-processor may be developed which will utilise eigenvector methods to allow more complex cluster analysis. For most

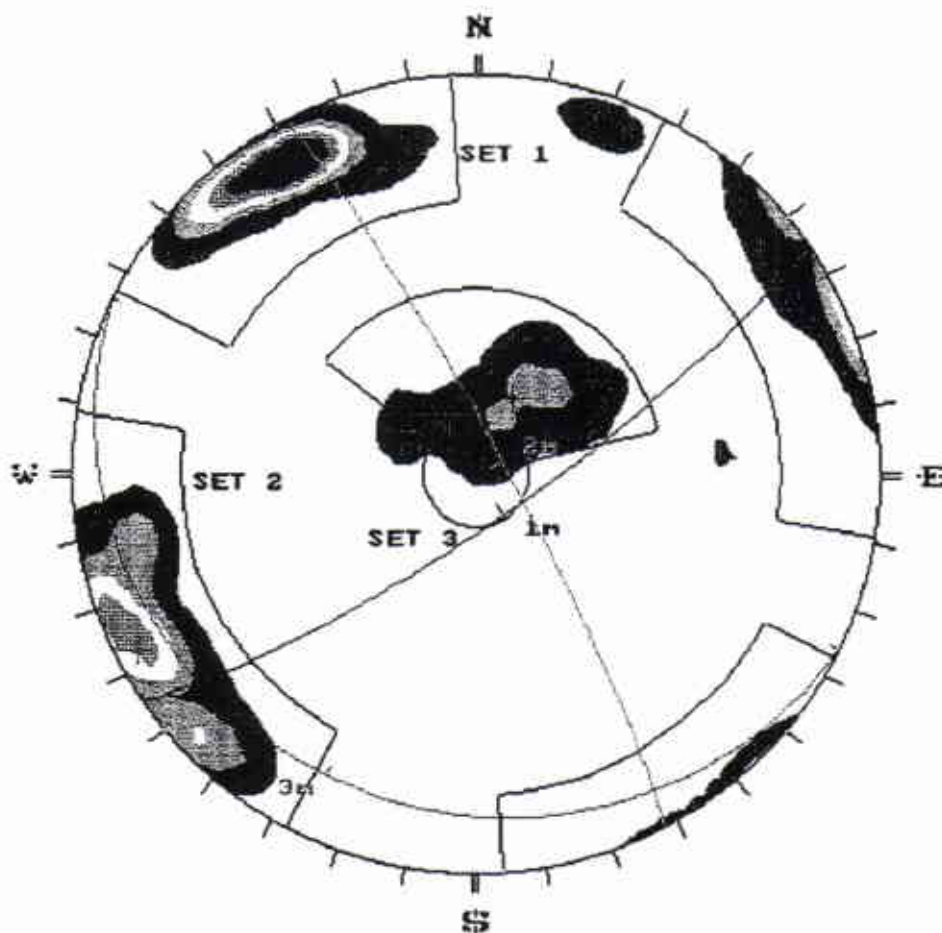applications and user requirements, the method used in DIPS was deemed to be sufficient.

Figure 5.23: DIPS windows and calculated mean planes

The set numbers assigned to the data within a window may be used internally, for the creation of joint-set-specific histograms for various feature attributes (figure 5.24). This is useful when performing a rigorous Q classification (Barton 1974), for example. Files may also be written to disk which contain processed orientations, bias correction weights and set numbers. These can be easily incorporated as input to additional packages such as visualization tools or block size and geometry analysis packages (Peaker 1990).
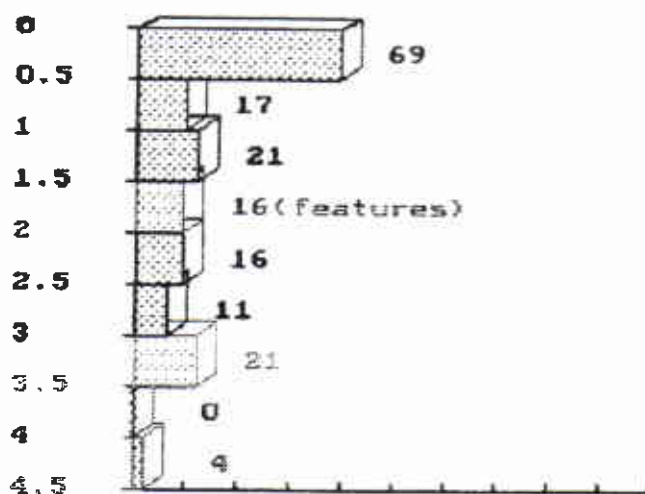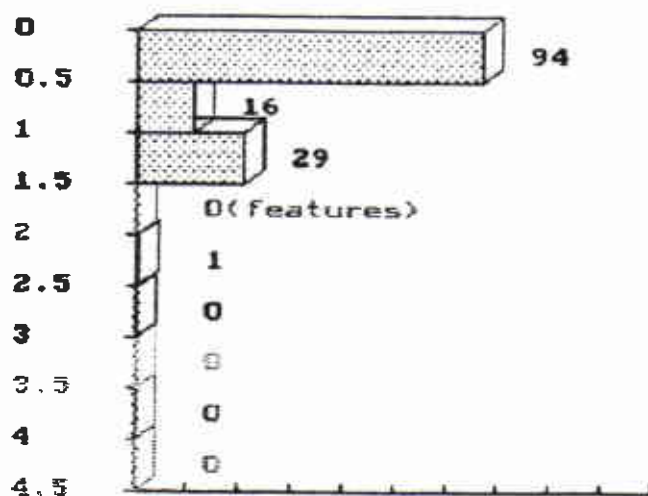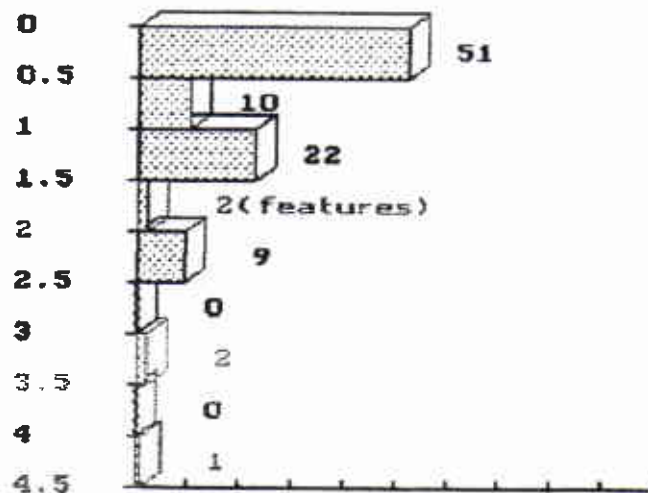
Figure 5.24: Set-specific attribute histograms (joint spacing)

5.3.9   Manipulation of Distinct Planes

DIPS permits plotting of selected and calculated orientations on a separate plot if desired. The planes are generated using the vector rotation method described earlier in this section. A legend can be generated giving the exact orientations represented.

A number of tools may be used with any of the various plot options described. Those most useful at this stage include the polar and equatorial grid overlays. The equatorial grid may be plotted at any meridian trend to illustrate a variety of relationships. DIPS also allows the plotting of small circles centred about any orientation on the stereonet. These are useful when performing stability assessment on the DIPS stereonet. In addition a rubber-band great circle may be moved throughout the stereonet and may be combined with a pitch or apparent dip grid for visual assessment of such relationships as the angle between intersecting planes (fig. 5.25). As discussed earlier, the intent of these and other interactive graphical tools is to mimic the flexibility of the original manual stereonet method.

Any or all of the data, as well as the selected distinct orientations may be rotated about any arbitrary axis. This is particularly useful for generating inclined hemisphere projections (fig. 5.28). These projections are identical to the lower hemisphere stereonet discussed throughout this work, with the exception that the stereonet equator is no longer horizontal. The inclined hemisphere is used for assessment of free wedge formation in inclined excavation backs or sidewalls (Priest 1980).

Rotation of data can also be useful for comparing different data sets which may be geometrically similar but sympathetic to a folded bedding, for example. Rotation of the data in one set by the relative angle of folding may confirm suspicions that the data sets are similar and allow prediction of geometries farther along the fold (Carter,1989).

Several features in the DIPS package are illustrated in the following figures and more are described in detail in the manual in appendix B.
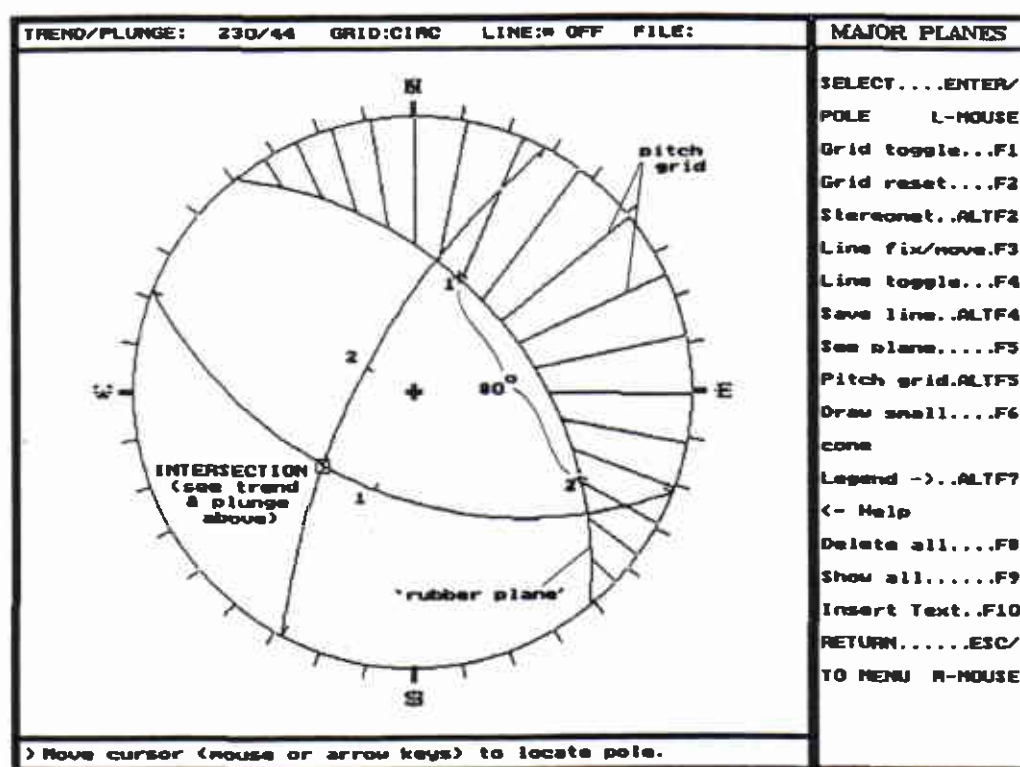

Figure 5.25: Solution for angle of intersection for two planes using rubber plane and pitch grid options.
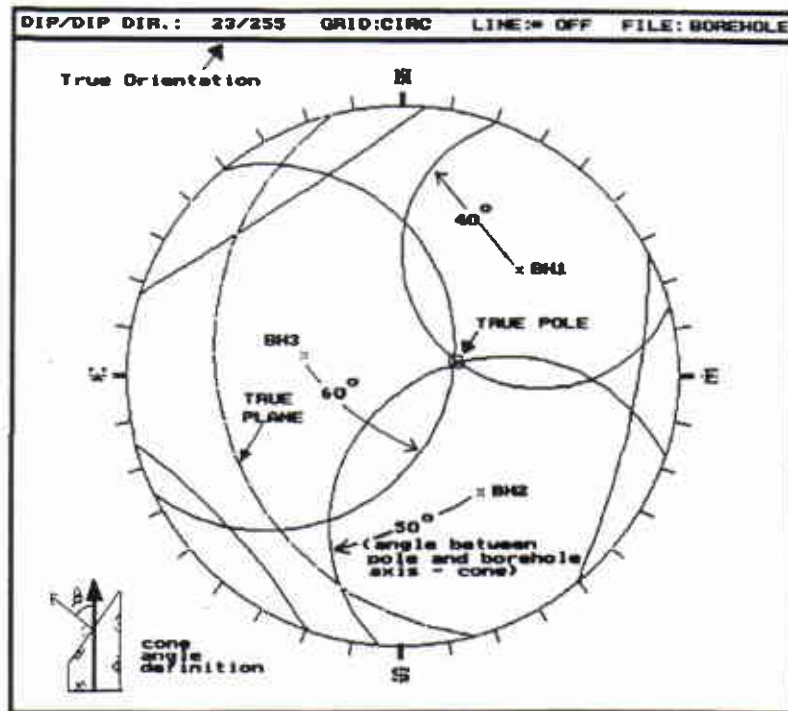
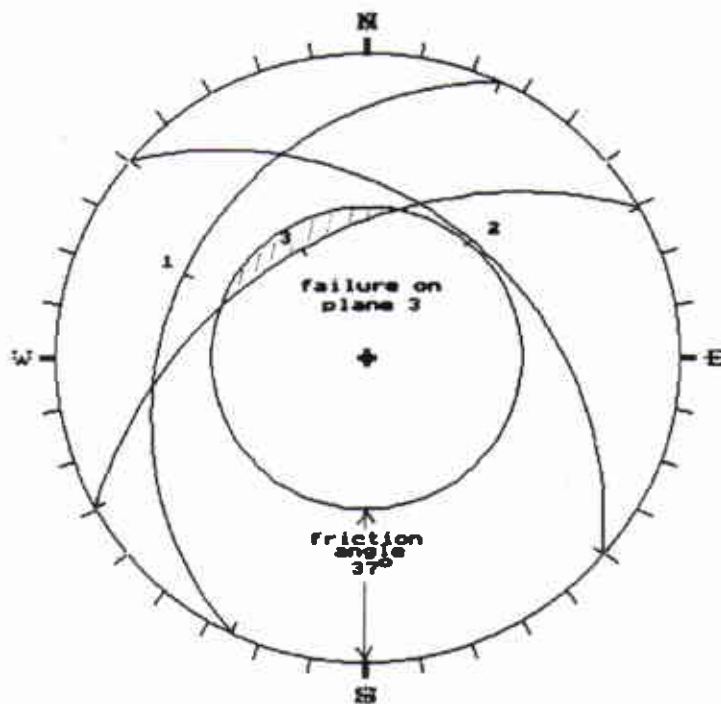**Figure 5.26:** Small circles used to solve true orientation of marker bed from unoriented core.

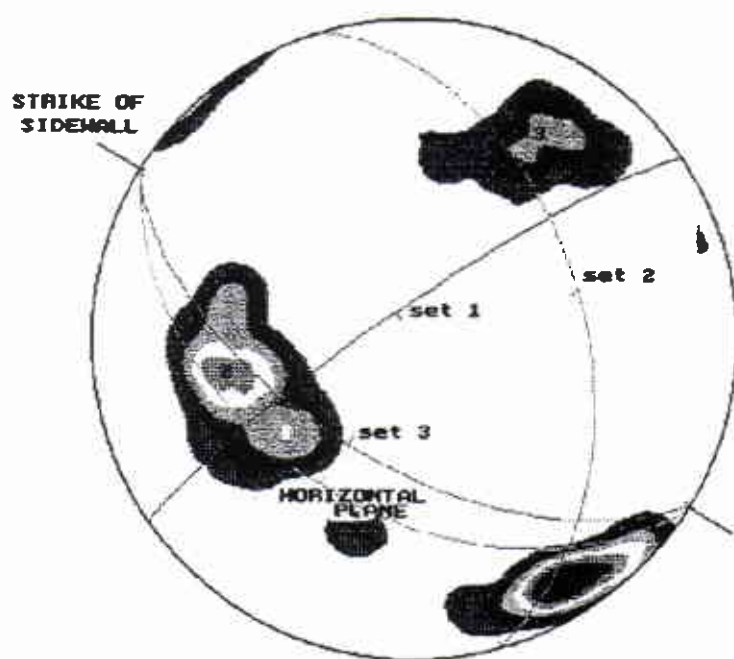**Figure 5.27:** Kinematic and stability study using small circles

Figure 5.28: Inclined hemispherical projection using rotate data option (data from fig 5.23)

5.3.10 The DIPS Database

One of the unique features of DIPS as a integral stereographic analysis package is its easily accessible data base. Any of the columns in the data file may be used in parallel, to filter and select, from a main data file, a subset of data which meets any combination of selection criteria. This can be useful for assessment of structural domains. All measured data from a project may be stored in a single data file and subsets corresponding to spatial locations or rock domain, as examples, may be interactively selected and plotted. The example in figure 5.29 illustrates how subsets corresponding to spatial location and rock type yield different structural domains.
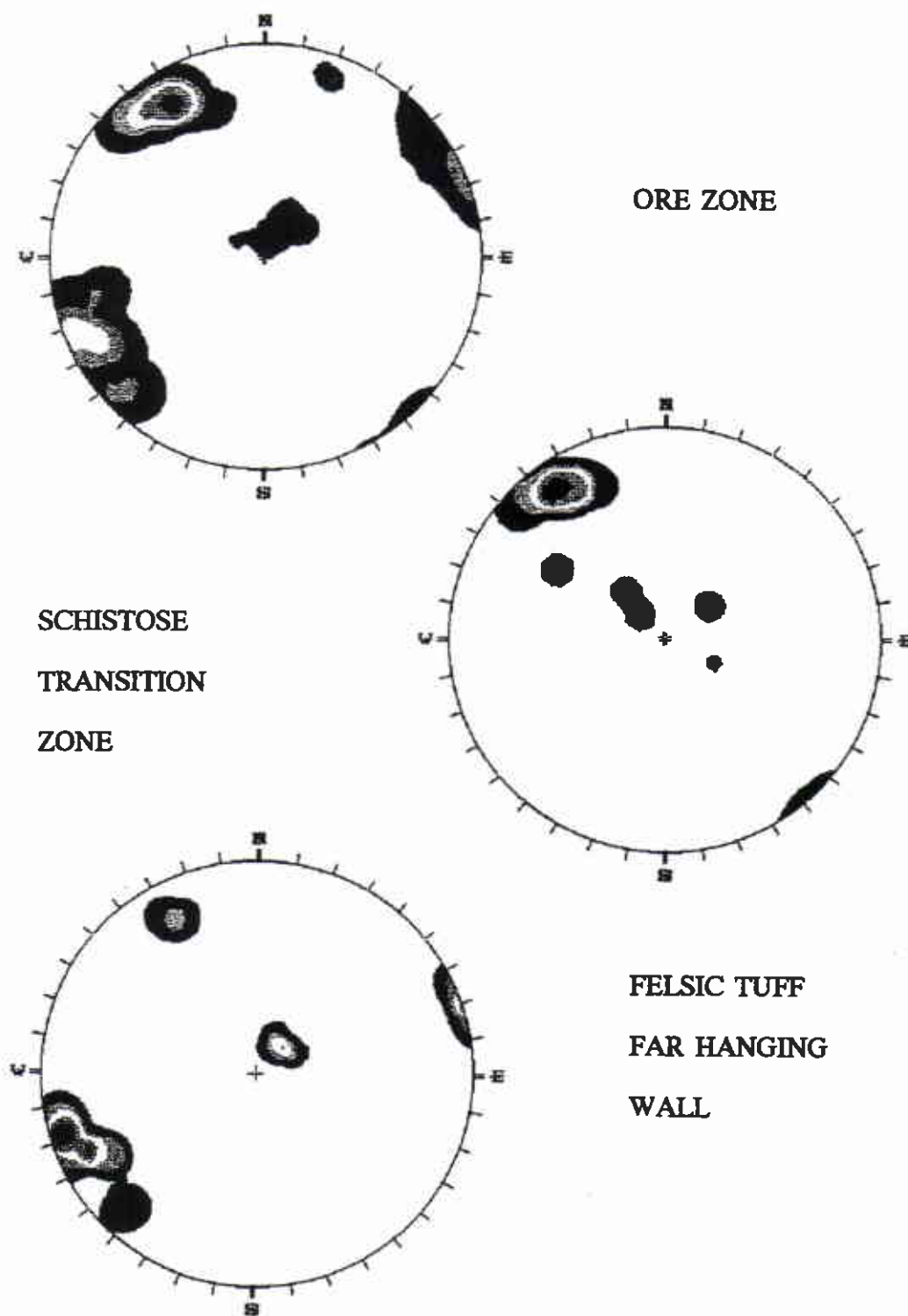
ORE ZONE

SCHISTOSE

TRANSITION

ZONE

FELSIC TUFF

FAR HANGING

WALL

Figure 5.29: Structural domains revealed through data screening (data from fig 5.2)

This database may also be used to filter data according to joint continuity or aperture, for example. If the data set is difficult to interpret, such filtering may be necessary in order to assess dominant structure.

The data base also allows local assessment of structure from a mine-wide data base. Such databases are becoming more common in canadian mining practice (Noranda 1989).

5.3.11 Hard Copy Output

It was decided early in this and other software development projects at the University of Toronto, that it was not the mandate of the group to invest a great deal of time developing printer drivers for the vast array of different printers on the market. Instead, it was seen as more efficient to prepare the screen in a fashion which would allow a screen dump to a printer or file using commercially available utilities. Pizzazz Plus by Applications Techniques Incorporated is one such utility and the one most commonly utilized at the time of this work by the group at the University of Toronto. This utility, and others like it, support a wide variety of printers and screen graphics cards.

DIPS has HARD COPY options in all of the plot menus. This option prepares the screen with titles and a legend. This display can then be captured by a print screen utility. The screen display can be printed directly to a printer or saved to a file which can be imported by a word processing package.

A file creation option has also been created which writes the plots and associated legend information to a Drawing Exchange File (DXF) which can then be imported by AutoCad (A computer aided drafting and design package by AutoDesk). AutoCad supports a wide range of plotters and printers and can be used as a picture editor to customize DIPS plots to fit company forms for example. The screen capture plots can be seen throughout this work while examples of DXF output are shown in figures 5.30 and 5.31.
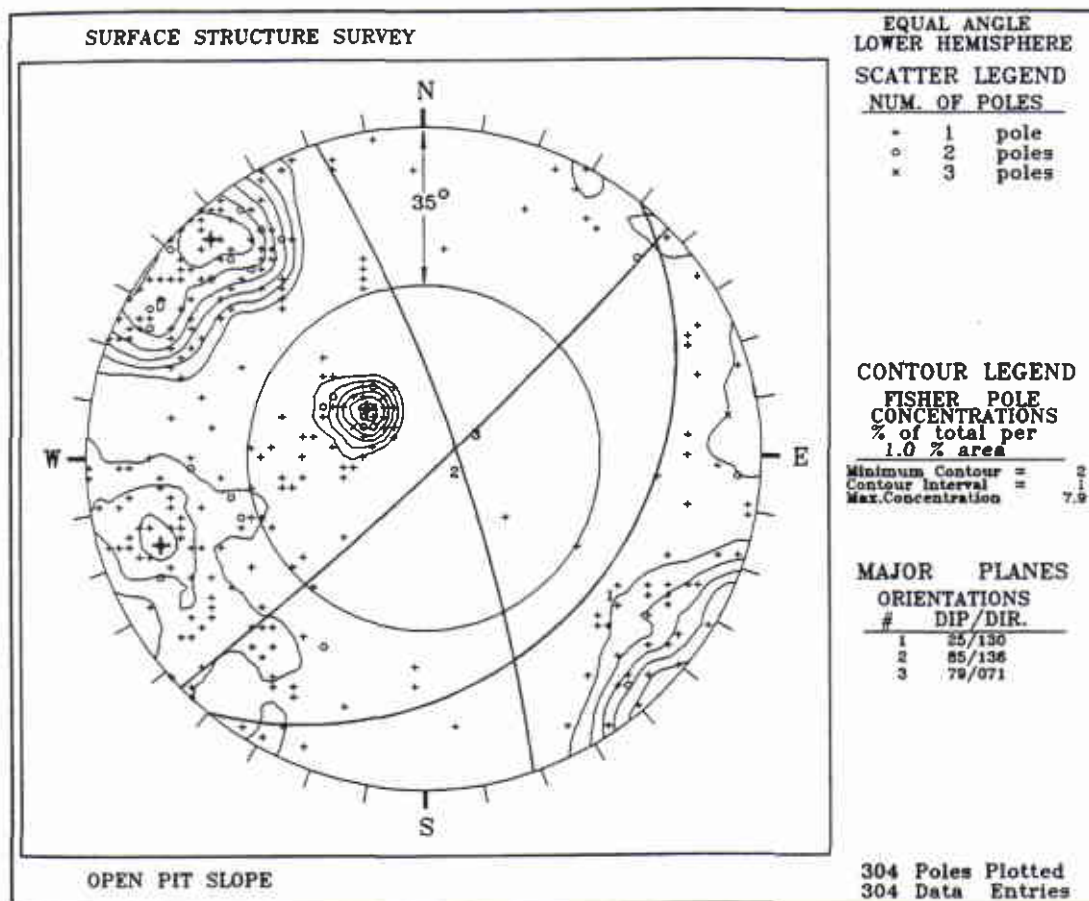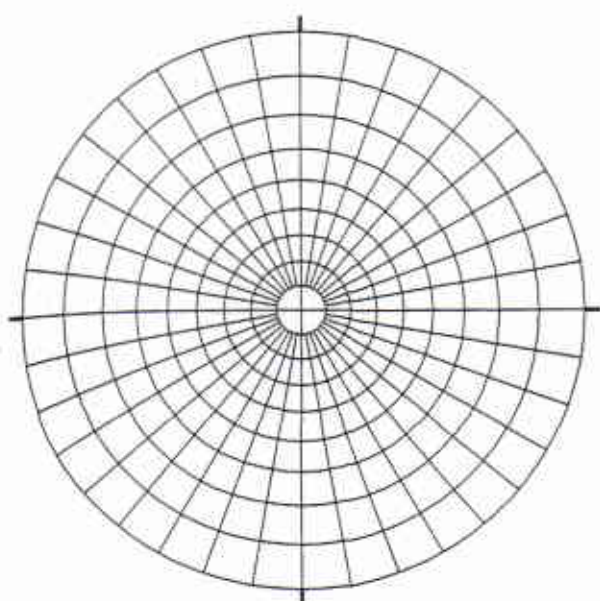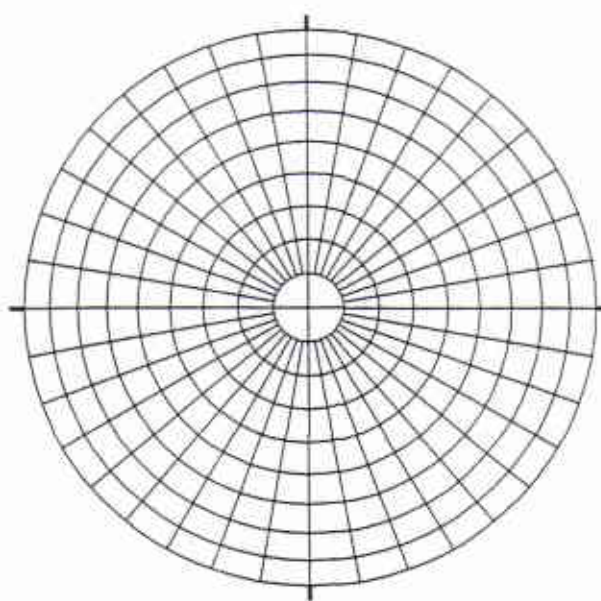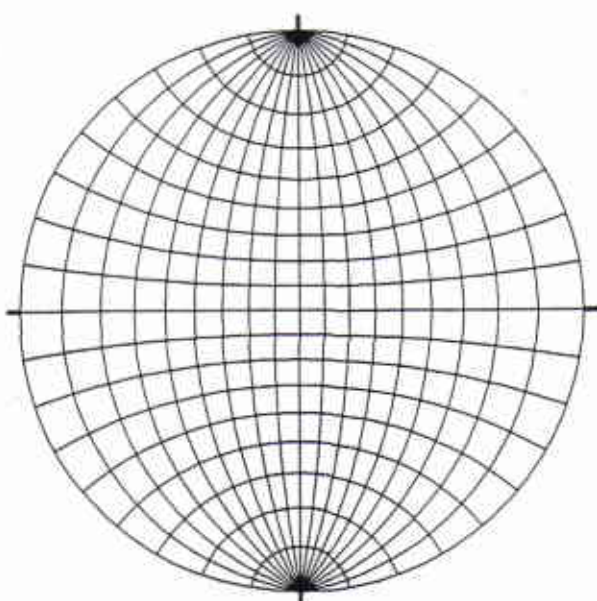

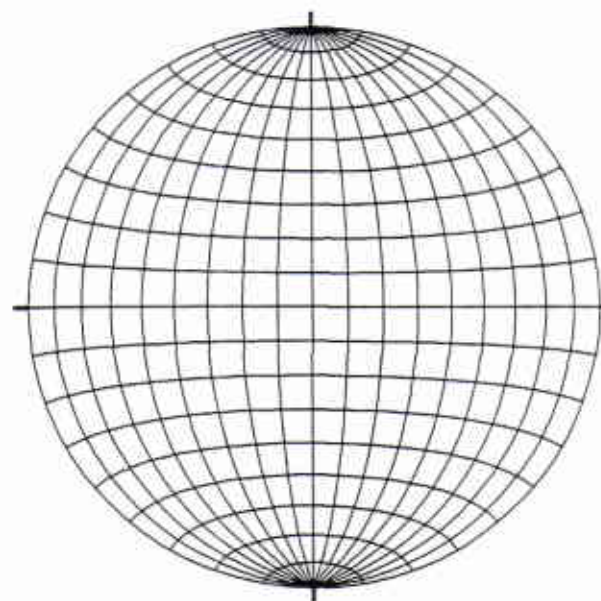**Figure 5.30:** ACAD output using DXF file creation with DIPS

POLAR EQUAL ANGLE NET

POLAR EQUAL AREA NET

EQUATORIAL EQUAL ANGLE NET

EQUATORIAL EQUAL AREA NET

Figure 5.31: DXF reference grids from DIPS - compare to figure 3.7

6.0   CONCLUSION

The main objective of this project was not to merely improve on the static presentation tools previously developed using spherical projection, nor was it an objective to create a black box statistical analysis tool for orientation data. The primary goal was to bring to the computer environment the interactive and illustrative nature of manual stereographic analysis, and to create an integrated package which would permit varying degrees of subjective as well as computational analysis through most phases of orientation analysis.

Although the background of the author dictated a design philosophy influenced by the requirements of engineering structural analysis, it was also felt that such a tool should accommodate any application in which orientation formed an important component of the data base. Within each field of application, it was felt that no preferred conventions existed among practitioners regarding either input format, data notation, or desired presentation style. A computer package would have to take the form of a toolkit and be as flexible and as robust as possible in these regards.

By utilising the computation power of the computer, it was felt that any simplifying approximations in the manual method, such as fixed and inaccurate statistical counting windows for density contouring, as well as errors introduced by contouring on the two dimensional projection, could be efficiently eliminated by performing all calculations in three dimensions on the surface of the reference sphere, using the projection only for presentation.

Since visualization is a major advantage of stereographic analysis, any package created during this work would have to utilize up to date computer graphics and animation techniques wherever possible both for interactive analysis and final report quality presentation.

Finally, it was the opinion of this author that the package should be able to treat an input file as a database from which data could be selectively screened to interactively retrieve user defined subsets for analysis. This data base would also have to accommodate non-orientation data associated with each data unit. This additional data could then be analyzed in various ways in addition to orientations.

The program DIPS, developed as part of this work at the University of Toronto, satisfies all of these initial criteria. The program has gained wide acceptance internationally as both an educational and practical engineering tool. Feedback from a wide variety of users regarding the interactive and graphical format of the program indicates that most of the authors initial objectives have been adequately met.

6.1   FUTURE DEVELOPMENT

At this stage, it is the feeling of the author that any further additions to the DIPS package within the main program would only increase the complexity of the working environment and would take away from the "user-friendly" nature of the program. Future enhancements to the program would therefore be more desirable in the form of add-on modules.

One desirable addition would be a customised data input program for DIPS file creation. This would eliminate the need to use a third party program for creating data files. This was originally thought to be an important component of this work, with the current system considered an unnecessary bother. It seems, however, that most users have been accustomed to storing their data in files created by commercial spreadsheet programs or ASCII editors. Others have developed customised electronic databases as part of their own systems. The free format of the text input file has permitted easy adaptation to systems already in place. This input module is, therefore, deemed less vital to the package then it was originally thought Such a tool would, nevertheless, be a useful addition to the DIPS package.

Once data clusters have been delineated by the user, it may be desirable to perform more complex analyses on the individual sets. Examples of such applications can be found in Peaker 1990, Zanbak 1977, Fisher 1953, Markland 1974, and others. There has been some limited demand for a statistical post-processor as part of the DIPS package, primarily from academic users. The simple mean vector calculation performed within DIPS was deemed to satisfy most field requirements. A more

sophisticated external module could be created, which would accept a processed output file from DIPS. Such a file can already be created and has been used for rigorous statistical processing of orientation and spacing data for joint sets (Peaker 1990).

The author intends, at a later date, to incorporate DIPS as a pre-processor for a statistical rock block analysis and structure visualisation package for underground excavations. At the time of writing, suitable keyblock analysis codes (Shi and Goodman 1990) are being evaluated for incorporation as an integrated support design tool for blocky ground.

The free format input and output files for DIPS have been designed to facilitate incorporation into other systems without the need to alter the internal coding of the DIPS program. The program in its present form should be adaptable to a wide variety of applications as they become available.

REFERENCES

ATTEWELL, P.B. and I.W. FARMER (1976). Principles of Engineering Geology. London: Chapman and Hall, pp 328-335.

ATTEWELL P.B. and J.P. WOODMAN (1972) "Stability of discontinuous rock masses under polyaxial stress systems." Proceedings. 13th Symposium on Rock Mechanics. ASCE. New York. pp 665-683.

BARTON, N., R. LIEN and J. LUNDE (1974) "Engineering classification of rock masses for the design of tunnel support." Rock Mechanics. 6. pp 189-236.

BAWDEN, W.F. (1989) Personal communication.

BOURKE, P.D. (1987). "A contouring subroutine." BYTE. June 1987. pp 143-150.

CANMET (1977). Pit Slope Manual, Ch. 2: Structural Geology, CANMET Report 77-41. Ottawa: Dept. of Energy Mines & Resources Canada. 123 pages.

CARTER, T.G. (1989) Personal Communication

CORKUM, B.T. (1990) FEINT Programmers manual. University of Toronto

DE AZEVEDO, C. (1990) "The use of numerical models for design of underground excavations in hard rock." MASc. Thesis submitted to the University of Toronto.

DENNESS, B. (1972) "A revised method of contouring stereograms using variable curvilinear cells." Geol. Mag. v. 109, no. 2, pp 157-163.

DIGGLE, J.P. and N.I. FISHER (1985) "SPHERE: A contouring program for spherical data." Computers and Geosciences. VII, No. 6. pp 725-766.

EINSTEIN, H.H. and G.B. BAECHER (1983). "Probabilistic and statistical methods in engineering geology." Rock Mechanics and Rock Engineering. 16, pp 39-72.

FISHER, R. (1953). "Dispersion on a sphere." Proceedings, Royal Society of London, A 217, pp 295-305.

FRANKLIN, S.A. and DUSSEAULT, M.B. (1989). Rock Engineering. McGraw - Hill. 600 pgs.

GOLDER ASS. (1979). STEREO - Version 2.0 Users Manual. Internal Publication. Vancouver: Golder Associates.

GOODMAN, R.E. (1976) Methods of Geological Engineering in Discontinuous Rocks. West Publ. Co. pp 88 - 223.

HOEK, E. and J.W. BRAY (1974). Rock Slope Engineering, 3rd. Edition. London: Institute of Mining and Metallurgy. 358 pages.

HOEK, E. and E.T. BROWN (1980). Underground Excavations in Rock. London: Institute of Mining and Metallurgy. 527 pages.

LUCAS, J.M. (1980). "A general stereographic method for determining the possible mode of failure of any tetrahedral rock wedge." Int. Jour. Rock Mech. Min. Sci. & Geomech Abstr. v. 17, pp 57-61.

MARKLAND, J. (1974). "The analysis of principal components of orientation data." Int. Jour. Rock Mech. Min. Sci. & Geomech Abstr. v. 11, pp 157-163.

MCMAHON, B.K. (1971). "A statistical method for the design of rock slopes." Proc. 1st Australia - N.Z. Conf. Geomech. Melbourne. 1. pp 314-321

NORANDA - Noranda Technology Centre (1989) Personal communication with research staff

PARK, R.G. (1983). Foundations of Structural Geology. London: Blackie. 135 pages.

PEAKER, S. (1990). "Development of a simple block size distribution model for the classification of rock masses." MASc. thesis submitted to the University of Toronto.

PHILLIPS, F.C. (1971). The Use of Stereographic Projection in Structural Geology, 3rd. Edition. London: Edward Arnold. 90 pages.

PRIEST, S.D. (1980). "The use of inclined hemisphere projection methods for the determination of kinematic feasibility, slide direction and volume of rock blocks." Int. Jour. Rock Mech. Min. Sci. & Geomech Abstr. v. 17, pp 1-23.

PRIEST, S.D. (1983). "Computer generation of inclined hemisphere projections." Int. Jour. Rock Mech. Min. Sci. & Geomech Abstr. v. 20,no. 1, pp 43-47.

PRIEST, S.D. (1985). Hemispherical Projection Methods in Rock Mechanics. London: George Allen & Unwin. 124 pages.

RAGAN, D.M. (1973). Structural Geology, An Introduction to Geometrical Techniques, 2nd. Edition. New York: Wiley. 208 pages.

SHI, GEN-HUA and R.E. GOODMAN (1989). Basic Programs for Block Theory - General Key Blocks. Berkeley: University of California.

SHI, GEN-HUA and GOODMAN (1990). "Finding 3-d maximum key blocks on unrolled joint trace maps of tunnel surfaces." Rock Mechanics Contributions and Challenges - Proc. of the 31st. U.S. Symposium. Rotterdam: A.A. Balkema.

SPIEGEL, M.R. (1974). Vector Analysis and an Introduction to Tensor Analysis, Schaum's Outline Series. New York: Mcgraw Hill.

STAUFFER, M.R. (1966) "An empirical-statistical study of three-dimensional fabric diagrams as used in structural analysis." Canadian Journal of Earth Science. v. 3. pp 473-498.

TERZAGHI, RUTH D. (1965). "Sources of error in joint surveys." Geotechnique, v. 15, no. 3, pp 287-304.

TOCHER, F.E. (1979) "The computer contouring of fabric diagrams." Computers and Geosciences. v.5. pp 73-80.

TOCHER, F.E. (1978) "Some modifications of a point-counting computer program for fabric analysis of axial orientations." Computers and Geosciences. v.4. pp 1-3.

TOCHER, F.E. (1978) "Petrofabric point-counting program fabric (FORTRAN IV)." Computers and Geosciences. v.4. pp 5-21.

TUFTE, E.R. (1983) The Visual Display of Quantitative Information. Cheshire, Conn.:Graphics Press. 197 pages.

WALLACH, J. (1990). Personal Correspondence. AECL. Ottawa.

WATSON, G.S. (1966). "The statistics of orientation data." J.Geology 75, no 5, pp 796-798.

WOOD, D. (1989) Personal Communication

ZANBAK, C. (1977). "Statistical interpretation of discontinuity contour diagrams." Int. Jour. Rock Mech. Min. Sci. & Geomech Abstr. v. 14, pp 111-120.
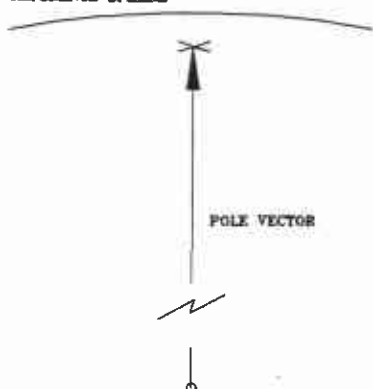

ZHANG, S. and G. TONG (1988). "Technical Note: Computerized pole concentratrion graphs using the Wulff stereographic projection." Int. Jour. Rock Mech. Min. Sci. & Geomech Abstr. v. 25, no. 1, pp 45-51.

APPENDIX A

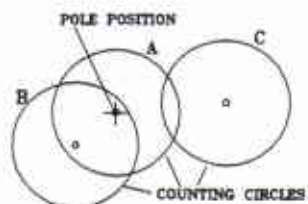## DERIVATION OF FISHER INFLUENCE FUNCTION

## DERIVATION OF SCHMIDT COUNTING CIRCLE CONCEPT:

REFERENCE SPHERE

POLE VECTOR

SCHMIDT METHOD ASSUMES 100% PROBABILITY THAT THE ACTUAL POLE POSITION IS AT THAT WHICH WAS MEASURED.

ON SURFACE OF REFERENCE SPHERE:

POLE POSITION

COUNTING CIRCLES

IN ARRANGEMENT AT RIGHT, THE POLE WHICH IS COINCIDENT WITH THE CENTRE OF COUNTING CIRCLE A, HAS A 100 % PROBABILITY OF FALLING WITHIN CIRCLE A AND B AND A 0 % PROBABILITY OF FALLING WITHIN CIRCLE C.

EQUIVALENT DERIVATION OF FISHER CONTOURING CONCEPT:

POLE VECTOR
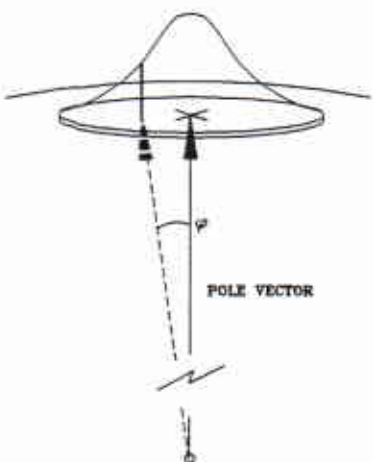
IN THIS METHOD THE FISHER DISTRIBUTION DESCRIBES THE PROBABILITY THAT THE TRUE ORIENTATION IS AN ANGULAR DISTANCE φ FROM THE MEASURED POLE (ON WHICH THE DISTRIBUTION IS CENTRED)

NOTE THAT THE DISTRIBUTION IS TRUNCATED AT THE COUNTING CIRCLE PERIMETER AND DERIVED SO THAT THIS LIMIT IS THE 96 % CONFIDENCE LIMIT. THIS MUST BE DONE SINCE THE ACTUAL DISTRIBUTION COVERS THE WHOLE SURFACE OF THE SPHERE.

ON SURFACE OF REFERENCE SPHERE:
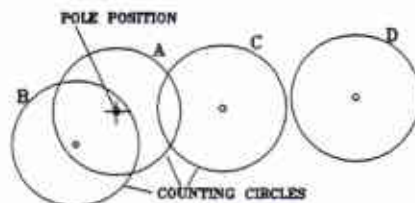
POLE POSITION

COUNTING CIRCLES

IN ARRANGEMENT AT RIGHT, THE POLE WHICH IS COINCIDENT WITH THE CENTRE OF COUNTING CIRCLE A, HAS A 100 % PROBABILITY OF FALLING WITHIN CIRCLE A A PROBABILITY BETWEEN 0 and 100 % OF FALLING IN CIRCLES B OR C AND 0 % PROBABILITY OF FALLING IN D.
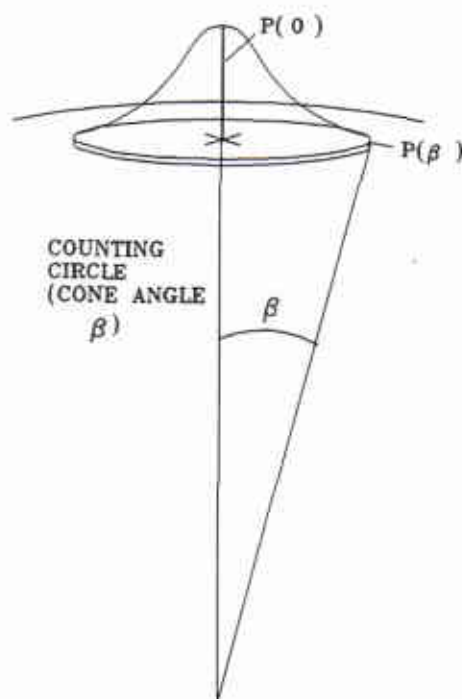
GIVEN A MEAN POLE ORIENTATION AT $\varphi = 0$ DEGREES

φ = THE PROBABILITY THAT THE ACTUAL POLE POSITION IS BETWEEN

φ & $\varphi + d\varphi$ FROM THIS MEASURED POSITION (ASSIGNED MEAN ORIENTATION)

$$P(\varphi) = \left(\frac{K}{4\pi \sinh(K)} \right) e^{K \cos(\varphi)} \, d\varphi$$

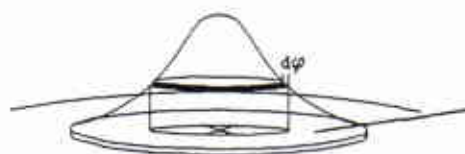TO DERIVE THE INFLUENCE FUNCTION, FIRST SOLVE FOR K FOR A GIVEN COUNTING CIRCLE CONE ANGLE β :

$$\frac{P(\beta)}{d\varphi} = 0.05 \frac{P(0)}{d\varphi}$$

COUNTING CIRCLE (CONE ANGLE β)

$$\frac{\left(\dfrac{K}{4\pi \sinh(K)} \right) e^{K \cos(\beta)}}{\left(\dfrac{K}{4\pi \sinh(K)} \right) e^{K \cos(0)}} = 0.05$$
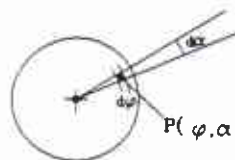
$$e^{K\cos(\beta - 1)} = 0.05$$

$$K = \frac{\ln(0.05)}{\cos(\beta - 1)}$$

NEXT NUMERICALLY CALCULATE TOTAL VOLUME UNDER DOME CORRESPONDING TO 100 % PROBABILITY OF OCCURANCE WITHIN A ANGULAR DISTANCE OF β FROM THE MEAN POLE.

$$V = \sum_{\varphi=0}^{\varphi=\beta} \left[\left(\frac{K}{4\pi \sinh(K)} \right) e^{K \cos(\varphi)} \right] \cdot d\varphi$$
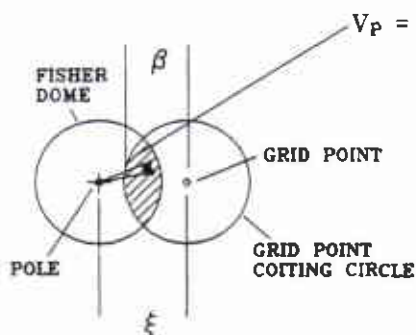
NOW DERIVE THE PROBABILITY THAT THE ACTUAL ORIENTATION
WILL BE SOME ANGULAR DISTANCE φ AND SOME ROTATIONAL
ANGLE α FROM THE MEAN POSITION:

$$P(\varphi,\alpha) = \left(\frac{K}{4\pi\sinh(K)}\right) e^{(K\cos\varphi)} d\varphi \frac{d\alpha}{2\pi}$$

$$P(\varphi,\alpha) = \left(\frac{K}{8\pi^2\sinh(K)}\right) e^{(K\cos\varphi)} d\varphi\, d\alpha \qquad (\text{ a })$$

CALCULATE THE VOLUME UNDER THE PROBABILITY DOME WHICH FALLS
WITHIN A COUNTING CIRCLE (RADIUS β) CENTRED ON A GRID POINT
SOME ANGULAR DISTANCE ξ FROM THE POLE POINT:

$V_P = $ THE NUMERICAL SUM OF THE VALUES OF P
IN EQUATION a ABOVE FOR ALL INTEGRATION
POINTS (φ,α) WHICH FALL INSIDE OF THE
GRID POINT COUNTING CIRCLE.

THIS PARTIAL VOLUME DIVIDED BY THE TOTAL
VOLUME OF THE FISHER DOME AS CALCULATED
ON THE PREVIOUS PAGE YIELDS THE PROBABILITY
THAT A POLE WITH MEASURED ORIENTATION AS
SHOWN WILL ACTUALLY FALL WITHIN THE GRID
POINT COUNTING CIRCLE. THIS IS THE VALUE WHICH
IS ASSIGNED TO THE GRID POINT FOR EACH POLE
INSTEAD OF THE 0 OR 1 VALUES IN THE SCHMIDT
METHOD.

THE PROBABILITY VALUE V_P / V CAN BE SHOWN TO
BE INDEPENDANT OF THE VALUE OF β WHEN
REPRESENTED AS A FUNCTION OF THE RATIO ξ/β .
THIS RELATIONSHIP SHOWN BELOW IS THE BASIS FOR
THE CALCULATION OF INFLUENCE IN DIPS. ACTUAL
VALUES ARE INTERPOLATED FROM A STORED SET
OF VALUES SHOWN BELOW.

Applied weights to grid points

probability weighting to grid point

(pole—grid separation)/(counting angle)

□ Fisher weighting
—— Schmidt weighting